INFLUENCE DES FACTEURS DU MILIEU SUR LA VARIABILITÉ SPATIO-TEMPORELLE DES COMMUNAUTÉS PHYTOPLANCTONIQUES ESTIVALES LE LONG DE LA CÔTE EST DE LA BAIE JAMES

Mémoire présenté

dans le cadre du programme de maîtrise en océanographie

en vue de l'obtention du grade de maître ès sciences (M.Sc)

PAR

© MARIE-ANNE BAUDIN

Août 2024

Composition du jury :

André Rochon, président du jury, Institut des sciences de la mer de Rimouski

Michel Gosselin, directeur de recherche, Institut des sciences de la mer de Rimouski

Michel Poulin, examinateur externe, Musée canadien de la nature

Dépôt initial le 29 avril 2024 Dépôt final le 15 août 2024

« La surface des eaux demeure l'éternel miroir, elle réfléchit le ciel et garde son intégrité. En se penchant vers l'épaisseur des eaux, chacun n'y verra que le reflet de lui-même; en se relevant, son regard se perdra dans le cercle d'horizon. »

Anita Conti, *Le carnet viking*

REMERCIEMENTS

Je tiens tout d'abord à remercier mon directeur de recherche, Michel Gosselin, pour m'avoir donné l'opportunité de travailler sur ce projet. Tes conseils et tes attentes élevées m'ont permis d'évoluer et ont été une véritable source d'inspiration pour moi. Merci également pour ta patience à chaque fois que je faisais irruption à ton bureau pour te poser des questions. Enfin, merci de m'avoir donné l'opportunité de participer à une campagne d'échantillonnage dans l'Arctique canadien, cette expérience sur le terrain a vraiment été enrichissante.

Je tiens également à remercier André Rochon et Michel Poulin pour avoir accepté de faire partie du jury en tant que président et membre externe, respectivement.

Je tiens à remercier celles et ceux qui ont rendu possible les analyses en laboratoire : Virginie Galindo et Mélanie Simard pour l'analyse des pigments, Sylvie Lessard pour l'identification et le dénombrement du phytoplancton, Amélie Évrard pour l'analyse de la CDOM, Claude Belzile pour les analyses de DOC, TDN et de cytométrie en flux, Pascal Rioux pour l'analyse des nutriments et Pascal Guillot pour le traitement des données CTD.

Merci particulier à toute l'équipe administrative de l'ISMER : Martine, Marielle, Nancy, Katia et Brigitte pour votre gentillesse et votre disponibilité.

Merci à Chloé, pour avoir été d'aussi bons conseils et avoir toujours été à l'écoute quand j'étais perdue, mais aussi pour ton soutien qui m'a vraiment permis de tenir le coup dans le rush des dernières semaines. Nos randonnées et nos road trips (plus ou moins improvisés) ont été de véritables moments revivifiant pour moi. Hâte de voir où les prochains vont nous mener !

Merci à Flavie, pour nos dates de soirée et fin de semaine à l'université où on passait plus de temps à choisir quelles couleurs utiliser plutôt que de comprendre pourquoi R ne fonctionnait pas (un beau graphique ça n'a pas de prix). Tes idées farfelues et ton enthousiasme ont égayé les moments qu'on a passés ensemble, et ta persévérance m'a également motivée à me dépasser.

Merci également à toutes les personnes de la cale : Cloé, Pauline, Rachel, Christian, Arthur, pour votre bonne humeur, nos fous rires et les bons moments qu'on a passés ensemble et qui ont rendu ces deux années incroyables.

Merci à tou.te.s mes ami.e.s de Rimouski, mais aussi celles et ceux qui se trouvent outre-Atlantique, pour votre soutien tout au long de ce parcours académique.

Je tiens particulièrement à remercier mes parents, mes frères et ma sœur, pour m'avoir toujours encouragée et soutenue dans mes choix tout au long de la maîtrise et ce, malgré la distance.

Finalement, merci aux différents organismes qui ont financé ce projet : le Conseil de recherches en sciences naturelles et en génie du Canada (CRSNG), le Fonds de recherche du Québec – Nature et technologies (FRQNT) *via* le groupement stratégique Québec-Océan et la société Niskamoon.

AVANT-PROPOS

Ce mémoire, qui s'inscrit dans le cadre du Projet sur l'océanographie côtière de l'est de la baie James (Coast-JB), porte sur l'influence des variables du milieu sur la structure et la dynamique des communautés phytoplanctoniques des eaux côtières de l'est de la baie James. Il est composé de trois parties : une introduction générale rédigée en français, un chapitre central rédigé en anglais sous la forme d'un article scientifique, et une conclusion générale rédigée en français. L'article, qui s'intitule *Environmental drivers of summer phytoplankton community structure in a subarctic nearshore ecosystem influenced by river inputs*, sera soumis ultérieurement à une revue scientifique avec comité de lecture.

Les résultats de ce projet de recherche ont été présentés sous forme d'affiches et de présentations orales lors d'atelier et conférences scientifiques, et ont également servi de support pour des projets de vulgarisation.

Présentations d'affiches :

Baudin M.-A., Gosselin M. 2023. Photoacclimation of phytoplankton communities along the eastern coast of James Bay. *Réunion scientifique Sentinelle Nord*, Québec, Canada.

Baudin M.-A, Gosselin M. 2023. Variabilité spatiale des communautés phytoplanctoniques le long de la côte est de la baie James durant les étés 2018 et 2019. *Réunion scientifique annuelle de Québec-Océan*, Rivière-du-Loup, Canada.

Présentations orales :

Baudin M.-A, Gosselin M. 2023. Variabilité spatiale des communautés phytoplanctoniques le long de la côte est de la baie James. *Finale provinciale du concours de vulgarisation Mon projet nordique, Journées nordiques de l'Institut nordique du Québec*, Trois-Rivières, Canada.

Baudin M.-A, Gosselin M. 2023. Variabilité spatiale des communautés estivales phytoplanctoniques le long de la côte est de la baie James. *Séminaire de recherche*, Université du Québec à Rimouski, Rimouski, Canada.

RÉSUMÉ

Au cours des dernières décennies, le changement climatique et l'endiguement de grands fleuves pour la production hydroélectrique ont modifié le cycle hydrologique, le débit des rivières et les apports en matière dissoute et particulaire, notamment dans la baie James. Les eaux côtières de cette région subarctique, encore peu étudiées, sont caractérisées par une importante turbidité, si bien que la disponibilité de la lumière se trouve limitée, affectant les communautés phytoplanctoniques. L'objectif principal de ce projet était de caractériser la structure des communautés phytoplanctoniques et d'examiner leur état de photoacclimatation le long de la côte est de la baie James durant la saison estivale. La signature pigmentaire, combinée à la microscopie et à la cytométrie en flux, a été utilisée pour identifier les principaux groupes de phytoplancton présents au début et à la fin de l'été. Les concentrations des pigments caroténoïdes photosynthétiques (PSC) et caroténoïdes photoprotecteurs (PPC) ont également été déterminées afin d'étudier le potentiel d'acclimatation du phytoplancton face aux variations de lumière *in situ*. L'utilisation des pigments s'est révélée être une bonne approche pour estimer la biomasse relative des principaux groupes phytoplanctoniques, montrant que les eaux côtières de la baie James étaient dominées par des cellules flagellées, notamment des cryptophytes et des prasinophytes, bien que les diatomées étaient très présentes au début de l'été. La disponibilité de la lumière, atténuée par de fortes concentrations en matière particulaire en suspension (SPM) et matière organique dissoute colorée (CDOM), jouait un rôle dans la composition phytoplanctonique, avec les eaux chaudes et turbides littorales dominées par de petites cellules flagellées, et les eaux plus claires du large dominées par des diatomées. Les rapports PSC:PPC suivaient également le gradient côte-large de la lumière, avec des rapports qui augmentaient à mesure que la distance à la côte augmentait. Cela a permis d'avancer que la limitation de la lumière n'impliquait pas une maximisation de la concentration en PSC, mais favorisait la croissance de petites cellules mixotrophes. Ces résultats ont également mis en évidence l'impact des dérivations des rivières, comme celle de la rivière Eastmain, où une importante diminution du débit a induit un changement dans les communautés de phytoplancton, remplaçant les diatomées par des cellules flagellées. À l'inverse, le débit de La Grande Rivière a plus que doublé depuis 1980, si bien que la communauté phytoplanctonique de son panache est maintenant caractérisée par des taxons d'eau saumâtre.

Mots clés : baie James, CHEMTAX, microscopie, pigments, photoacclimatation, phytoplancton

ABSTRACT

In the last decades, climate change and the construction of dams on major rivers for hydroelectric production have altered the hydrological cycle, river flow and the input of dissolved and particulate matter, especially in James Bay. The coastal waters of this subarctic region, still poorly studied, are characterized by high turbidity, which limits light availability and affects phytoplankton communities. The main objective of this project was to characterize the structure of phytoplankton communities and examine their photoacclimation state along the eastern coast of James Bay during the summer. Pigment signatures, combined with microscopy and flow cytometry, were used to identify the main phytoplankton groups present in early and late summer. Concentrations of photosynthetic carotenoids (PSC) and photoprotective carotenoids (PPC) were also determined to study the acclimation potential of phytoplankton to light variations *in situ*. The use of pigments proved to be a good approach for estimating the relative biomass of the major phytoplankton groups, showing that the coastal waters of James Bay were dominated by flagellated cells, particularly cryptophytes and prasinophytes, although diatoms were present in early summer. Light availability, attenuated by suspended particulate matter (SPM) concentrations and colored dissolved organic matter (CDOM), played a role in phytoplankton composition, with warm and turbid nearshore waters dominated by small flagellate cells, and less turbid offshore waters dominated by diatoms. PSC:PPC ratios also followed the coast-offshore gradient of light, with ratios increasing with distance from the coast. This suggested that light limitation did not involve maximization of PSC concentrations but favored the growth of small mixotrophic cells. These results also highlighted the impact of river diversions, such as the Eastmain River, where a significant reduction in flow induced a change in phytoplankton communities, replacing diatoms with small flagellated cells. In contrast, the flow of the La Grande River has more than doubled since 1980, its phytoplankton plume community is now characterized by brackish-water taxa.

Keywords: James Bay, CHEMTAX, Microscopy, Pigments, Photoacclimation, Phytoplankton

TABLE DES MATIÈRES

REMERCIEMENTS ix

AVANT-PROPOS xi

RÉSUMÉ xiii

ABSTRACT xv

TABLE DES MATIÈRES xvii

LISTE DES TABLEAUX xix

LISTE DES FIGURES xxi

LISTE DES ABRÉVIATIONS, DES SIGLES ET DES ACRONYMES xxv

INTRODUCTION GÉNÉRALE 1

1. RÔLE DU PHYTOPLANCTON SUR LES CYCLES BIOGÉOCHIMIQUES DES MILIEUX CÔTIERS 1

2. IMPORTANCE ET RÔLES DES PIGMENTS 4

3. APPROCHES TAXONOMIQUES POUR LE PHYTOPLANCTON 6

4. CARACTÉRISTIQUES DE LA BAIE JAMES 13

5. OBJECTIFS 15

ENVIRONMENTAL DRIVERS OF SUMMER PHYTOPLANKTON COMMUNITY STRUCTURE IN A SUBARCTIC NEARSHORE ECOSYSTEM INFLUENCED BY RIVER INPUTS 17

1.1 INTRODUCTION 17

1.2 METHODOLOGY 20

1.2.1 Study site 20
1.2.2 Sampling 20
1.2.3 Chemical analysis 22
1.2.4 Light microscopy and flow cytometry 23

1.2.5 HPLC pigments 24
1.2.6 Chemotaxonomy 24
1.2.7 Statistical analysis 28

1.3 RESULTS AND DISCUSSION 29

1.3.1 Identification of taxonomic groups 30
1.3.2 Contribution of phytoplankton classes to total chlorophyll *a* biomass 34
1.3.3 Phytoplankton community composition 37
1.3.4 Spatial distribution and environmental drivers of phytoplankton community composition 39
1.3.5 Physiology and photoacclimation 47

1.4 CONCLUSION 53

1.5 ACKNOWLEDGEMENTS 53

CONCLUSION GÉNÉRALE 55

MATÉRIEL SUPPLÉMENTAIRE 59

RÉFÉRENCES 78

LISTE DES TABLEAUX

Tableau 1. Liste des marqueurs pigmentaires des différentes classes algales (Roy et al. 1996; Wright & Jeffrey 2006; Tremblay et al. 2009; Jeffrey et al. 2011; Coupel et al. 2015a). Les groupes en gras correspondent aux groupes majoritaires dans lesquels le pigment associé est retrouvé. MgDVP : magnesium 2,4-divinylpheoporphyrin a_5 ester monoéthylique ; BFU : 19'-butanoyloxyfucoxanthin ; HFU : 19'-hexanoyloxyfucoxanthin. 8

Tableau 2. Résumé des caractéristiques des cinq méthodes d'évaluation de la composition des communautés phytoplanctoniques: les pigments par HPLC, le séquençage d'amplicons de gènes d'ARN ribosomique 16S et 18S, l'imagerie cellulaire quantitative et la cytométrie en flux (Adapté de Kramer et al. 2024). ASV : variant de séquence d'amplicon. 11

Table 1. Initial matrix of ratios of accessory pigment to total chlorophyll *a* (TChl *a*) for different phytoplankton classes. Ratios were determined from [a] Higgins et al. (2011), [b] Coupel et al. (2015a) and [c] Matthes et al. (2021). Chl *b*: chlorophyll *b*; Chl c_2: chlorophyll c_2; Chl c_3: chlorophyll c_3; Allo: alloxanthin; Fuco: fucoxanthin; Neo: neoxanthin; Peri: peridinin; Pras: prasinoxanthin; Lut: lutein; Zea: zeaxanthin. TChl *a*: total chlorophyll *a*, Diato-I and Diato-II: Diatoms under low and high light levels, respectively, Chloro: chlorophytes, Crypto: cryptophytes, Cyano: cyanobacteria, including freshwater and marine colonial forms and marine coccoid planktonic species (e.g., *Synechoccocus*), Dino-1: dinoflagellates type 1 (containing peridinin), Prasino-2: prasinohytes type 2, including nanoplanktonic species (e.g., *Pyramimonas*), Prasino-3: prasinophytes type 3, including picoplanktonic species (e.g., *Micromonas*).....26

Table 2. Optimized final matrix of ratios of accessory pigment to total chlorophyll *a* (TChl *a*) for different phytoplankton classes during early and late summer. RMS = root mean sqare. Abbreviations are defined in Table 1. 27

Table S1. Relative contribution of accessory pigment to total chlorophyll *a* (%) photoacclimation index (mean ± SD) during early and late summer. 66

Table S2. List of planktonic protist and cyanobacteria (> 2 µm) from the eastern coast of James Bay during late summer 2018. Minimum (Min), mean and maximum (Max) abundance (cells L^{-1}) for each taxon, and occurrence (O) is shown in percent of the total number of samples collected (n = 28). n.d. = not

detected. Note that the limit of detection is 730 cells L^{-1}, however a value of zero was used when calculating the mean abundance. 67

Table S3. Summary of mean values (± standard deviation) for environmental and biological variables measured in the surface waters for five groups of stations with a taxonomically similar phytoplankton classes (determined with the group-average clustering) during early summer. The Kruskal-Wallis test (with p-value) and Dunn's post hoc test were performed to seek differences between groups for each variable (letters depict significant differences between groups where a<b<c). n.s.: non significant. PicoPCcyan: pico-phycocyanin-containing cyanobacteria, NanoPCcyan: nano-phycocyanin-containing cyanobacteria, PicoPEcyan: pico-phycoerythrin-containing cyanobacteria, NanoPEcyan: nano-phycoerythrin-containing cyanobacteria, Picoeuk: photosynthetic picoeukaryotes, Nanoeuk: photosynthetic nanoeukaryotes. 76

Table S4. Summary of mean values (± standard deviation) for environmental variables measured in the surface waters for four groups of stations with a taxonomically similar phytoplankton classes (determined with the group-average clustering) during late summer. The Kruskal-Wallis test (with p-value) and Dunn's post hoc test was performed to seek differences between groups for each variable (letters depict significant differences between groups where a<b<c). n.s.: non significant. Abbreviations are defined in Table S3. 77

LISTE DES FIGURES

Figure 1. Location of sampling stations along the east coast of James Bay during early (2019) and late (2018) summer. 21

Figure 2. Relationship between **(A)** total dinoflagellate abundance and peridinin concentration, **(B)** cryptophyte abundance and alloxanthin concentration, **(C)** total cyanobacteria abundance and zeaxanthin concentration, and **(D)** picoeukaryote abundance and prasinoxanthin concentration. The data is from the late summer. The linear regression line is shown. 33

Figure 3. Relative contributions of major phytoplankton groups to **(A)** total cell abundance (determined by light microscopy) and **(B)** total chlorophyll *a* (TChl *a*) concentration (determined by CHEMTAX) during late summer (n = 28). Total cell abundance and TChl *a* concentration are superposed on the graph (black line). Stations are sorted by latitude (from north on the left to south on the right). Pigment abbreviations are defined in Table 1. 35

Figure 4. Relative contributions of major phytoplankton groups to total chlorophyll *a* (TChl *a*) concentration during **(A)** early and **(B)** late summer. TChl *a* concentration is superposed on the graph for both periods (black line). Samples were collected at the same stations during both periods. Stations are sorted by latitude (from north on the left to south on the right).....38

Figure 5. Maps showing groups of stations with similar phytoplankton composition (based on CHEMTAX and determined with the group-average clustering) during **(A)** early (n = 114 stations) and **(B)** late (n = 68 stations) summer. Note that there are only four groups of stations in late summer. 41

Figure 6. Relative contribution of major phytoplankton groups to total chlorophyll *a* for groups of stations with similar pigment composition (determined by group-average clustering) during **(A)** early and **(B)** late summer. The Shannon diversity index (H') is indicated above each group.....43

Figure 7. Redundancy analysis (RDA) ordination plots of axis I and II showing taxonomic groups of phytoplankton based on CHEMTAX (red bold) in relation with environmental variables (black arrows) at stations collected during **(A)** early and **(B)** late summer. Colors represent the stations with a similar phytoplankton composition (determined with the group-average clustering).....46

Figure 8. Maps showing the mass ratio of photosynthetic carotenoids to photoprotective carotenoids (PSC:PPC) during **(A)** early and **(B)** late summer. 49

Figure 9. Relationships between **(A)** photosynthetic carotenoid pigment (PSC) concentration and total chlorophyll *a* (TChl *a*) concentration, and **(B)** photoprotective carotenoids (PPC) concentration and TChl *a* concentration. Relationships between PSC:PPC ratio and **(C)** water temperature, **(D)** Secchi depth, **(E)** relative contribution of prasinophytes to TChl *a*, and **(F)** relative contribution of diatoms I+II to TChl *a* during early (circles) and late (triangles) summer. The linear regression line is shown in all panels. 51

Figure S1. Heat map of the Spearman correlation coefficients between environmental and biological variables. The size of the circle is proportional to the correlation coefficient which shown in color. 59

Figure S2. Relationship between **(A)** relative contribution of total cyanobacteria to total chlorophyll *a* concentration and total cyanobacteria cell abundance and **(B)** relative contribution of total prasinophytes (type 2 + type 3) to total chlorophyll *a* concentration and picoeukaryote cell abundance during both sampling periods. Cell abundances were counted by flow cytometry. The linear regression line is shown. 60

Figure S3. Relationships between unidentified flagellate abundance and **(A)** alloxanthin concentration, **(B)** chlorophyll *b* concentration **(C)** neoxanthin concentration, and **(D)** lutein concentration. Cell abundances were counted by flow cytometry. The linear regression line is shown. 61

Figure S4. Relative contributions of phytoplankton groups to total chlorophyll *a* concentration during **(A)** early and **(B)** late summer. Stations are sorted by latitude (from north on the left to south on the right). 62

Figure S5. Group-average clustering showing groups of stations with taxonomically similar phytoplankton classes (as determined by CHEMTAX) during **(A)** early (n = 114, similarity level of 70%) and **(B)** late (n = 68, similarity level of 75%) summer. 63

Figure S6. Two-dimensional non-metric multidimensional scaling (NMDS) of stations during **(A)** early (n = 114) and **(B)** late (n = 68) summer. Groups of stations with taxonomically similar phytoplankton classes, as determined with the group-average clustering (see Figure S5), are superimposed on the NMDS. 64

Figure S7. Degradation pigment concentrations during **(A)** early and **(B)** late summer, and pheophorbide *a*:pheophytin *a* (Pb:Pp) ratio during early (circles with solid line) and late (triangles with dashed line) summer. Stations are sorted

by latitude (from north on the left to south on the right). LGR = La Grande River, MR = Maquatua River, VCR = Vieux Comptoir River, ER = Eastmain River.....65

LISTE DES ABRÉVIATIONS, DES SIGLES ET DES ACRONYMES

$a_{CDOM}(440)$	Coefficient d'absorption de la matière organique dissoute colorée à 440 nm (*Absorption coefficient of colored dissolved organic matter at 440 nm*)
Allo	Alloxanthine (*Alloxanthin*)
ANOSIM	Analyse de similarité (*Similarity analysis*)
BFU	19'-butanoyloxyfucoxanthine (*19'-Butanoylxyfucoxanthin*)
CDOM	Matière organique colorée dissoute (*Colored dissolved organic matter*)
CHEMTAX	*Chemical taxonomy*
Chl *a*	Chlorophylle *a* (*Chlorophyll a*)
Chl *b*	Chlorophylle *b* (*Chlorophyll b*)
Chl c_2	Chlorophylle c_2 (*Chlorophyll* c_2)
Chl c_3	Chlorophylle c_3 (*Chlorophyll* c_3)
Chloro	Chlorophytes (*Chlorophytes*)
Crypto	Cryptophytes (*Cryptophytes*)
Cyano	Cyanobactéries (*Cyanobacteria*)
Diato-I	Diatomées sous faible intensité lumineuse (*Diatoms under low light intensity*)

Diato-II	Diatomées sous forte intensité lumineuse (*Diatoms under high light intensity*)
Dino-1	Dinoflagellés type 1 (*Dinoflagellates type 1*)
Fuco	Fucoxanthine (*Fucoxanthin*)
HFU	19'-hexanoyloxyfucoxanthin (*19'-Hexanoyloxyfucoxanthin*)
HPLC	Chromatographie liquide à haute performance (*High-performance liquid chromatography*)
Lut	Lutéine (*Lutein*)
MgDVP	Magnesium 2,4-divinylpheoporphyrine a_5 ester monoéthylique (*Magnesium 2,4-divinylpheoporphyrin a_5 monomethyl ester*)
NanoPCcyan	Nanocyanobactéries contenant de la phycocyanine (*Nano-phycocyanin-containing cyanobacteria*)
NancoPEcyan	Nanocyanobactéries contenant de la phycoérythrine (*Nano-phycoerythrin-containing cyanobacteria*)
Nanooeuk	Nanoeucaryotes photosynthétiques (*Photosynthetic nanoeukaryotes*)
Neo	Néoxanthine (*Neoxanthine*)
NMDS	Cadrage multidimensionnel non-métrique (*Non-metric multidimensional scaling*)
NO_3 + NO_2	Nitrate + Nitrite (*Nitrate + Nitrite*)
Pb	Phéophorbide *a* (*Pheophorbide a*)
Peri	Péridinine (*Peridinin*)
Picoeuk	Picoeucaryotes photosynthétiques (*Photosynthetic picoeukaryotes*)

PicoPCcyan	Picocyanobactéries contenant de la phycocyanine (*Pico-phycocyanin containing cyanobacteria*)
PicoPEcyan	Picocyanobactéries contenant de la phycoérythrine (*Pico-phycoerythrin containing cyanobacteria*)
PO_4	Phosphate (*Phosphate*)
Pp	Phéophytine *a* (*Pheophytin a*)
PPC	Caroténoïdes photoprotecteurs (*Photoprotective Carotenoids*)
PSC	Caroténoïdes photosynthétiques (*Photosynthetic Carotenoids*)
Pras	Prasinoxanthine (*Prasinoxanthin*)
Prasino-2	Prasinophytes type 2 (*Prasinophytes type 2*)
Prasino-3	Prasinophytes type 3 (*Prasinophytes type 3*)
RDA	Analyse de redondance (*Redundancy analysis*)
$Si(OH)_4$	Acide silicique (*Silicic acid*)
SPM	Matière particulaire en suspension (*Suspended particulate matter*)
TChl *a*	Chlorophylle *a* totale (somme de la chlorophylle *a* et de la chlorophyllide *a*) (*Total chlorophyll a (sum of chlorophyll a and chlorophyllide a)*)
Zea	Zéaxanthine (*Zeaxanthin*)

INTRODUCTION GÉNÉRALE

1. RÔLE DU PHYTOPLANCTON SUR LES CYCLES BIOGÉOCHIMIQUES DES MILIEUX CÔTIERS

Les milieux côtiers jouent un rôle important sur les cycles biogéochimiques, en particulier celui du carbone, en raison de leur grande production autochtone de matière organique (production primaire) par rapport à l'océan ouvert, et des apports allochtones supplémentaires provenant des bassins versants environnants (Smith & Hollibaugh 1993; Liu et al. 2000; Kuzyk et al. 2010). Les régions de hautes latitudes jouent un rôle crucial sur les cycles biogéochimiques mondiaux, car elles abritent un grand nombre de systèmes d'eau douce et drainent de vastes zones de tourbières et de sols riches en matière organique. Cette matière organique représente jusqu'à 50% du stock mondial de carbone des sols, faisant de ces régions une composante essentielle du cycle du carbone de la planète (Freeman et al. 2001; Findlay 2005; de Melo et al. 2022).

Les milieux côtiers arctiques et subarctiques sont des systèmes relativement complexes, puisque leur dynamique est régie non seulement par le forçage des marées et les apports d'eau douce terrestres, mais également par la saisonnalité des glaces (McClelland et al. 2012). Les réseaux fluviaux jouent un rôle clé dans les processus biogéochimiques des eaux côtières, puisqu'ils sont en effet considérés comme des vecteurs de sédiments, de matière organique particulaire et dissoute, et de nutriments, soutenant l'importante production primaire de ces écosystèmes (Cole et al. 2007; Kuzyk et al. 2010; Raymond et al. 2013; McClelland et al. 2014; de Melo et al. 2022). La production primaire des zones côtières de hautes latitudes est soutenue par la présence des macroalgues (notamment les fucoïdes et les varechs), des herbiers marins (tels que la zostère marine), du microphytobenthos et du phytoplancton. L'ensemble de ces producteurs primaires contribue de manière significative

à la production de l'écosystème côtier (Gattuso et al. 2006; Woelfel et al. 2010; Arrigo & van Dijken 2015; Lebrun et al. 2022). La combinaison du forçage des marées et le ruissellement des rivières crée des zones de transition, générant des gradients environnementaux, notamment de la lumière et des nutriments (Jacquemot et al. 2021), influençant la productivité primaire (Muylaert et al. 2009; Vigil et al. 2009; Bazin et al. 2014; Jacquemot et al. 2021). Bien que la croissance des producteurs primaires soit favorisée par la hausse des températures et la réduction du couvert de la glace de mer, elle peut être limitée par l'atténuation de la lumière dans la colonne d'eau, induite par l'apport des sédiments *via* le ruissellement des rivières ou des glaciers (Krause-Jensen et al. 2020). La glace de mer, cependant, fournit un habitat de choix pour les communautés microbiennes (Poulin et al. 2011), impliquées, entre autres, dans la production primaire (Vancoppenolle et al. 2013). Les échanges de dioxyde de carbone (CO_2) à travers la glace de mer, la précipitation du carbonate de calcium ($CaCO_3$) dans la glace, l'émission de méthane (CH_4) et de diméthyle sulfure (DMS) vers l'atmosphère et la chute d'algues dans la colonne d'eau pendant la fonte de la glace sont également considérés comme des processus biogéochimiques clés caractérisant la glace de mer (Vancoppenolle et al. 2013).

Toutefois, les modifications environnementales actuelles et futures affecteront la production primaire sympagique, pélagique et benthique, et influenceront à plus grande échelle les cycles biogéochimiques et la dynamique des réseaux trophiques (Tremblay et al. 2012), en particulier dans les systèmes de hautes latitudes, considérés comme les plus vulnérables face aux changements climatiques (Lee et al. 2023). Les impacts de ces modifications sur la production primaire demeurent cependant encore difficiles à prédire. En effet, l'augmentation de la température des eaux de surface et des apports d'eau douce pourrait intensifier la stratification de la colonne d'eau, limitant les apports verticaux des nutriments, et causant par conséquent une diminution de la production primaire (Carmack et al. 2016). Il en résulterait alors une modification dans la structure et le fonctionnement des réseaux trophiques, le phytoplancton de grande taille comme les diatomées alimentant les réseaux trophiques herbivores (Tremblay et al. 2012). D'autre part, l'amincissement continu de la glace de mer accentuerait la fréquence et l'étendue des proliférations

phytoplanctoniques, augmentant ainsi la production primaire de la colonne d'eau (Horvat et al. 2017; Ardyna et al. 2020), mais réduisant en contrepartie la production attribuable aux algues de glace (Arrigo 2017; Hop et al. 2020; Lannuzel et al. 2020). Également, les modifications environnementales futures pourraient conduire à une augmentation des précipitations et de l'érosion côtière, phénomènes qui s'amplifient au fil des années dans l'Arctique (McCrystall et al. 2021; Nielsen et al. 2022). Cela induira par conséquent une augmentation de la turbidité de ces eaux côtières, en raison d'un apport accru de sédiments (Klein et al. 2021). La pénétration réduite de la lumière dans la colonne d'eau deviendrait alors limitante pour la photosynthèse des producteurs primaires (Klein et al. 2021).

Ce projet de maîtrise met plutôt l'emphase sur l'étude des communautés phytoplanctoniques, pour lesquelles des changements dans la taille des cellules peuvent être induits par les modifications climatiques, en favorisant notamment la croissance du phytoplancton de petite taille (Lovejoy et al. 2007; Tremblay et al. 2012). Ces modifications dans la structure de taille se reflètent également dans les groupes fonctionnels de phytoplancton. En effet, les diatomées, qui dominent actuellement les communautés phytoplanctoniques, pourraient être remplacées par des cellules flagellées plus petites, qui possèdent une meilleure capacité de croissance dans des conditions de faible intensité lumineuse et de limitation en nutriments (Tremblay et al. 2009), et qui sont moins sujettes à la sédimentation (Li et al. 2009). Les diatomées, qui dominent aussi généralement les eaux très productives, sont broutées par le zooplancton métazoaire (Tremblay et al. 2012), mais un remplacement par de plus petites cellules serait plus favorable à des organismes protozooplanctoniques tels que les ciliés (Klauschies et al. 2012). La structure de taille est une caractéristique importante des communautés phytoplanctoniques qui détermine, en partie, l'ampleur du carbone fixé et exporté vers les niveaux trophiques supérieurs (Waite et al. 1997; Li et al. 2009) et les profondeurs marines (Armstrong et al. 2001; Schloss et al. 2007). Bien que la production primaire phytoplanctonique soit principalement déterminée par la disponibilité de la lumière et des nutriments (Tremblay et al. 2012), elle est également modulée par d'autres facteurs tels que la température, la salinité ou le pH (Tremblay et al. 2019; Jacquemot et al. 2021). L'importance relative des différents facteurs et leurs

interactions varient dans l'espace (localement et régionalement) et dans le temps (selon les saisons et les années) (Legendre et al. 1996; Kuzyk et al. 2010), et peuvent affecter différemment le phytoplancton qui peuple la colonne d'eau des habitats côtiers (Tremblay et al. 2019). La lumière joue cependant un rôle fondamental dans la régulation de la productivité, de l'abondance, de la biomasse et de la composition phytoplanctonique, en particulier dans les écosystèmes côtiers turbides peu profonds (Paerl & Justic 2011). En effet, dans ces milieux, l'atténuation de la lumière dans la colonne d'eau est principalement causée par la matière particulaire en suspension et la matière organique dissoute colorée (CDOM) (Gallegos et al. 1990; Paerl & Justic 2011; Mabit et al. 2022). En condition de faibles intensités lumineuses, le phytoplancton tend à augmenter son contenu cellulaire en pigments et à réorganiser leur disposition au sein de ses unités photosynthétiques (PSU) (Falkowski & Raven 2007).

2. IMPORTANCE ET RÔLES DES PIGMENTS

Les cellules phytoplanctoniques ont développé toute une gamme de pigments capable d'absorber le rayonnement solaire photosynthétiquement actif (PAR, 400 – 700 nm), afin d'effectuer la photosynthèse (Roy et al. 1996). Parmi ces pigments, trois types peuvent être chimiquement distingués : les chlorophylles, les caroténoïdes et les phycobilines (Kirk 2011; Roy et al. 2011). Les chlorophylles et les caroténoïdes sont essentiellement synthétisés chez les cellules procaryotes et eucaryotes photosynthétiques, ce qui les différencie des autres communautés d'organismes, telles que les bactéries hétérotrophes et les protozoaires (Wright & Jeffrey 2006). Dans les océans, les pigments photosynthétiques, en particulier la chlorophylle *a* (Chl *a*), sont depuis longtemps reconnus comme des marqueurs moléculaires uniques de la biomasse phytoplanctonique (Gibb et al. 2001). Quant aux caroténoïdes, considérés comme des composés naturels très diversifiés (Lohr 2011), la quantité synthétisée annuellement a été estimée par Pfander (1992) et Hendry (1993) à 200×10^6 tonnes. Ces caroténoïdes (plus de 700) peuvent être divisés en carotènes et en xanthophylles (Lohr 2011).

Enfin, les phycobilines sont plutôt retrouvées chez les algues rouges, les cryptomonades et les cyanobactéries (Chakdar & Pabbi 2016), mais leur quantité annuelle synthétisée demeure encore inconnue.

La composition pigmentaire du phytoplancton peut varier qualitativement au sein d'un même genre, voire entre les souches d'une même espèce (Zapata et al. 2004; Kramer et al. 2024). Cette variation peut être considérée comme une réponse rapide face aux conditions environnementales changeantes (Kuczynska et al. 2015). Des études antérieures ont observé les effets de plusieurs facteurs environnementaux sur les concentrations pigmentaires, parmi lesquels il est possible de citer : l'intensité lumineuse, le spectre de la lumière, le rayonnement ultraviolet, la longueur du jour, le cycle diurne, le statut nutritionnel, la concentration en macronutriments et en fer, le mélange vertical et la phase de croissance (Higgins et al. 2011). Néanmoins, ce sont les effets de la lumière et des nutriments sur la composition pigmentaire qui sont les facteurs les plus examinés dans les études (Goericke & Montoya 1998; Schlüter et al. 2000; Henriksen et al. 2002; Rodriguez et al. 2002; Falkowski & Raven 2007). La limitation en azote et en fer, ou éventuellement de la lumière, conduit généralement à une augmentation des rapports pigments accessoires:Chl *a*, principalement en raison de la diminution de la Chl *a* intracellulaire, car les caroténoïdes ne contiennent pas d'azote et les modifications de leurs concentrations intracellulaires sont plus faibles (Higgins et al. 2011). Le phytoplancton ajuste donc son contenu cellulaire en pigments photosynthétiques pour maximiser l'efficacité de la photosynthèse sous différents régimes lumineux et synthétise des pigments photoprotecteurs pour minimiser les dommages causés par un excès de rayonnement (Falkowski & Raven 2007).

Les produits de dégradation de la Chl *a*, communément appelés phéopigments, peuvent survenir lors de la photooxydation (plus de 50% des phéopigments en surface), de la sénescence, de la sédimentation et de la remise en suspension des cellules phytoplanctoniques, ainsi que du broutage induit par le zooplancton (Gibb et al. 2001). La phéophytine *a*, par exemple, est un indice de la sénescence des cellules phytoplanctoniques. La présence de phéophorbide *a* suggère une pression de broutage par le zooplancton

métazoaire, notamment sur les diatomées. Parallèlement, l'hydroxy-méthyl-phéophorbide *a* et la pyrophéophorbide *a* sont plutôt des marqueurs de broutage par le microzooplancton sur les cellules flagellées de petite taille. La chlorophyllide *a* et l'allomère de la chlorophylle *a* résultent généralement de la dégradation artificielle de la Chl *a* lors de la manipulation des échantillons (filtration, extraction, stockage) (Suzuki & Fujita 1986; Jeffrey & Hallegraeff 1987; Roy et al. 2011).

3. APPROCHES TAXONOMIQUES POUR LE PHYTOPLANCTON

Les pigments, en plus de fournir des indications quant à l'état physiologique du phytoplancton, sont utilisés comme biomarqueurs taxonomiques de ces organismes. En effet, en plus de la Chl *a* qui est largement utilisée comme proxy de la biomasse algale, d'autres pigments chlorophylliens et caroténoïdes peuvent être employés en tant que traceurs de certains groupes spécifiques au sein des communautés algales (Roy et al. 1996; Coupel et al. 2015a; Kuczynska et al. 2015). La chimiotaxonomie, plus particulièrement, vise à classer les organismes vivants en fonction de leur composition chimique, notamment des métabolites secondaires qu'ils produisent (Gibb et al. 2001). L'utilisation des pigments pour l'analyse chimiotaxonomique a été suggérée dans les années 1970 lorsque Jeffrey (1961, 1968) a décelé une grande diversité de pigments dans le phytoplancton, grâce à l'utilisation de la chromatographie sur couche mince. Au cours des 35 dernières années, la chimiotaxonomie du phytoplancton a été à l'origine d'une grande amélioration de notre compréhension de la répartition et de la composition des populations océaniques de phytoplancton. Plus récemment, des progrès ont également été réalisés dans l'utilisation des données sur les pigments pour permettre des estimations quantitatives de la biomasse chlorophyllienne des classes individuelles (ex. Mackey et al. 1998). Les pigments accessoires sont utilisés comme indicateurs de la biomasse relative des principaux groupes taxonomiques d'algues unicellulaires et offrent un moyen d'évaluer les changements ou les différences dans la

composition des groupes fonctionnels phototrophes dans les assemblages mixtes (Kuczynska et al. 2015; Kramer et al. 2024).

L'analyse de ces pigments se fait à l'aide de la chromatographie liquide à haute performance (HPLC), et permet la séparation, l'identification et la quantification des pigments chlorophylliens, des caroténoïdes et des pigments de dégradation. L'application de l'HPLC permet une estimation plus précise de la Chl *a*, ainsi qu'une séparation et une quantification jusqu'à 50 chloropigments et caroténoïdes supplémentaires dans le plancton marin (Wright et al. 1991). La méthode HPLC est intéressante car elle est relativement rapide. Les pigments représentent des marqueurs précieux pour les classes algales (Tableau 1), en particulier pour les fractions pico- et nanoplanctoniques, qui sont difficilement identifiables à la microscopie optique (Higgins et al. 2011). Ainsi, sans recourir aux longs comptages microscopiques, il est devenu possible d'avoir une information globale et synthétique de la biomasse et de la composition de la communauté phytoplanctonique (Gibb et al. 2001).

Tableau 1. Liste des marqueurs pigmentaires des différentes classes algales (Roy et al. 1996; Wright & Jeffrey 2006; Tremblay et al. 2009; Jeffrey et al. 2011; Coupel et al. 2015a). Les groupes en gras correspondent aux groupes majoritaires dans lesquels le pigment associé est retrouvé. MgDVP : magnésium 2,4-divinylphéoporphyrine a_5 ester monométhylique ; BFU : 19'-butanoyloxyfucoxanthine ; HFU : 19'-hexanoyloxyfucoxanthine.

Pigment	Classe
Chlorophylles	
Chlorophylle *b*	**Chlorophyceae de type 1 et 2**, Euglénophyceae, **Prasinophyceae de type 1, 2A, 2B, 3A et 3B**
Chlorophylle c_1	Chrysophyceae, **Diatomées de type 1 et 3**, Prymnésiophyceae de type 1 à 5
Chlorophylle c_2	Chrysophyceae, Cryptophyceae, **Diatomées de type 1 à 3**, Dinoflagellés de type 1 à 4, Prymnésiophyceae de type1 à 8
Chlorophylle c_3	**Chrysophyceae**, Diatomées de type 2 et 3, Dinoflagellés de type 2, **Prymnésiophyceae de type 4 à 8**
MgDVP	Chrysophyceae, Diatomées de type 1 à 3, Dinoflagellés de type 1 à 4, **Prasinophyceae de type 2B, 3A et 3B**, Prymnésiophyceae de type 1 à 8
Carotènes	
β, β-carotène	Chlorophyceae de type 1 et 2, Chrysophyceae, Cyanophyceae de type 1 à 3, Diatomées de type 1 à 3, Dinoflagellés de type 1 à 4, Euglénophyceae, Prasinophyceae de type 1, 2A, 2B, 3A et 3B, Prymnésiophyceae de type 1 à 8
Xanthophylles	
Alloxanthine	**Cryptophyceae**
Antheraxanthine	Chrysophyceae
BFU	**Chrysophyceae, Prymnésiophyceae de type 6 à 8**
Crocoxanthine	Cryptophyceae
Diatoxanthine	Chrysophyceae, Diatomées de type 1 à 3, Dinoflagellés de type 1 à 3, Prymnésiophyceae de type 1 à 8
Diatodinoxanthine	Chrysophyceae, Diatomées de type 1 à 3, Dinoflagellés de type 1 à 3, Prymnésiophyceae de type 1 à 8
Fucoxanthine	Chrysophyceae, **Diatomées de type 1 à 3**, Dinoflagellés de type 2 et 3, Prymnésiophyceae de type 1 à 8
HFU	**Prymnésiophyceae de type 6 à 8**
Lutéine	**Chlorophyceae de type 3 et 4**, Euglénophyceae, Prasinophyceae de type 1, 2A, 2B, 3A et 3B
Néoxanthine	Chlorophyceae de type 1 et 2, Euglénophyceae, Prasinophyceae de type 1, 2A, 2B, 3A et 3B
Péridinine	**Dinoflagellés de type 1**
Prasinoxanthine	**Prasinophyceae de type 3A et 3B**
Violaxanthine	Chlorophyceae de type 1 et 2, Prasinophyceae de type 1, 2A, 2B, 3A et 3B
Zéaxanthine	Chlorophyceae de type 1 et 2, **Cyanophyceae de type 1 à 5**, Prasinophyceae de type 1, 2A, 2B, 3A et 3B

Néanmoins, malgré les avantages que présente cette méthode, quelques critiques peuvent être formulées. Premièrement, il est toujours difficile de trouver un pigment biomarqueur exclusif d'une classe algale, puisque peu de pigments sont considérés comme des marqueurs non ambigus, la plupart étant répartie sur plusieurs groupes algaux (Tableau 1; Higgins et al. 2011; Jeffrey et al. 2011; Kramer et al. 2024). Il est donc encore nécessaire d'améliorer la connaissance des pigments caractéristiques des souches isolées en laboratoire et d'avoir, de préférence, une bonne connaissance des espèces présentes dans le milieu étudié. Certains groupes présentent des signatures pigmentaires différentes, comme les Prymnésiophyceae, montrant six types de pigments (Zapata et al. 2004; Jeffrey et al. 2011). Deuxièmement, il est parfois possible de trouver des pigments biomarqueurs d'une classe algale à l'intérieur d'un autre groupe, s'expliquant par le phénomène d'endosymbiose. Certaines cellules phytoplanctoniques sont fonctionnelles à l'intérieur d'une cellule hôte appartenant en général à un autre groupe. C'est le cas, en particulier, des dinoflagellés, qui comptent des espèces hétérotrophes et mixotrophes. L'application de la chimiotaxonomie des pigments sera beaucoup mieux établie grâce aux progrès de la taxonomie et de la phylogénie, associés à une meilleure analyse des pigments et à des identifications chimiques plus rapides. Grâce à ces techniques améliorées, il serait possible de découvrir une plus grande diversité de pigments et de taxons chez les populations de phytoplancton marin et de mieux comprendre leur rôle dans les cycles biogéochimiques des océans (Nair et al. 2008; Hallegraeff 2010).

La microscopie optique, souvent complémentaire à l'utilisation des pigments, est une technique relativement courante qui permet l'identification et le dénombrement des cellules phytoplanctoniques (Roy et al. 1996; Coupel et al. 2015a). Pendant de nombreuses années, la microscopie a été la seule méthode d'identification du phytoplancton. Pour les mesures de biomasse, les cellules d'algues étaient comptées et mesurées au microscope, et les volumes des cellules calculés en attribuant des formes géométriques simples aux cellules et convertis en carbone cellulaire à l'aide des rapports carbone/volume (Hillebrand et al. 1999). La microscopie peut produire une identification fiable des grosses cellules, mais les cellules pico- et nanophytoplanctoniques sont souvent négligées voir non identifiées. De plus, la

détermination de la biomasse carbonée des algues dépend à la fois de l'habileté du taxonomiste, mais également du nombre de cellules comptées et mesurées (Higgins et al. 2011).

En complément des approches pigmentaire et microscopique, d'autres méthodes existent pour caractériser la composition des communautés phytoplanctoniques, telles que le séquençage d'amplicons de gènes ARN ribosomique 16S (Needham & Fuhrman 2016) et 18S (Catlett et al. 2020), l'imagerie cellulaire quantitative (Dashkova et al. 2017), ou encore la cytométrie en flux (Sosik et al. 2010). Ces méthodes se différencient essentiellement par leur capacité à identifier taxonomiquement les cellules, leurs normes de standardisation, et leurs échelles d'observation (Tableau 2; Kramer et al. 2024). Cependant, quelle que soit la méthode employée, seule une fraction des cellules phytoplanctoniques est prise en compte, et la présence de cellules inconnues voire non identifiées représente également une proportion non négligeable (Kramer et al. 2024). Ainsi, aucune des méthodes citées ci-dessus ne permet une estimation parfaite de la composition phytoplanctonique, raison pour laquelle une caractérisation plus robuste pourrait être supportée par la combinaison de ces méthodes (Kramer et al. 2024).

Tableau 2. Résumé des caractéristiques de quatre méthodes d'évaluation de la composition des communautés phytoplanctoniques : les pigments par HPLC, le séquençage d'amplicons de gènes d'ARN ribosomique 16S et 18S, l'imagerie cellulaire quantitative et la cytométrie en flux (Adapté de Kramer et al. 2024). ASV : variant de séquence d'amplicon.

Méthode	**Pigments**	**Séquençage d'amplicons**	**Imagerie cellulaire quantitative**	**Cytométrie en flux**
Cellules	Eucaryotes et procaryotes	Eucaryotes (18S et 16S) et procaryotes (16S)	Eucaryotes et quelques procaryotes	Eucaryotes et procaryotes
Taille	> 0.3 µm	> 0.22 µm	~ 6 – 150 µm	~ 0.5 – 64 µm
Résolution taxonomique	Groupes	Classes à espèces	Classes à espèces	*Prochlorococcus* *Synechococcus* Nanoeucaryotes Picoeucaryotes
Mesure	Concentrations pigmentaires	Comptages ASV	Comptages cellulaires et biovolumes	Comptages cellulaires
Avantages	• Liens directs avec les propriétés optiques • Accessibilité des données • Méthode hautement standardisée • Résolution élevée pour les eucaryotes • Approches de normalisation en cours de développement	• Résolution élevée pour les eucaryotes et les procaryotes (18S et 16S) • Accessibilité des données (18S et 16S) • Approches de normalisation en cours de développement (18S et 16S)	• Biovolume plus facilement lié au carbone • Taxonomie au niveau cellulaire (détermination du gène ou du pigment par biovolume) • Possibilité d'identification taxonomique itérative	• Mesure au niveau cellulaire pour les procaryotes et quelques eucaryotes • Estimations du carbone possibles avec certaines hypothèses • Méthode hautement standardisée pour les groupes ciblés
Limites	• Variation inter- et intra-groupes des pigments • Impacts environnementaux sur la concentration • Résolution taxonomique limitée	• Nombre de copies de gènes différent d'un taxon à l'autre (18S) • Différences de méthode pouvant fausser les résultats (18S et 16S) • Attribution incomplète des ASVs (18S et 16S) • Pas de procaryotes photosynthétiques (18S) • Impossible d'identifier les dinoflagellés (16S)	• Forte proportion de cellules non-identifiées • Impossibilité de quantifier les petites cellules • Faible volume échantillonné qui peut exclure les cellules rares et de grande taille	• Forte proportion de cellules non-identifiées (eucaryotes) • Gamme de taille limitée • Très petit volume échantillonné • Pas d'indication précise de la forme et du biovolume

Notre étude a combiné l'utilisation de la cytométrie en flux, la chimiotaxonomie pigmentaire et la microscopie, permettant le comptage des petites cellules procaryotes et eucaryotes photosynthétiques, l'identification des différentes fractions de taille cellulaires et des principaux groupes phytoplanctoniques, ainsi qu'une résolution taxonomique élevée. Bien que la microscopie optique confirme généralement les résultats obtenus par les pigments, elle n'est pas en mesure d'identifier les petites cellules flagellées (< 5 µm), entraînant une sous-estimation de leur présence par rapport aux groupes de phytoplancton identifiés par l'analyse pigmentaire (Higgins et al. 2011). La microscopie fournit néanmoins des informations taxonomiques précieuses qui sont essentielles pour l'évaluation qualitative des résultats chimiotaxonomiques. Une certaine connaissance des communautés phytoplanctoniques de la zone échantillonnée est essentielle pour obtenir des résultats fiables des biomasses chlorophylliennes calculées (Wright et al. 1996; Henriksen et al. 2002). Les informations issues de la microscopie doivent être utilisées pour déterminer les principaux types d'algues à inclure dans les matrices CHEMTAX (*CHEMical TAXonomy*), un programme permettant de déterminer la contribution des groupes phytoplanctoniques à la biomasse chlorophyllienne totale (voir Ansotegui et al. 2003; Coupel et al. 2015a; Nemcek et al. 2023). Ainsi, des cellules algales avec différentes signatures pigmentaires peuvent être identifiées, par exemple les dinoflagellés dépourvus de péridinine (ex. Rodriguez et al. 2002; Irigoien et al. 2004), plusieurs sous-types différents d'haptophytes avec une teneur en pigments différente (Zapata et al. 2004; Ardyna et al. 2020; Wang et al. 2021) ou de prasinophytes (Latasa et al. 2004; Ardyna et al. 2020). Ces cellules peuvent sinon induire des erreurs dans les analyses chimiotaxonomiques. Les associations symbiotiques présentent un risque continu d'erreur d'identification complète si la microscopie est négligée. Les exemples incluent les cyanobactéries dans les diatomées (Hallegraeff & Jeffrey 1984), les diatomées dans les dinoflagellés (Takano et al. 2008) et les cryptophytes dans les ciliés (Llewellyn et al. 2005) ou dans les dinoflagellés (Hackett et al. 2003).

4. CARACTÉRISTIQUES DE LA BAIE JAMES

Située dans le nord du Québec, la baie James est le territoire traditionnel du peuple autochtone cri (Eeyou Istchee, qui signifie la terre du peuple en Eeyou/Eenou) (de Melo et al. 2022). Cette grande baie (67 000 km^2 ; El-Sabh & Koutitonsky 1977) s'étend sur les régions septentrionales de deux provinces canadiennes, l'Ontario et le Québec, et le territoire le plus au sud du Nunavut (Keller et al. 2014). Elle fait partie du vaste système de la baie d'Hudson qui chevauche la région arctique et subarctique du Canada (Estrada et al. 2012). Ce système comprend la baie d'Hudson, le détroit d'Hudson, le bassin Foxe et la baie James (El-Sabh & Koutitonsky 1977; Prinsenberg 1984), formant ensemble la plus grande mer intérieure polaire au monde (Keller et al. 2014). Bien que la baie James soit une région subarctique, elle connaît un cycle climatique et de glace de mer similaire aux plateformes continentales bordant l'océan Arctique (Hochheim & Barber 2010; Andrews et al. 2018). Malgré sa faible profondeur (moyenne de 60 m), la baie James joue un rôle important dans l'introduction d'eau douce dans l'ensemble du système de la baie d'Hudson (Déry et al. 2016). Il existe deux principales sources d'eau douce dans la baie James, soit la fonte des glaces de mer et le débit fluvial (Déry et al. 2011; Granskog et al. 2011).

Les eaux froides et salées de la baie d'Hudson pénètrent au nord-ouest de la baie James et y circulent de manière cyclonique pour ressortir le long de la côte est pour retourner dans la baie d'Hudson (Prinsenberg 1984). À mesure que les eaux circulent dans la baie James, elles se réchauffent *via* l'ajout d'eau douce provenant de grandes rivières, entraînant également une diminution de la salinité des eaux de surface (Prinsenberg 1984). Par conséquent, la moitié est de la baie James est plutôt caractérisée par des eaux relativement chaudes de plus faible salinité, comparativement à la moitié ouest (El-Sabh & Koutitonsky 1977). Cela s'explique également par le débit fluvial important de La Grande Rivière, considérée comme l'une des plus grandes rivières se déversant dans le système de la baie d'Hudson, contribuant à elle seule à plus de 16% de l'apport annuel total de débit mesuré dans la baie d'Hudson (Hernández-Henríquez et al. 2010). En plus d'influencer la température et la salinité, les apports fluviaux affectent également la turbidité, qui à leur tour

ont des implications majeures sur le fonctionnement et la productivité des eaux côtières (de Melo et al. 2022). En effet, les rivières représentent les principaux vecteurs de matière dissoute et particulaire (Cole et al. 2007; Battin et al. 2008), notamment la CDOM et la matière particulaire en suspension (SPM), composantes importantes dans les eaux de la baie James (Mabit et al. 2022). Ces dernières modifient la disponibilité de la lumière dans la colonne d'eau, si bien qu'elles affectent la photosynthèse et donc la production primaire (Mabit et al. 2022). De plus, la baie James est considérée comme un point chaud de l'exportation fluviale de carbone organique dissous vers les mers septentrionales, en raison des forts rendements annuels en eau douce (c'est-à-dire le rapport entre le taux de ruissellement annuel d'une rivière et la superficie du bassin versant) (Mundy et al. 2010; de Melo et al. 2022).

La baie James, et plus largement le système de la baie d'Hudson, est confronté à un rythme de changement environnemental beaucoup plus rapide que d'autres régions de l'Arctique (Gagnon & Gough 2005; Keller et al. 2014), notamment en raison de sa proximité avec les systèmes terrestres (Westmacott & Burn 1997; Gough & Wolfe 2001; Gagnon & Gough 2005; Kuzyk et al. 2010). En effet, au cours des dernières décennies, les conditions climatiques froides et relativement stables typiques de la région ont cédé la place à une nette tendance au réchauffement (Gagnon & Gough 2005; Hochheim & Barber 2010; Bhiry et al. 2011). Les modifications des régions de hautes latitudes, comme la baie James, sont entraînées par l'augmentation des températures de l'air en surface (Chapman & Walsh 1993), comprenant une augmentation de la température des eaux de surface (Galbraith & Larouche 2011), une diminution de l'épaisseur et de l'étendue des glaces de mer (Stroeve & Notz 2018), une diminution de l'épaisseur et de la durée de la couverture nivale (Brown & Braaten 1998; Curtis et al. 1998), un réchauffement et un dégel du pergélisol (Osterkamp & Romanovsky 1996; Stieglitz et al. 2003), ainsi que l'augmentation des tempêtes et des précipitations (Walsh 2000; McCabe et al. 2001). De tels changements dans les milieux de hautes latitudes affectent tous le débit d'eau douce de manière complexe. Cependant, des observations récentes suggèrent une accélération du cycle hydrologique dans de nombreuses régions du Nord, y compris une augmentation du débit d'eau douce (Peterson et al. 2002;

Ziegler et al. 2003), et une réduction de la saisonnalité du débit des cours d'eau (Wang et al. 2024) en réponse au réchauffement climatique (Clair et al. 1998; Brown 2010), avec des implications majeures pour la production primaire (Hopwood et al. 2020).

En plus d'être exposée aux changements climatiques, la baie James est soumise à des modifications anthropiques. En effet, au début des années 1970, le gouvernement du Québec et Hydro-Québec ont mis en œuvre le développement de grands complexes hydroélectriques dans le centre et le nord du Québec (Warner 1999). Dans le cadre de ce projet, plusieurs rivières de l'est de la baie James ont été affectées (par endiguement ou dérivation), entraînant par conséquent des modifications de débit (Roy & Messier 1989; Déry et al. 2016). C'est le cas en particulier de La Grande Rivière, qui possède une série de barrages et de grands réservoirs, et pour laquelle le débit annuel moyen a plus que doublé depuis la mise en place de ces infrastructures en 1980 (de 1 700 en 1980 à 3 780 $m^3 s^{-1}$ en 2019; de Melo et al. 2022). La construction du complexe La Grande a nécessité la dérivation de plusieurs rivières régionales, telles que les rivières Eastmain, Opinaca, Rupert et Sakami au sud, et les rivières Caniapiscau et Grande rivière de la Baleine au nord (Messier et al. 1986; Déry et al. 2016). Le détournement de ces rivières a conduit à une diminution de leur débit, comme c'est le cas des rivières Eastmain (de 910 en 1978 à 65 $m^3 s^{-1}$ en 2019) et Rupert (de 845 en 2009 à 395 $m^3 s^{-1}$ en 2019) (de Melo et al. 2022). Cela induit par conséquent des changements physico-chimiques, comme Messier et al. (1986) l'ont rapporté avec des augmentations de salinité dans les eaux de la rivière Eastmain, après que 90% de son débit ait été détourné vers La Grande Rivière en 1980 (Déry et al. 2011).

5. OBJECTIFS

Cette étude, qui s'inscrit dans le cadre du projet sur l'océanographie des eaux côtières de l'est de la baie James (COast-JB), a pour objectif principal de documenter la structure spatiale des communautés phytoplanctoniques le long de la côte est de la baie James au début et à la fin de l'été. Les objectifs spécifiques sont de (i) caractériser les changements de la

composition taxonomique de ces communautés en utilisant des approches microscopique, cytométrique et pigmentaire, (ii) identifier les facteurs abiotiques et biotiques à l'origine des variations spatio-temporelles de ces communautés pendant l'été, et (iii) documenter le potentiel de photoacclimatation des communautés phytoplanctoniques en utilisant la signature pigmentaire.

ENVIRONMENTAL DRIVERS OF SUMMER PHYTOPLANKTON COMMUNITY STRUCTURE IN A SUBARCTIC NEARSHORE ECOSYSTEM INFLUENCED BY RIVER INPUTS

1.1 INTRODUCTION

Marine phytoplankton exhibit a high degree of diversity that varies between and within taxonomic groups (Otero et al. 2020). This diversity, which can be metabolic or morphological, is a critical factor influencing the overall structure and dynamics of marine ecosystems (Naeem et al. 2012) and leads to different biogeochemical functions (Van Oostende et al. 2017). The function of pelagic ecosystems is influenced by environmental gradients, and the diversity of phytoplankton within these communities determines their ability to survive along these gradients (Irwin & Finkel 2018; Otero et al. 2020). Both biotic and abiotic factors influence phytoplankton biodiversity (Sarker et al. 2018). The composition of phytoplankton communities changes in response to seasonal variations, with species abundances being affected by light conditions, temperature, nutrient inputs and the presence of consumers (Wiltshire et al. 2015). Phytoplankton have adapted to grow under different light (low to high) and nutrient (oligotrophic to mesotrophic) regimes that exist in the ocean (Van Oostende et al. 2017).

The size structure of phytoplankton assemblages is also characteristic of their environment (Van Oostende et al. 2017). Indeed, phytoplankton size is associated with physiological traits such as growth, photosynthetic and respiration rates, light-absorptive properties (Finkel 2001; Hernando et al. 2015), and nutrient uptake rates and requirements (Hein et al. 1995; Hernando et al. 2015). Low concentrations (< 1 mg m^{-3}) of chlorophyll *a* (Chl *a*), an indicator of phytoplankton biomass, are generally observed in environments with low nutrient supply (Van Oostende et al. 2017). Small cells like pico- and nanophytoplankton

(< 20 µm), which make up the main part of total Chl *a*, are therefore prevalent in these environments (Raimbault 1988; Chisholm 1992; Marañón et al. 2012; Van Oostende et al. 2017).

Coastal environments are highly productive areas compared to the open ocean (Kuzyk et al. 2010). They are areas where marine and freshwater biomes meet and interact, creating unique ecosystems with physico-chemical gradients that depend on hydrodynamic processes (e.g., currents, waves, tides) and rivers inputs (e.g., suspended particulate matter (SPM), colored dissolved organic matter (CDOM), nutrients; Jacquemot et al. 2021). SPM and CDOM inputs from rivers can limit the light availability for phytoplankton growth in coastal environments (Uncles et al. 2002; Domingues et al. 2012; Burchard et al. 2018), whereas riverine nutrient inputs can enhance their production (Ferland et al. 2011; Lee et al. 2023). In Arctic and sub-Arctic environment, river runoff has been shown to influence the growth conditions of primary producers and their taxonomic composition (Ingram et al. 1985; Jacquemot et al. 2021; Nozais et al. 2021; Leblanc et al. 2022).

Information on the distribution of the main phytoplankton groups is crucial to improving our understanding of their role in marine ecosystems and biogeochemical cycles (Bracher et al. 2017). In contrast to other subarctic and temperate environments, few studies have been conducted in James Bay coastal waters (Bazin et al. 2014; Keller et al. 2014). Since the late 1970s, the development of large hydroelectric complexes in James Bay has led to anthropogenic modifications that have changed the flow of some rivers due to damming or deviation (Roy & Messier 1989; Déry et al. 2016). In particular, the La Grande River complex required the diversion of several regional rivers, such as the Eastmain, Opinaca, Rupert and Sakami rivers to the south, and the Caniapiscau and Great Whale rivers to the north (Roy & Messier 1989; Déry et al. 2016). The diversion of these rivers has decreased their flow, as in the case of the Eastmain (from 910 $m^3 s^{-1}$ in 1978 to 65 $m^3 s^{-1}$ in 2019) and Rupert (from 845 $m^3 s^{-1}$ in 2009 to 395 $m^3 s^{-1}$ in 2019) rivers, while increasing the annual flow of the La Grande River (from 1,700 $m^3 s^{-1}$ in 1980 to 3,780 $m^3 s^{-1}$ in 2019) (de Melo et al. 2022). In addition, this region is becoming warmer: the average summer air temperature

at the La Grande Rivière Airport, approximately 90 km east of the coast, increased by 1.56°C between 1982 and 2020 (Leblanc et al. 2022).

Historically, few scientific studies have been carried out in James Bay, with significant data collection having begun to accumulate in the 1970s (Prinsenberg 1984). The only studies of the taxonomic composition of eukaryotic phytoplankton in James Bay were conducted by Foy & Hsiao (1976), Legendre & Simard (1978), Ingram et al. (1985) and De Sève (1993), and focused on diatom communities. In addition, the available data for the region are sparse both spatially and temporally. As a result, little information is available on the variability of current phytoplankton communities along the entire coast of James Bay and the factors that may influence their distribution.

The main objectives of this study, part of the Coastal Oceanography of eastern James Bay (COast-JB) project, is to document the structure of phytoplankton communities along the east coast of James Bay in early and late summer. The specific objectives are to (i) characterize changes in the composition of these communities using microscopic, cytometry and pigmentary approaches, (ii) identify the abiotic and biotic factors responsible for spatio-temporal variations in the communities during both summer period, and (iii) document the photoacclimation potential of phytoplankton communities using pigment signatures.

Microscopy, chemotaxonomy and flow cytometry are complementary methods for identifying phytoplankton composition. Microscopy is a commonly used approach that accurately identifies cells > 2 µm with a low taxonomic rank (i.e., at the genus or species levels). However, this technique is complex for small flagellated cells, which may dominate phytoplankton biomass in oligotrophic systems. Chemotaxonomy, on the other hand, allows the identification of major phytoplankton groups but at lower taxonomic resolution (i.e., class level) (Kramer et al. 2024). Finally, flow cytometry, although having a low taxonomic resolution, can quantify the abundance of pico- and nanophytoplankton, and distinguish PC- and PE-cyanobacteria. Therefore, by combining these three methods, it is possible to identify the main phytoplankton groups with greater certainty (see Ansotegui et al. 2003; Irigoien et al. 2004; Brito et al. 2015). This combination of methods provides a good understanding of

the phytoplankton communities present in the study area, which is essential to obtain accurate results of the calculated biomasses (Wright et al. 1996; Henriksen et al. 2002; Kramer et al. 2024).

1.2 METHODOLOGY

1.2.1 Study site

James Bay, spanning an area of 67,000 km^2, is situated at the southern extremity of the Hudson Bay system in subarctic Canada (Figure 1; El-Sabh & Koutitonsky 1977). The Hudson Bay system, which includes Hudson Bay, Hudson Strait, Foxe Basin and James Bay, collectively forms the world's largest polar inland sea (Prinsenberg 1984; Keller et al. 2014). Although shallow, with an average depth of 60 m, James Bay plays a crucial role in supplying freshwater to the entire Hudson Bay system and northern seas (Mundy et al. 2010; Déry et al. 2016; Meilleur et al. 2023). The cold, salty surface waters of Hudson Bay enter northwestern James Bay, circulate there cyclonically, and emerge along the east coast into Hudson Bay (Prinsenberg 1984). As the waters circulate through James Bay, they are warmed up by the addition of freshwater from large rivers, also leading to a decrease in surface water salinity (Prinsenberg 1984). River inputs affect not only the temperature and salinity of James Bay, but also its turbidity and color due to its high concentrations of SPM and CDOM (Mabit et al. 2022).

1.2.2 Sampling

Sampling was carried out aboard freighter canoes guided by Cree land users along the east coast of James Bay (between 52.03° and 54.12°N) from early to mid-summer (3 July to 16 August 2019) and mid-summer (1 to 18 August 2018) (Figure 1). For simplicity, these two sampling periods are hereafter referred to as early and late summer. In total, 114 and 68

stations were visited during early and late summers, respectively. At each station, a vertical profile of water temperature and salinity was obtained with a conductivity, temperature, depth (CTD) probe (Sea-Bird SBE 19plus V2 or SonTek CastAway). A 30 cm diameter Secchi disk was also used to determine water transparency (Kirk 2011).

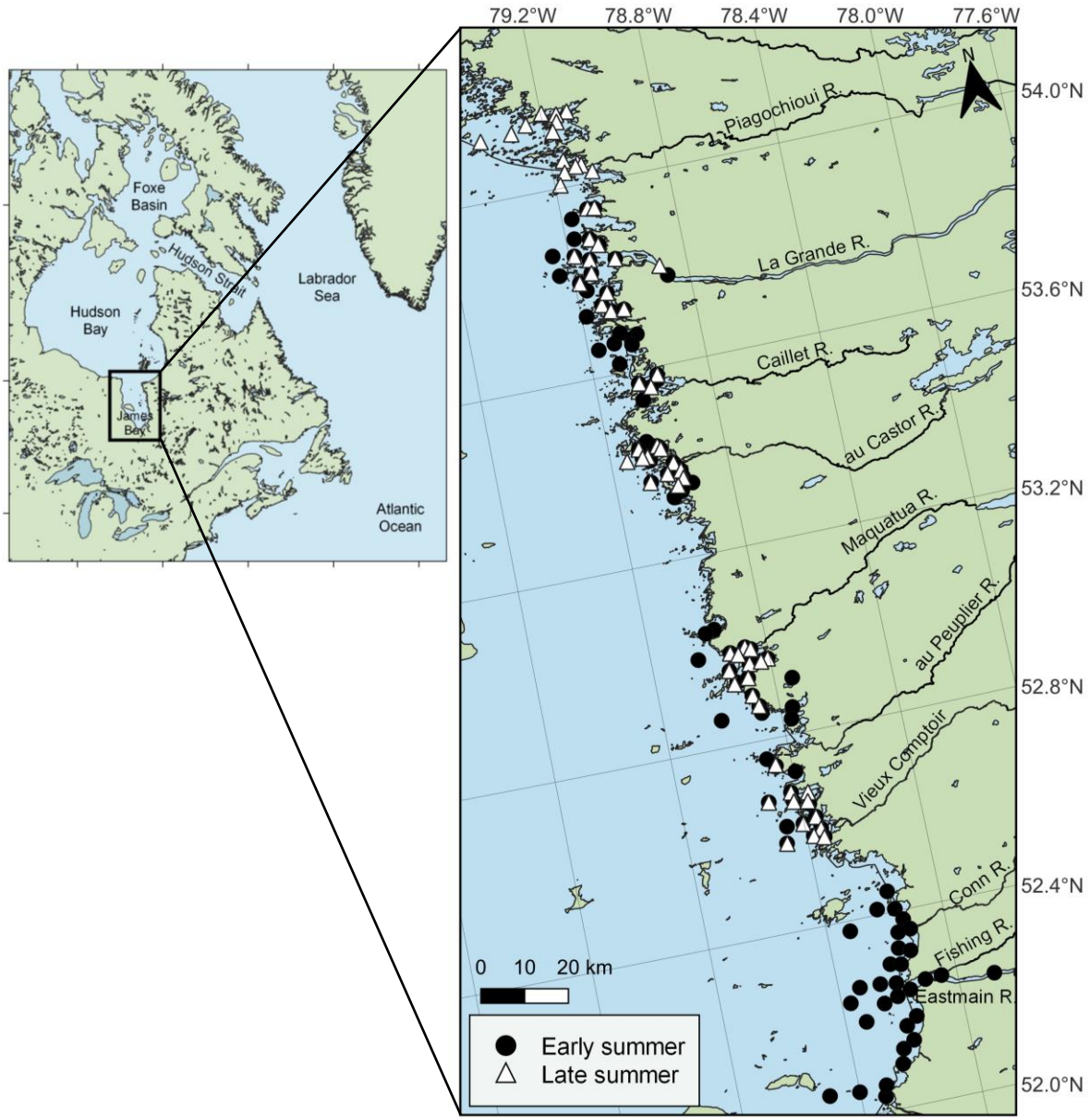

Figure 1. Location of sampling stations along the east coast of James Bay during early (2019) and late (2018) summer.

Water samples were collected from the surface (0.5 m) using a 5 L Niskin bottle. CDOM samples were transferred from the Niskin bottle into 120 mL borosilicate glass bottles with Teflon-lined caps and filtered in a land-based laboratory (see section 1.2.3). DOC and nutrient samples were transferred into polypropylene sterile specimen containers and filtered aboard the freighter canoe (see section 1.2.3). The chemical samples were stored in the dark at 4°C.

The remaining water samples for SPM, pigments, and phytoplankton abundance determination were stored in an acid washed Coleman cooler (20 L) for processing at the land-based laboratory.

1.2.3 Chemical analysis

The CDOM samples were filtered through Nanopure water-rinsed 0.2 µm Supor®polyethersulfone membranes (Pall Laboratory) under low vacuum conditions within hours of collection in a land-based laboratory. After filtration, the samples were collected into 60 mL clear borosilicate glass bottles with Teflon-lined caps and stored in the dark at 4°C until analysis within one month of sample collection at the Université du Québec à Rimouski (UQAR). The absorption coefficient of CDOM at 440 nm ($a_{CDOM}(440)$) was measured using a Perkin-Elmer Lambda-35 spectrophotometer (dual beam UV-visible) according to the method described by Évrard et al. (2023). This wavelength was chosen to indicate CDOM abundance: 440 nm being the optimal wavelength for to retrieve a_{CDOM} from space in Quebec's coastal waters, including the eastern James Bay (Mabit et al. 2022).

The DOC and nutrient samples were filtered through a pre-combusted (450°C for 5 h) 25 mm Whatman GF/F filter aboard the freighter canoe. The DOC samples were acidified with 2 N HCl and stored at 4°C in the dark, until analysis at UQAR with a Shimadzu TOC-V_{CPN} analyzer, as described in Évrard et al. (2023). Nutrient samples, namely nitrate plus nitrite ($NO_3 + NO_2$), phosphate (PO_4), and silicic acid ($Si(OH)_4$), were frozen at –80°C until

analysis at UQAR using a Bran-Luebbe 3 nutrient autoanalyzer (adapted method from Grasshoff et al. 1999). SPM samples were filtered through a pre-weight and pre-combusted 48 mm Whatman GF/F filter and dried at 75°C for 24 h at the land-based laboratory following the protocol of Neukermans et al. (2012). Filters were redried and reweighed on the Mettler Toledo MX5 microbalance at UQAR.

1.2.4 Light microscopy and flow cytometry

During late summer, samples for the identification and enumeration of filamentous cyanobacteria and protist cells > 2 µm were collected in 250 mL glass bottles and preserved in acidic Lugol's solution (Parsons et al. 1984). The bottles were stored in the dark at 4°C until analysis. Cells were identified to the lowest possible taxonomic rank using an inverted microscope (Zeiss Axiovert 10) according to Utermöhl (1958). For each 25 mL settling chamber, at least 400 cells (accuracy ± 10%) were counted (Lund et al. 1958) over a minimum of three transects of 20 mm at a magnification of 400×. The main taxonomic references used to identify the protist cells were Bourrelly (1970), Tomas (1997), Bérard-Therriault et al. (1999), Joosten (2006), Throndsen et al. (2007), Komárek & Anagnostidis (2008), John et al. (2011) and Komárek (2013).

In early and late summer, the abundance of pico- (0.2 – 2 µm) and nano- (2 – 20 µm) photosynthetic prokaryotes (PC- and PE-cyanobacteria) and eukaryotes was determined on 5 mL subsamples (in duplicate) fixed with 20 µL of 25% glutaraldehyde (Grade I, Sigma-Aldrich G5882). Samples were stored and kept frozen at −80°C for later analysis using a CytoFLEX flow cytometer (Beckman Coulter Inc.) equipped with a blue (488 nm) and a red (638 nm) laser (Araújo et al. 2022). The results were analyzed with CytExert v2.3 software (Beckman Coulter).

1.2.5 HPLC pigments

Phytoplankton pigment identification (photosynthetic, photoprotective, and degradation pigments) and concentration were determined in early and late summer by reverse-phase high-performance liquid chromatography (HPLC). Samples were filtered through 48 mm Whatman GF/F filters and stored immediately at −80°C. The retained pigments were extracted in 95% methanol and extracts were filtered through 0.22 µm polytetrafluoroethylene membrane filters. Pigments were analyzed with an Agilent Technologies 1200 Series system with a Symmetry C8 column (150 × 4.6 mm, 3.5 µm particle size; Waters Corporation). The pigments were separated as described in Zapata et al. (2000). Then, marker pigments were identified by comparing the retention time and spectral properties of external pigment standards. The limits of detection and quantification were estimated and pigments with concentrations below the limit of detection were not reported. A pigment-based index of diversity (Shannon diversity index (H')) was calculated using the formula:

$$H' = -\Sigma ((n_i / n) \times \ln(n_i / n))$$

where n is the total concentration of photosynthetic and photoprotective pigments (Chl *a* excluded; Table S1) and n_i is the concentration of each pigment.

1.2.6 Chemotaxonomy

The CHEMTAX (CHEMical TAXonomy) software (Mackey et al. 1996, version 1.95 used in Wright et al. 2009; Wright 2017) was used to determine the contribution of major algal classes to total chlorophyll *a* (TChl *a* = chlorophyll *a* + chlorophyllide *a*). At the same time, a confirmation of the microscopic analysis was performed for late summer. CHEMTAX was used separately for each year. Initial pigment ratio matrix (Table 1) was based on previous CHEMTAX analyses from polar water studies (Higgins et al. 2011; Coupel et al.

2015a; Matthes et al. 2021). The initial matrix (F0) was optimized by generating a series of 60 variants of F0, calculated using the random function:

$$F = 1 + S \times (R - 0.5)$$

where S is the scaling factor (typically 0.7), and R is a random number between 0 and 1 (generated using the RAND function in Microsoft Excel) (Wright et al. 2009). The average of the six best output matrices (equivalent to 10% of the total matrix corresponding to the smallest root mean square (RMS)) was calculated and used as the new input matrix. A new series of 60 variants of the new input matrix was generated with S = 0.3 to reduce the standard deviation of the results, as recommended by Latasa (2007). The results of the six best output matrices were used as the optimized output to calculate the means of the final relative biomass estimates and pigment ratios (Table 2).

Table 1. Initial matrix of ratios of accessory pigment to total chlorophyll *a* (TChl *a*) for different phytoplankton classes. Ratios were determined from [a] Higgins et al. (2011), [b] Coupel et al. (2015a) and [c] Matthes et al. (2021). Chl *b*: chlorophyll *b*; Chl c_2: chlorophyll c_2; Chl c_3: chlorophyll c_3; Allo: alloxanthin; Fuco: fucoxanthin; Neo: neoxanthin; Peri: peridinin; Pras: prasinoxanthin; Lut: lutein; Zea: zeaxanthin, TChl *a*: total chlorophyll *a*, Diato-I and Diato-II: Diatoms under low and high light levels, respectively, Chloro: chlorophytes, Crypto: cryptophytes, Cyano: cyanobacteria, including freshwater and marine colonial forms and marine coccoid planktonic species (e.g., *Synechoccocus*), Dino-1: dinoflagellates type 1 (containing peridinin), Prasino-2: prasinophytes type 2, including nanoplanktonic species (e.g., *Pyramimonas*), Prasino-3: prasinophytes type 3, including picoplanktonic species (e.g., *Micromonas*).

	Chl *b*	Chl c_2	Chl c_3	Allo	Fuco	Neo	Peri	Pras	Lut	Zea	TChl *a*
Diato-I [a, c]	-	0.174	0.066	-	0.590	-	-	-	-	-	1
Diato-II [a]	-	0.310	0.089	-	0.498	-	-	-	-	-	1
Chloro [a]	0.339	-	-	-	-	0.036	-	-	0.187	0.047	1
Crypto [c]	-	-	-	0.256	-	-	-	-	-	-	1
Cyano [a]	-	-	-	-	-	-	-	-	-	0.227	1
Dino-1 [b]	-	-	-	-	-	-	0.600	-	-	-	1
Prasino-2 [b]	0.786	-	-	-	-	0.056	-	-	0.038	-	1
Prasino-3 [b]	0.953	-	-	-	-	-	-	0.241	0.008	-	1

Table 2. Optimized final matrix of ratios of accessory pigment to total chlorophyll *a* (TChl *a*) for different phytoplankton classes during early and late summer. RMS = root mean square. Abbreviations are defined in Table 1.

	Chl *b*	Chl c_2	Chl c_3	Allo	Fuco	Neo	Peri	Pras	Lut	Zea	TChl *a*
Early summer (RMS = 0.044)											
Diato-I	-	0.012	0.005	-	0.542	-	-	-	-	-	1
Diato-II	-	0.456	0.011	-	0.577	-	-	-	-	-	1
Chloro	0.275	-	-	-	-	0.031	-	-	0.225	0.043	1
Crypto	-	-	-	0.284	-	-	-	-	-	-	1
Cyano	-	-	-	-	-	-	-	-	-	0.216	1
Dino-1	-	-	-	-	-	-	0.811	-	-	-	1
Prasino-2	0.891	-	-	-	-	0.153	-	-	0.047	-	1
Prasino-3	0.572	-	-	-	-	-	-	0.448	0.008	-	1
Late summer (RMS = 0.050)											
Diato-I	-	0.019	0.014	-	0.700	-	-	-	-	-	1
Diato-II	-	0.492	0.066	-	0.376	-	-	-	-	-	1
Chloro	0.321	-	-	-	-	0.037	-	-	0.153	0.049	1
Crypto	-	-	-	0.303	-	-	-	-	-	-	1
Cyano	-	-	-	-	-	-	-	-	-	0.326	1
Dino-1	-	-	-	-	-	-	0.638	-	-	-	1
Prasino-2	0.758	-	-	-	-	0.169	-	-	0.043	-	1
Prasino-3	0.681	-	-	-	-	-	-	0.464	0.008	-	1

1.2.7 Statistical analysis

A limited number of environmental data was missing from the database. To facilitate the statistical analysis, some values have been substituted for missing data. As $a_{CDOM}(440)$ was highly correlated with DOC concentration in the eastern James Bay (see Fig. 7 of Évrard et al. (2023)), the missing $a_{CDOM}(440)$ values for stations C34-03 and C1-27 (in 2019) were determined from DOC by a Pearson linear regression. Missing nutrients values (NO_3 + NO_2, PO_4 and $Si(OH)_4$) for station C1-05 (in 2018) were obtained by averaging values obtained at stations C1-01, C1-08, C1-06, C1-07 and C1-10, all of which are located in the La Grande River plume with similar salinity values.

For statistical analysis, only the most abundant phytoplankton classes obtained by microscopy were selected: cryptophytes (crypto), diatoms (diato-I and diato-II), prasinophytes (prasino-2 and prasino-3), dinoflagellates (dino-1), and cyanobacteria (cyano), which made up at least 70% of the total phytoplankton abundance. Chlorophytes (chloro) were also considered, despite their low contribution (< 15%) to the total abundance, as they share many pigments with prasinophytes. This step helped to prevent the overestimation of prasinophytes. All pigments identified were kept for statistical analysis (using the software R; RStudioTeam 2021), but those that were absent in more than 20% of the stations were removed. Afterwards, each pigment concentration was divided by the TChl *a*. Finally, these data were square-root transformed to decrease the range between extreme values (Clarke & Warwick 2001).

A non-metric multidimensional scaling (NMDS) into 2-D representation was carried out using a Bray-Curtis similarity matrix to better visualize similarities between stations (Clarke 1993). Associated with this ordination, a group-average clustering was also performed to identify groups of samples with similar taxonomic composition (Clarke & Warwick 2001). Similarity analysis (ANOSIM) was also applied to the Bray-Curtis similarity matrix to identify groups of stations with significant differences in taxonomic composition (Clarke 1993).

As the data did not meet the conditions for a parametric test (i.e., normality of distribution and homogeneity of variance), a Kruskal-Wallis one-way analysis of variance by ranks was performed for each environmental variable to seek significant differences among the groups of stations identified by the clustering analysis. If any significant differences were found, a post-hoc multiple comparison test (Dunn's test) was applied.

A redundancy analysis (RDA) was carried out to estimate the interactions between the major taxonomic groups and environmental variables. The relative contribution of each phytoplankton class to TChl *a* was used to perform the analysis. Each environmental variable was standardized (i.e., the mean value was subtracted and divided by the standard deviation) because of the different units among variables (Legendre & Legendre 2012). Spearman correlations between each variable were carried out to determine potential collinearity (Figure S1), and the significant environmental variables best explaining the interactions were selected.

1.3 RESULTS AND DISCUSSION

During this study, sampling was carried out along the shoreline of the eastern James Bay. Surface water samples were collected from Loon Point, south of Eastmain River, to Paul Bay, north of La Grande River, during early summer, and from Conn River, south of Vieux Comptoir River, to Attikuan Point, north of Piagochioui River, during late summer (Figure 1). Microscopic, cytometric and pigment approaches were combined to determine the composition of major phytoplankton classes. The stations were then grouped according to the similarity of the phytoplankton composition in order to identify the different environmental variables that characterize the different ecological niches along the coast.

1.3.1 Identification of taxonomic groups

1.3.1.1 Light microscopy

The accuracy of the results obtained with CHEMTAX depends on accurate pigment analysis, a good knowledge of the phytoplankton composition of the study area, and appropriate pigment ratios (Mackey et al. 1996; Irigoien et al. 2004; Nemcek et al. 2023). The most abundant taxa > 2 µm along the east coast of James Bay in late summer 2018 were Cryptophyceae (5 – 20 µm), the centric diatom *Skeletonema* cf. *costatum*-like species, the cryptophyte *Hemiselmis* spp., the prasinophyte *Pyramominas* spp. (5 – 10 µm) and the thecate dinoflagellate *Heterocapsa rotundata*. All these taxa were present in at least 89% of the collected samples (Table S2). It is interesting to note the very low abundance of prymnesiophytes (< 2% of total cells counted), a phytoplankton class that is generally abundant in other sub-Arctic and Arctic marine environment such as the Estuary and Gulf of St. Lawrence (Roy et al. 2008), the Hudson Bay (Jacquemot et al. 2021), the Labrador fjords (particularly *Chrysochromulina* spp. and *Phaeocystis pouchetii*, Simo-Matchim et al. 2017), and the Beaufort Sea (Balzano et al. 2012; Coupel et al. 2015a). Since the presence of prymnesiophytes was not reported in previous studies of phytoplankton composition in James Bay between 1974 and 1993 (Foy & Hsiao 1976; Legendre & Simard 1978; Ingram et al. 1985; De Sève 1993), this may indicate that they were not abundant relative to other taxa.

The dominance of cryptophytes along the James Bay coast may be explained in part by the light spectrum of the water column. Indeed, James Bay is characterized by turbid, CDOM-rich waters (Mabit et al. 2022) that absorb and scatter light. In these turbid/colored waters, the irradiance spectrum is dominated by red wavelengths due to the preferential absorption of violet and blue wavelengths by compounds such as tannins, humic acids, or other macromolecules that make up the CDOM pool (Blough & Del Vecchio 2002; Lawrenz et al. 2010). Because cryptophytes possess phycobiliproteins (phycoerythrin, phycocyanin

and allophycocyanin) with absorption maxima at red wavelengths (Roy et al. 2011; Richardson 2022), they have a competitive advantage over other eukaryotic phytoplankton.

Filamentous cyanobacteria, which are photosynthetic prokaryotes, were also observed along the coast at 17 of 28 stations sampled during late summer (Table S2). This phylum was also detected in the La Grande and Eastmain river plumes in September 1974 (Foy & Hsiao 1976). As cryptophytes, they possess phycobiliproteins and other pigments that give them a competitive advantage in fresh and low-salinity waters that are rich in CDOM. In the present study, 93 genera and 105 species were identified, diatoms were the largest group with 35 genera and 35 species (Table S2). In September 1974, 92 genera and 202 species were observed, of which 53 genera and 179 species were diatoms (Foy & Hsiao 1976). In the future, phytoplankton diversity in James Bay should be compared to other subarctic coastal environments using current molecular tools.

Some of the algal taxa identified in this study are known to be potentially toxic or harmful. These include the dinoflagellates *Amphidinium* spp., *Gymnodinium*/*Gyrodinium* spp., *Dinophysis acuminata*, *Dinophysis* spp., *Heterocapsa* spp., *Prorocentrum* spp. and *Scrippsiella* spp., the diatoms *Leptocylindrus minimus* and *Skeletonema costatum*; the cyanobacteria *Anabaena* spp., *Dolichospermum* spp., *Lyngbya* spp. and *Oscillatoria* spp., the prymnesiophytes *Chrysochromulina* spp. and *Phaeocystis pouchetti*, the chrysophytes *Mallomonas* spp.; and the photosynthetic ciliate *Mesodinium rubrum* (Table S2). All these taxa had an average occurrence of 27% (range: 4 – 96%), but a major part of the taxa (68%) had an occurrence < 22%, and the other portion (32%) had an occurrence > 42% Taxa with higher occurrence were *Chrysochromulina* spp. (96%), *Skeletonema costatum* (96%) and *Gymnodinium*/*Gyrodinium* spp. (71%). Some of these taxa have been previously observed in the La Grande and Eastmain rivers, in particularly *Anabaena* spp., and *Dinophysis acuminata*, although they were present at very low abundances (Foy & Hsiao 1976). In addition, Legendre & Simard (1978) mentioned the presence of the filamentous cyanobacteria *Oscillatoria* spp. in Rupert Bay. However, none of these harmful algae were numerous (Table S2).

1.3.1.2 Flow cytometry

Since microscopic identification of taxa was done on a limited number of water samples and included only cells > 2 µm, flow cytometric analyses were performed on all collected samples to determine the abundance of photosynthetic eukaryotic and procaryotic cells between 0.2 and 2 µm (i.e., picophytoplankton). Cells between 2 and 20 µm (i.e., nanophytoplankton) were also counted by flow cytometry for comparison. In contrast to photosynthetic eukaryotes and PC-cyanobacteria, which were ubiquitous along the coast, PE-cyanobacteria were detected at only a few stations during early (8 out of 114 stations; range: $0.14 – 11.4 \times 10^6$ cells L^{-1}) and late (14 out of 68 stations; range: $0.11 – 6.2 \times 10^6$ cells L^{-1}) summer. The highest abundances were observed near au Castor River in early summer and near au Castor and Maquatua rivers in late summer. The dominance of PC-cyanobacteria over PE-cyanobacteria was also observed by Callieri (2008) in shallow, turbid freshwaters.

Photosynthetic picoeukaryotes were more abundant than photosynthetic nanoeukaryotes during early ($20.1 \pm 31.9 \times 10^6$ cells L^{-1} *vs.* $6.5 \pm 5.9 \times 10^6$ cells L^{-1}) and late ($18.3 \pm 18.6 \times 10^6$ cells L^{-1} *vs.* $5.4 \pm 3.6 \times 10^6$ cells L^{-1}) summer. Similar to eukaryotes, the abundance of picocyanobacteria was much higher than that of nanocyanobacteria during early ($6.0 \pm 14.0 \times 10^6$ cells L^{-1} *vs.* $0.27 \pm 0.60 \times 10^6$ cells L^{-1}) and late ($21.2 \pm 45.1 \times 10^6$ cells L^{-1} *vs.* $0.36 \pm 0.32 \times 10^6$ cells L^{-1}) summer. Pico-sized eukaryotes and cyanobacteria are up to 3 and 59 times more abundant than cells 2 – 20 µm, respectively. The predominance of picophytoplankton over larger cells is also observed in other coastal environments (Tremblay et al. 2009; Nemcek et al. 2023).

1.3.1.3 Pigment biomarkers

A regression analysis was performed to test the relationship between pigment biomarkers and the abundance of some phytoplankton classes (Figure 2). Peridinin, an excellent marker for tracing dinoflagellates type 2 (Roy et al. 2011), correlated very well with dinoflagellate counts ($r^2 = 0.94$, Figure 2A). Most of the dinoflagellate species identified

in this study contain peridinin, as in the case of *Heterocapsa rotundata* (Coupel et al. 2015a; Nemcek et al. 2023). It was the most abundant dinoflagellate species (10% of the total abundance across all samples). *Gyrodinium* and *Gymnodinium*, which do not possess peridinin, were not abundant (< 1% of total phytoplankton cells > 2 µm). The major pigment in these genera is fucoxanthin (Roy et al. 1996; Coupel et al. 2015a). In addition, few heterotrophic dinoflagellates (e.g., *Amphidinium sphenoides* and *Protoperidinium bipes*) were counted (< 1%), and most dinoflagellates having pigments are mixotrophic (Millette et al. 2017).

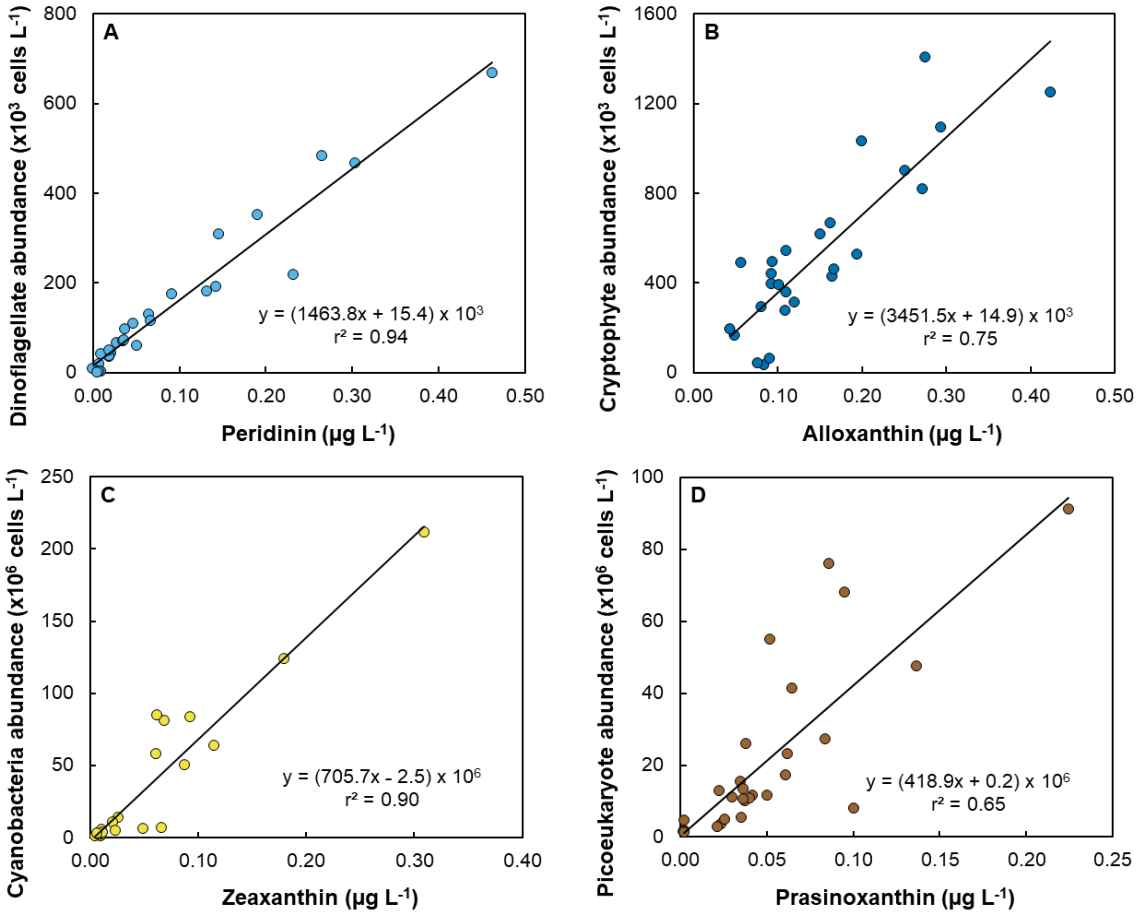

Figure 2. Relationship between **(A)** total dinoflagellate abundance and peridinin concentration, **(B)** cryptophyte abundance and alloxanthin concentration, **(C)** total cyanobacteria abundance and zeaxanthin concentration, and **(D)** picoeukaryote abundance and prasinoxanthin concentration. The data is from the late summer. The linear regression line is shown.

Alloxanthin, zeaxanthin and prasinoxanthin were also correlated with cryptophytes, cyanobacteria and picoeukaryote abundances, respectively ($r^2 > 0.65$, Figure 2B-D). These results suggest that the following three pigments are suitable for determining the abundance of cryptophytes, cyanobacteria, and prasinophytes type-3 (e.g., the picoeukaryote *Micromonas*). Since prasinoxanthin is only present in prasinophytes type-3 (e.g., the picoeukaryote, *Micromonas*), it can be used to distinguish them from the bigger prasinophytes type-2, which are abundant in our samples (i.e., *Pyramimonas* spp., Table S2).

Picophytoplankton are often underestimated by microscopy due to their small size (Coupel et al. 2015a; Del Bel Belluz et al. 2021). HPLC pigment analysis allows us to propose that the picoeukaryotes and picocyanobacteria counted by flow cytometry consist of the prasinophyte *Micromonas* and the prokaryote *Synechococcus*, respectively. *Micromonas polaris*, a psychrophilic alga restricted to polar waters (Simon et al. 2017), is a common species in Arctic and sub-Arctic waters (Lovejoy et al. 2007; Balzano et al. 2012; Coupel et al. 2015a; Jimenez et al. 2021; Nemcek et al. 2023). *Synechococcus* are present in Arctic lakes, subarctic rivers, and coastal plume (Rae & Vincent 1998; Blais et al. 2022). In coastal waters, picocyanobacterial such as *Synechococcus* and *Cyanobium*, can originate from rivers (Waleron et al. 2007; Callieri 2008).

1.3.2 Contribution of phytoplankton classes to total chlorophyll *a* biomass

CHEMTAX was used to estimate the contribution of the major phytoplankton classes to TChl *a* concentration. Figure 3 illustrates the contribution of each phytoplankton class to total abundance of cells > 2 µm and the TChl *a* biomass. It shows that cell counts underestimate the biomass of prasinophytes and cyanobacteria and overestimate the biomass of cryptophytes during late summer. This discrepancy is partly explained by the fact that the pico-sized cells were 10 to 100 times more abundant than the larger cells during this study. To test this hypothesis, we estimated the contribution of the picoprasinophytes to TChl *a* by multiplying their abundance by a value of 0.018 pg Chl *a* per cell for low-light culture of

Micromonas sp. (DuRand et al. 2002). These cells contributed an average of 24 and 29% to TChl *a* during early and late summer, respectively. These contributions are similar to those of prasinophytes (prasino-2 + prasino-3) estimated by CHEMTAX with averaged values of 17 and 21% during early and late summer, respectively (Figure 4). For comparison, the picoeukaryote contribution was estimated to be 7% in the Norwegian and Barents seas (Not et al. 2005) and 20 − 49% in the Canadian High Arctic waters (Tremblay et al. 2009) during late summer.

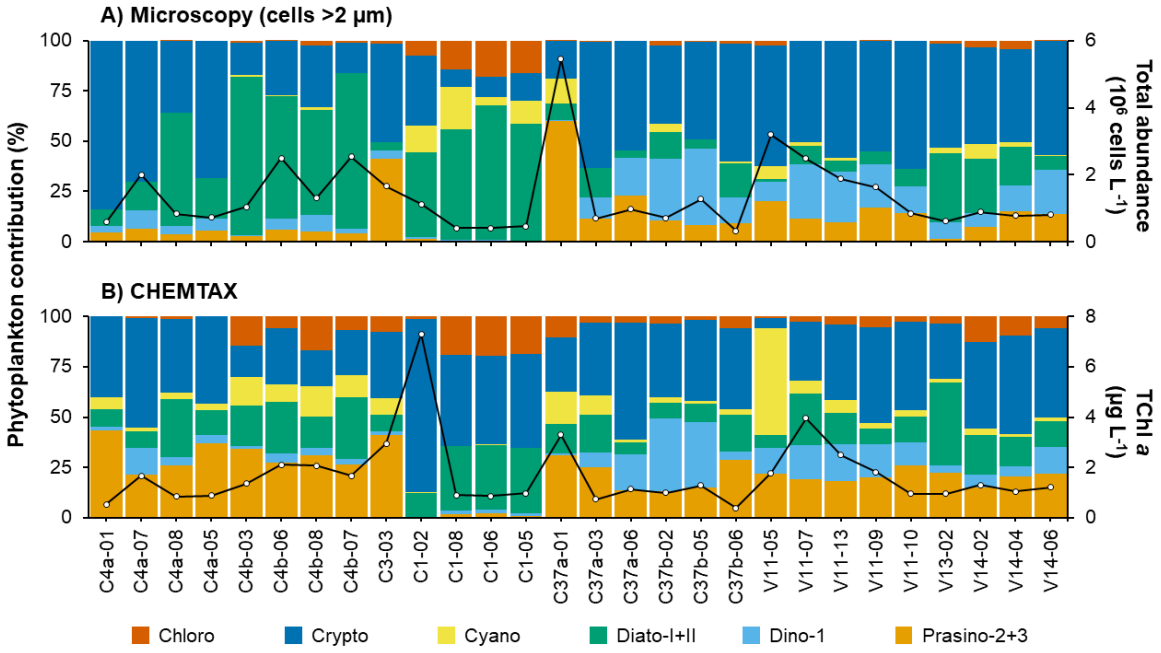

Figure 3. Relative contributions of major phytoplankton groups to **(A)** total cell abundance (determined by light microscopy) and **(B)** total chlorophyll *a* (TChl *a*) concentration (determined by CHEMTAX) during late summer (n = 28). Total cell abundance and TChl *a* concentration are superposed on the graph (black line). Stations are sorted by latitude (from north on the left to south on the right). Pigment abbreviations are defined in Table 1.

Its appears that CHEMTAX underestimates cyanobacteria and detects more cryptophytes than microscopy at brackish water stations, especially in the La Grande River plume (stations C1-02, C1-08, C1-06 and C1-05; Figure 3). The contribution of picocyanobacteria (determined by flow cytometry) to TChl *a* was estimated by assuming an

intracellular Chl *a* concentration of 1.26 fg cell^{-1}, measured in low-light culture of *Synechococcus* spp. (Morel et al. 1993). According to this cell quota, picocyanobacteria contributed little to TChl *a* (average of 0.39 and 1.75% during early and late summer, respectively).

Although zeaxanthin correlates strongly with cyanobacteria ($r^2 = 0.90$; Figure 2C), it is not the best tracer pigment. Its use as a diagnostic pigment was the best option, as it is the only pigment known to be present in all cyanobacteria. The use of pigments such as myxoxanthophyll, echinenone or canthaxanthin could be an alternative to detect the presence of cyanobacteria (Schlüter et al. 2006; Roy et al. 2011), especially since myxoxanthophyll and echinenone are preferentially used to detect freshwater cyanobacteria (Schagerl & Donabaum 2003). However, these pigments were not identified by HPLC analysis, they may have been below the detection limit. Also, phycobiliproteins (particularly phycocyanin and phycoerythrin) are more appropriate compounds for the detection of cyanobacteria (Roy et al. 2011). However, the hydrophilic nature of these compounds makes it impossible to extract them using the Zapata et al. (2000) method used in this study (Roy et al. 2011).

Finally, it should be noted that there is a significant linear relationship between the estimated contribution of cyanobacteria to TChl *a* and the total abundance of cyanobacteria counted by flow cytometry (i.e., PC- and PE-cyanobacteria < 20 µm) ($r^2 = 0.64$; $p < 0.001$; Figure S2A). In addition, a significant linear relationship between the estimated contribution of prasinophytes to TChl *a* and the abundance of picoeukaryotes counted by flow cytometry ($r^2 = 0.52$; $p < 0.001$; Figure S2B).

Another advantage of pigment biomarkers is that it can be used to identify fragile flagellated cells with altered morphological features (e.g., scaly cell wall) or cellular appendages (e.g., flagella haptonema and cell-wall projections). Although unidentified flagellated cell abundances were not included in the present study, they make up on average 38% of the total cells > 2 µm (range: 15 – 61%, Table S2). Their abundance is very well correlated with alloxanthin concentration ($r^2 = 0.29$, $p < 0.001$; Figure S3). Cryptophytes are known to be very fragile (Goldman & Dennett 1985; Goodenough et al. 2018). In the La

Grande River plume, the unidentified flagellates are probably fragile cryptophytes. Another explanation for overestimation cryptophytes is that they can be endosymbionts in some ciliates, particularly the genus *Mesodinium* (Llewellyn et al. 2005). This has already been reported by Blais et al. (2022) and Gustafson et al. (2000), with the species *Mesodinium rubrum* which contained cryptophyte chloroplasts and their associated pigments, notably alloxanthin, considered as an excellent tracer ($r^2 = 0.75$; Figure 2B). In addition, a higher abundance of the ciliate *Mesodinium* was found in the sampled stations, especially at station C1-02, compared to the other stations (420,480 cells L^{-1}; Table S2). This is also the station where CHEMTAX estimates a very high abundance of cryptophytes.

The abundance of chlorophytes is underestimated compared to their biomass. Their abundance is correlated with chlorophyll *b* ($r^2 = 0.43$, $p < 0.001$; Figure S3) and neoxanthin ($r^2 = 0.35$, $p < 0.001$; Figure S3). This suggest that a fraction of the unidentified flagellates may be chlorophytes, and the underestimation may be explained by the osmotic shock caused to freshwater chlorophytes by salt water, which deformed them and led to the loss of their flagella, making them difficult to identify.

1.3.3 Phytoplankton community composition

Phytoplankton community composition is generally similar between early and late summer in the northern part of James Bay (i.e., between the Piagochioui River (C3-03) and the Maquatua River (V11-04)) (Figure 4 and Figure S4 for all stations). Although the stations in the La Grande River plume (stations C1-02 to C1-24) appear to have similar composition (diatoms-I, cryptophytes and chlorophytes), it is possible to observe a relatively higher biomass of diatoms-I during early summer. The stations located south of the La Grande River up to the Maquatua River (stations C33-02 to V11-04) seem to be more diverse, with the presence of cryptophytes, prasinophytes, diatoms, dinoflagellates and cyanobacteria.

De Sève (1993) described a diatom bloom in the tidal freshwater zone of the turbid and shallow Rupert Bay estuary during summer 1991. Diatoms dominated the freshwater zone (30 – 80% abundance), while flagellates dominated the estuarine and coastal zones (60 – 95% abundance). Although we did not sample Rupert Bay, diatoms I+II biomass was relatively higher and less variable in early summer in the southern part of James Bay (south of the Maquatua). In general, stations with high chlorophyll biomass of diatoms-II are more numerous in early (21 stations with values > 0.2 µg L^{-1}) than in late (3 stations with values > 0.2 µg L^{-1}) summer. Moreover, diatoms-I dominates in biomass compared to diatoms-II at most stations.

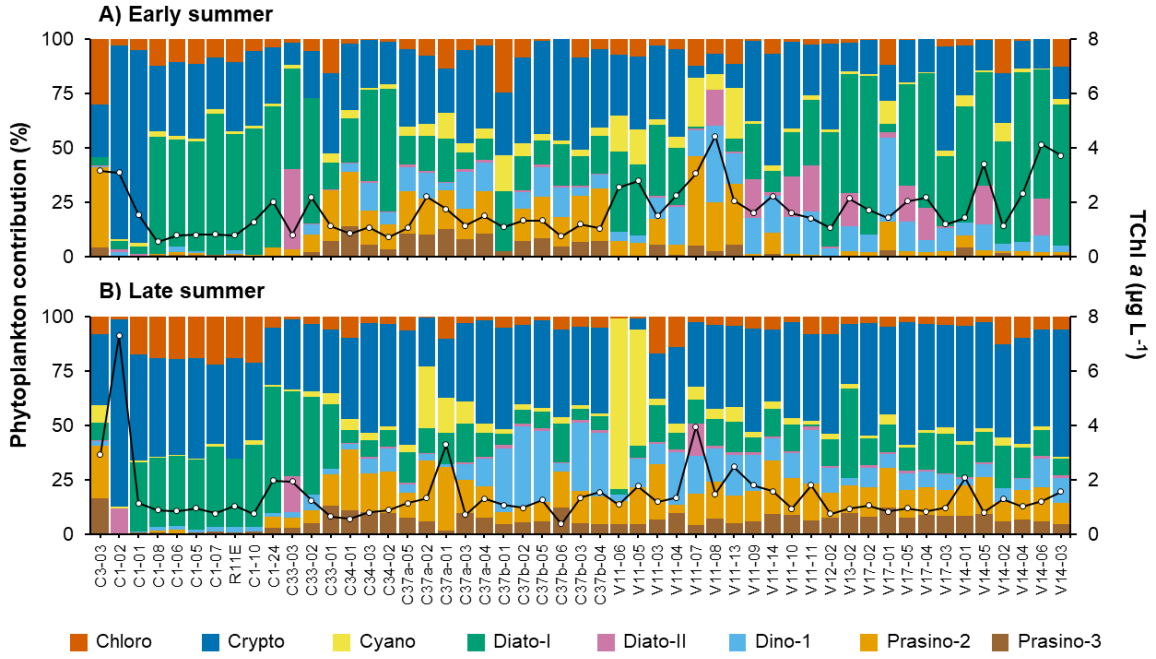

Figure 4. Relative contributions of major phytoplankton groups to total chlorophyll *a* (TChl *a*) concentration during **(A)** early and **(B)** late summer. TChl *a* concentration is superposed on the graph for both periods (black line). Samples were collected at the same stations during both periods. Stations are sorted by latitude (from north on the left to south on the right).

Groups of stations with a similar taxonomic composition were identified using a group-average clustering (similarity of 70 and 75% for early and late summer, respectively),

combined with NMDS (Figures 5, S5 and S6). Analysis of similarities (ANOSIM) revealed significant differences between the different groups with $R = 0.6464$ ($p < 0.001$) and $R = 0.8948$ ($p < 0.001$) for early and late summer, respectively. Group 1 contains the largest number of stations ($n = 79$ and $n = 55$ for early and late summer, respectively). The phytoplankton communities are diverse in group 1: the Shannon diversity indices (H') were 2.06 and 2.37 for early and late summer, respectively, with diatoms-I, cryptophytes and prasinophytes type 2+3 contributing most to TChl *a* (> 75%).

1.3.4 Spatial distribution and environmental drivers of phytoplankton community composition

1.3.4.1 La Grande River

In the La Grande River plume, the abundance ratio of the major phytoplankton classes determined by microscopy differed between late summer 1974 and 2018. In 2018, diatoms were more abundant than chlorophytes (diatoms:chlorophytes = 3.73 ± 3.00) and cyanobacteria (diatoms:cyanobacteria = 4.95 ± 0.80), whereas they were less abundant in 1974 (diatoms:chlorophytes = 0.74 ± 0.43; diatoms:cyanobacteria = 0.52 ± 0.45) (Foy & Hsiao 1976). The main species were also different between the two sampling years. In 2018, the centric diatom *Urosolenia eriensis* (as *Rhizosolenia eriensis*) and the chlorophytes *Scenedesmus bijugus*, two species which are found in Arctic and sub-Arctic freshwaters (Duthie 1979), made up, on average, 40% and 5.78% of the total abundance, respectively. The presence of *Urosolenia eriensis* and *Scenedesmus* spp. was also reported in 1974 by Foy & Hsiao (1976), but in lower abundance. The most abundant diatom species were *Tabellaria floculosa* at the mouth of the river and *Skeletonema costatum* in the offshore waters (18 and 30% of the total diatom abundance, respectively; Foy & Hsiao 1976). *Urosolenia eriensis* and *Aulacoseira* spp. (as *Melosira* spp.) were previously found in these waters, but more so in the estuarine zone of the La Grande River (Foy & Hsiao 1976). However, the natural hydrological regimes of the La Grande River have been altered with the deviation of several

rivers, rising the flow from ca. 58 km^3 yr^{-1} (in 1974) to ca. 138 km^3 yr^{-1} (in 2020) (Costanzo 2023). The flow increase has therefore reduced the salinity of the water in the La Grande River plume, favouring the presence of freshwater phytoplankton species such as the diatoms *Urosolenia eriensis* and *Aulacoseira* spp. and the chlorophytes *Scenedesmus bijugus*, *Monoraphidium* spp. and *Pediastrum* spp.

Here, we discussed which environmental factors are shaping the phytoplankton community composition of the La Grande River plume. During late summer, the plume was characterized by low salinity (5.79 ± 8.47), and relatively high concentrations of NO_3 + NO_2 (1.16 ± 0.87 µM) and $Si(OH)_4$ (26.13 ± 7.41 µM) (Group 2, Table S4). Axis I of the RDA analysis represents a salinity and nutrient gradient (Figure 7B) and explains 25.67% of the variation in taxonomic composition. The phytoplankton assemblage was more homogeneous during late summer (Group 2, Figure 6B), with the RDA analysis showing a correlation of diatoms-I and chlorophytes with this axis. However, the phytoplankton assemblage was more heterogeneous during early summer (Group 1, Figure 6A). This difference may be due to the flow of the La Grande River, which was higher in late summer than early summer (143 *vs.* 133 km^3 yr^{-1}, respectively) (Costanzo 2023), resulting in a difference in nutrient inputs (de Melo et al. 2022). However, it has already been reported that flow rivers in high latitude is not necessarily proportional to nutrient concentration (Holmes et al. 2012), especially in the La Grande River, where discharges are considerably lower in summer than winter (Lee et al. 2023), which could explain the low TChl *a* concentrations and total cell abundances. Indeed, NO_3 + NO_2 concentrations were higher in early summer (1.49 ± 1.11 *vs.* 1.11 ± 0.97 µM for the same stations in the La Grande River plume in early and late summer, respectively), while flow was lower, compared to early summer. In contrast, $Si(OH)_4$ concentrations were lower in early summer (17.17 ± 6.28 *vs.* 25.76 ± 7.76 µM for the same stations in the La Grande River plume in early and late summer, respectively), due to consumption by diatoms, whose abundance was higher at this period (56 *vs.* 43% for the same stations in the La Grande River plume). In late summer, flagellated cell development occurred after diatom bloom, with chlorophytes and cryptophytes being more abundant than in early summer (38 *vs.* 27% for cryptophytes, and 14 *vs.* 8% for chlorophytes).

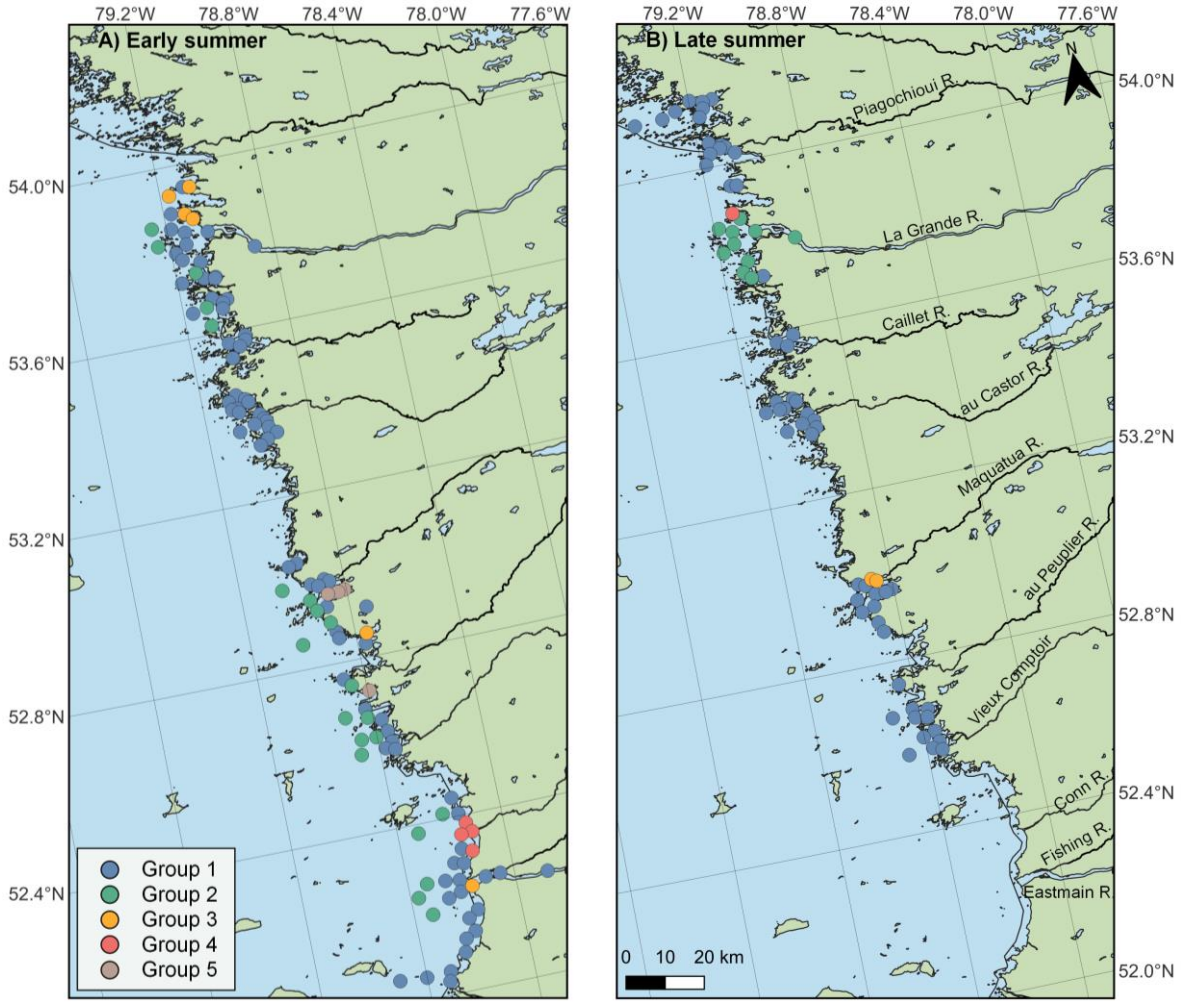

Figure 5. Maps showing groups of stations with similar phytoplankton composition (based on CHEMTAX and determined with the group-average clustering) during **(A)** early (n = 114 stations) and **(B)** late (n = 68 stations) summer. Note that there are only four groups of stations in late summer.

1.3.4.2 High abundance of cyanobacteria and mixotrophic flagellates at Maquatua River

During late summer, the phytoplankton community composition at two stations near the Maquatua River differed from the other stations (Group 3, Figures 5B and 6B), with a dominance of cyanobacteria (66% of TCh *a*). The development of this community was strongly related with axis II of the RDA analysis, which represents a gradient of light and

temperature, and explained 9.80% of the variability in phytoplankton groups (Figure 7B). The Maquatua River niche was mainly characterized by warm water temperatures (14.68 ± 0.59°C), low nutrient concentrations (NO_3 + NO_2 = 0.10 ± 0.03 µM) and low light availability, as indicated by high $a_{CDOM}(440)$ (5.21 ± 0.41 m^{-1}) and low Secchi depth values (1.35 ± 0.32 m) (Table S4). These environmental conditions are favorable for the development of small cells such as cyanobacteria, several observations having confirmed that cyanobacteria preferred warmer temperatures (Vincent 2000). With their surface/volume ratio, they can grow in oligotrophic waters. Most freshwaters in high latitude areas are generally characterized by low nutrient levels, which would explain the high abundance of picocyanobacterial in these ecosystems (Vincent & Quesada 2012). Bloom-forming cyanobacteria have been observed in subarctic waters and could become more abundant as a result of environmental changes in these high latitudes regions (Vincent & Quesada 2012).

The high abundance of PC-picocyanobacteria was confirmed by flow cytometry analysis (Table S4). It has already been previously shown that flow cytometry analyses report the presence of picocyanobacterial at high latitudes, although the average abundance and biomass are relatively low (Buitenhuis et al. 2012; Ibarbalz et al. 2019). In this study, these organisms are probably of freshwater origin. The success of cyanobacteria development depends in part on high temperatures (Vincent 2000). Indeed, their growth rate is relatively rapid with increasing temperature, allowing them to keep up with grazing by nanoflagellates or ciliates (Waleron et al. 2007). Picocyanobacteria are also more efficient at nutrient acquisition and light capture than larger cells (Stockner 1988; Blais et al. 2022). In this study, most filamentous cyanobacteria with a size of 2 – 5 µm formed colonies. Blais et al. (2022) also reported the presence of filamentous cyanobacteria and colonial form of picocyanobacteria near the Great Whale River in south-east Hudson Bay. In coastal waters, picocyanobacteria are thought to come from allochthonous sources, a hypothesis confirmed by Waleron et al. (2007) in the Mackenzie River of the Beaufort Sea using molecular tools.

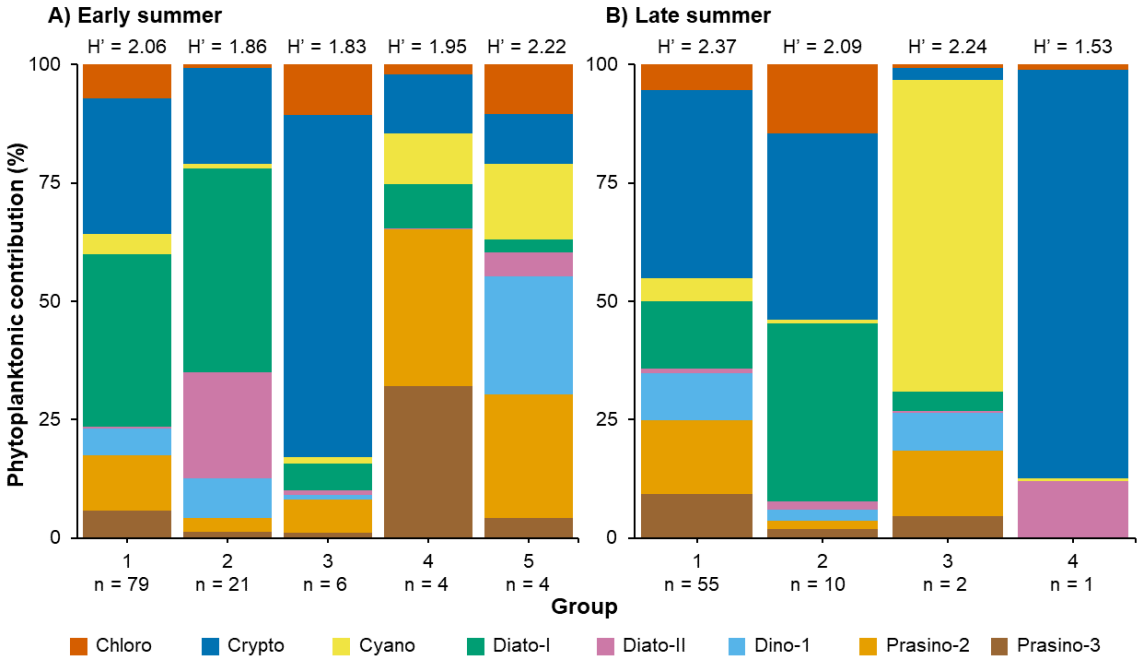

Figure 6. Relative contribution of major phytoplankton groups to total chlorophyll *a* for groups of stations with similar pigment composition (determined by group-average clustering) during **(A)** early and **(B)** late summer. The Shannon diversity index (H') is indicated above each group.

Prasinophytes type 2 represented 14% of the TChl *a* near the Maquatua River during late summer (Group 3, Figure 6B). The high turbidity and low nutrient concentrations ($NO_3 + NO_2 = 0.10 \pm 0.03$ µM) of this area may have favored the development of these small flagellated cells (Table S4). In addition, prasinophytes community was mainly composed of *Pyramimonas* spp. (2 – 10 µm), a mixotrophic taxon able to grow at low light intensity and nutrient concentrations (McKie-Krisberg et al. 2018; Blais et al. 2022; Pang et al. 2022). In early summer, flagellate cells also dominated the waters near the Maquatua River, with a predominance of prasino-2 (26.10%), dinoflagellates (24.92%), cyanobacteria (15.89%) and cryptophytes (15.89%) (Group 5, Figure 6A). The high temperature (14.72 + 1.81°C) and low nutrient concentrations ($NO_3 + NO_2 = 0.06 \pm 0.04$ µM) favored the development of these cells.

The development success of these groups may be due to their ability to realize mixotrophy. Indeed, mixotrophic phytoflagellates can make up a significant proportion of planktonic communities (McKie-Krisberg et al. 2018). It is now recognized that a significant number of protist taxa use phago-mixotrophy to obtain nutrients for growth and reproduction under conditions of light or nutrient limitation (Millette et al. 2023). This is particularly true for dinoflagellates, cryptophytes, chrysophytes and prymnesiophytes (Millette et al. 2017; Stoecker & Lavrentyev 2018; Pang et al. 2022).

Mixotrophy could also explain the high contribution of prasinophytes, especially prasino-2. Indeed, our microscopic counts estimated that 99% of prasinophytes identified were from the genus *Pyramimonas* spp., a taxon that would be considered mixotrophic (McKie-Krisberg et al. 2018; Bock et al. 2021). However, the phago-mixotrophy capacity of prasinophytes and green algae in general remains controversial (Pang et al. 2022). We proposed that prasinophytes type 3 are mainly composed of the picoeukaryote *Micromonas polaris*. However, the capacity of this species for phago-mixotrophy is still debated, so we cannot say with certainty that this taxon realizes mixotrophy.

1.3.4.3 Coast-to-sea gradient

During early summer, a coast-to-sea gradient in phytoplankton community composition was evident along the east coast of James Bay, particularly near the La Grande, Maquatua, Vieux Comptoir and Eastmain rivers (Figure 5A). The first and second axes of the RDA explained 23.83% and 14.15% of the variation in phytoplankton community composition, respectively (Figure 7A). Water temperature and Secchi depth (a proxy for light availability) were the two main variables correlating with axis 1, while salinity and SPM concentrations (a proxy of turbidity) were correlated with axis 2. The mean water temperature (11.45 ± 3.04°C) and SPM concentration (11 ± 18 mg L^{-1}) were relatively high and the mean salinity (12.65 ± 6.69°C) and Secchi depth value (1.41 ± 0.91 m) were relatively low near the coast (i.e., Group 1) compared to offshore waters (i.e., Group 2; Table S3). The nearshore phytoplankton communities, represented by group 1, was relatively diversified (Shannon

diversity index, H' = 2.06), with diatoms-I (36%, acclimated to low light level), cryptophytes (29%) and prasinophytes type 2 (11%) representing the main algal groups (> 75%; Figures 5A and 6A).

In this study, the phytoplankton community was similar between the Eastmain estuary and the offshore waters (Figure 5A). In contrast, it differed between these two zones in the late summer of 1974, with a greater proportion of chlorophytes, chrysophytes, and filamentous cyanobacteria in the estuary (Foy & Hsiao 1976). This change can be explained by the diversion of the Eastmain River for hydroelectric development (de Melo et al. 2022), which has resulted in significant decrease in its discharge in the 1980s (ca. 38 km^3 yr^{-1} prior 1980 to ca. 24 km^3 yr^{-1} since 1981; Ingram et al. 1985; de Melo et al. 2022). Consequently, the freshwater-saltwater transition is less pronounced, with saltwater from the bay penetrating further into the Eastmain River (Ingram et al. 1985; Déry et al. 2016). This change is reflected in the taxonomic composition of phytoplankton, with greater biomass of cryptophytes and lower abundance of freshwater taxa such as chlorophytes. These nearshore waters in the southern part of the bay are very turbid, with high SPM concentration and $a_{CDOM}(440)$ (Mabit et al. 2022). These observations are consistent with the measurements of de Melo et al. (2022) who mentioned that the presence of a high peatland cover and soil rich in organic matter in eastern James Bay is responsible of the high level of SPM (18.3 mg L^{-1}) and $a_{CDOM}(440)$ (10.3 m^{-1}) in the Eastmain River. In addition, the Eastmain River is associated with low Secchi depth (Table S3), suggesting high turbidity. It has already been mentioned that cryptophytes can form a dominant group in turbid waters (Hammer et al. 2002). Compared with other groups, cryptophytes are particularly sensitive to light (Richardson 2022), and the survival of this group at low light intensities is due to a highly efficient photosynthetic system, but also to a slow rate of cellular respiration (Thinh 1983; Hammer et al. 2002).

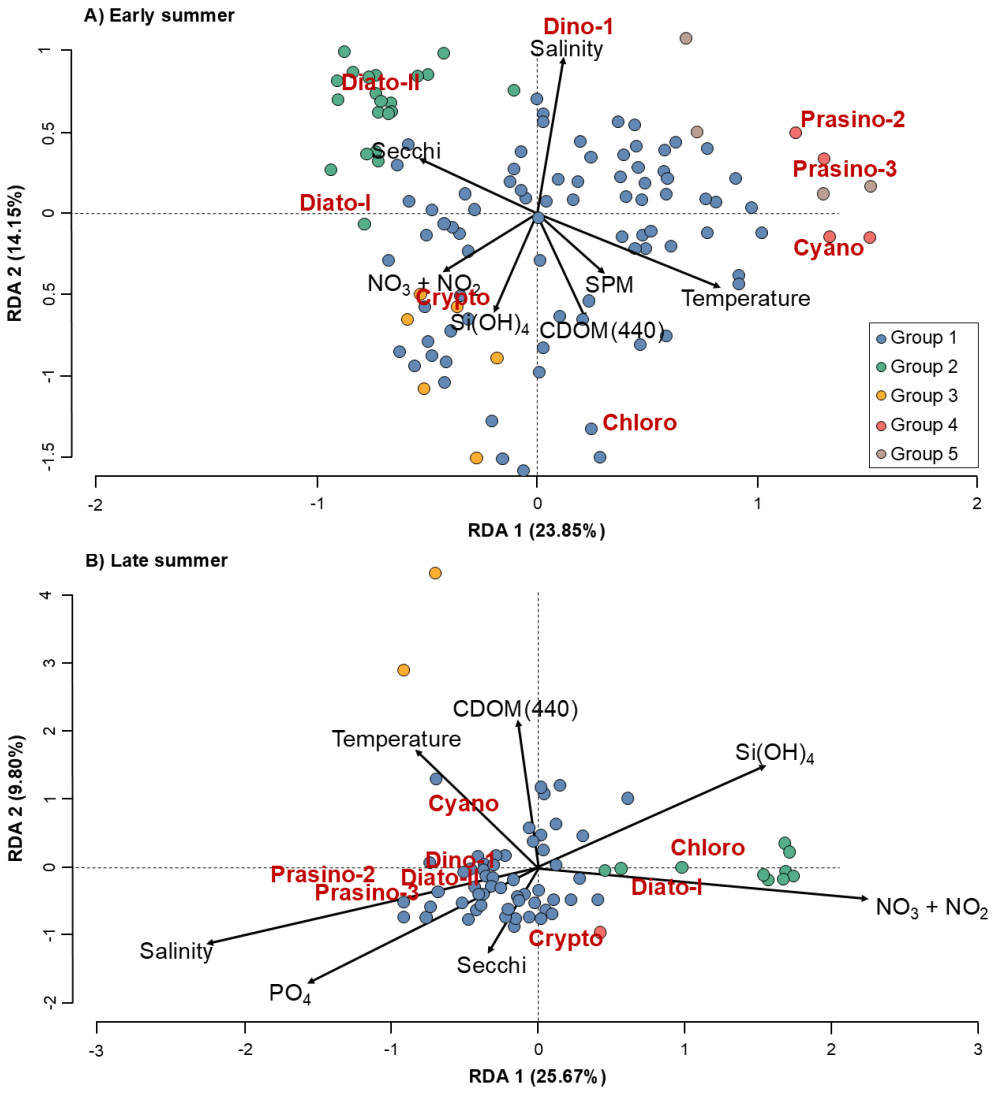

Figure 7. Redundancy analysis (RDA) ordination plots of axis I and II showing taxonomic groups of phytoplankton based on CHEMTAX (red bold) in relation with environmental variables (black arrows) at stations collected during **(A)** early and **(B)** late summer. Colors represent the stations with a similar phytoplankton composition (determined with the group-average clustering).

Offshore phytoplankton communities, represented by group 2, are less diversified than group 1 (H' = 1.86), with diatoms-I (43%) and diatoms-II (22%) dominating these stations (Figures 5A and 6A). These coastal waters are characterized by salty (16.70 ± 2.57), cold (7.03 ± 2.52°C) waters, compared to the other stations (Figure 7A, Table S3). In addition,

the light availability is greater, and is reflected by higher Secchi depth values (2.05 ± 0.79 m), and lower $a_{CDOM}(440)$ and SPM concentrations (2.31 ± 0.72 m^{-1} and 2.83 ± 1.51 mg L^{-1}, respectively). In addition, the chlorophyll biomass of diato-II was higher between turbid and less turbid waters (Mann-Whitney *U*-test, $p < 0.01$), supporting the hypothesis that heliophilic diatoms (as diatoms-II) seem to be generally found in the more transparent, deeper waters off the coast, particularly in early summer. The resuspension of sediments in shallow waters caused by tides and waves could be one of the mechanisms explaining the very low diatoms-II contribution close to the coast. This coast-to-sea gradient in phytoplankton communities was more visible during early summer, because a limited number of offshore stations were sampled during late summer. However, stations near the au Castor and Piagochioui rivers did not have a phytoplankton community composition distinct from other rivers, either during early or late summer.

1.3.5 Physiology and photoacclimation

Phytoplankton can be subject to several loss processes, such as grazing, cell death, viral lysis or sinking (Choi et al. 2017). Pheopigments (here chlorophyllide *a*, pheophorbide *a* and pheophytin *a*) are often used as indicators of degraded cells (Szymczak-Żyla et al. 2008), and their presence in water indicates zooplankton activity or cellular senescence (Bidigare et al. 1986; Coupel et al. 2015b), although chlorophyllide *a* can also result from artificial degradation of Chl *a* during sample handling (e.g., filtration, extraction, storage; Roy et al. 2011). The pheophorbide *a*:pheophytin *a* (Pb:Pp) ratio was higher in early than late summer (Figure S7), a period associated with diatom bloom. The highest ratios were found in offshore waters where diatoms I+II dominate the chlorophyll biomass. According to Sathish et al. (2020), a high Pb:Pp ratio correspond to increased grazing pressure. The pattern of pigment degradation suggests that the phytoplankton communities were under more intense grazing pressure during early summer, especially in the south (between the Maquatua and Eastmain rivers and in the north in the La Grande River plume).

In addition, pheophorbide *a* was the most abundant degradation pigment. These high concentrations could be influenced by taxonomic composition, as previous studies showed that the Pb:Pp ratio can depend on phytoplankton composition (Jeffrey & Hallegraeff 1987; Szymczak-Żyla et al. 2008). For example, the genus *Skeletonema*, the diatom genus that was most abundant in late summer, is known to produce high levels of pheophorbide *a*, due in part to its high chlorophyllase activity (Sathish et al. 2020). This characteristic associated with *Skeletonema*, in addition to enhanced grazing pressure, could partially explain the presence of higher chlorophyllide *a* concentrations in the southern bay during early summer. It could also explain the lower concentrations in the north, since chlorophyllase activity varies between species of the same taxonomic class (Jeffrey & Hallegraeff 1987); it was the genus *Urosolenia* that was present in the north, not *Skeletonema*.

In response to light variations, phytoplankton have developed physiological adjustments, that induce changes in enzymes, morphology and biochemical composition (Graff et al. 2016). Limited light availability can affect phytoplankton production in two ways: by regulating the maximum attainable biomass in the system (Wofsy 1983; Pennock 1985), or by stimulating physiological acclimation under low-light conditions (Falkowski & Owens 1980; Pennock & Sharp 1986). Variations in intracellular pigment concentrations (Gameiro et al. 2011; Graff et al. 2016) and ratio of photosynthetic carotenoids (PSC, sum of alloxanthin, fucoxanthin, peridinin and neoxanthin) to photoprotective carotenoids (PPC, sum of diadinoxanthin, diatoxanthin, violaxanthin, lutein, zeaxanthin and β, β-caroten) (Eisner & Cowles 2005; Alou-Font et al. 2016) are often used to estimate the acclimation potential of algal cells. The PSC:TChl *a* ratio has previously been shown to increase in response to low-light photoacclimation, while the opposite trend was observed for the PPC:TChl *a* ratio (Geider et al. 1996; Eisner & Cowles 2005; Ferreira et al. 2017; Kauko et al. 2019).

PSC:PPC mass ratio was on average higher during early than late summer (2.02 ± 0.93 *vs.* 1.11 ± 0.29, respectively) (Figure 8). Light availability was more limited in early summer, with lower Secchi depth values (1.48 ± 0.90 *vs.* 2.16 ± 1.22 m during early and late summer,

respectively), reflecting the need for phytoplankton communities to maximize their light-harvesting capacity, and to increase their photosynthetic efficiency (Grobbelaar 1990; Van De Poll et al. 2005; Gameiro et al. 2011). Our highest PSC:PPC ratios observed in early summer are consistent with those obtained by Kauko et al. (2019) for Arctic phytoplankton communities acclimated to low light intensity. However, the change in PSC:PPC ratio between the two sampling periods and among stations (Figure 8) may be due to a change in the phytoplankton community composition, as discussed below.

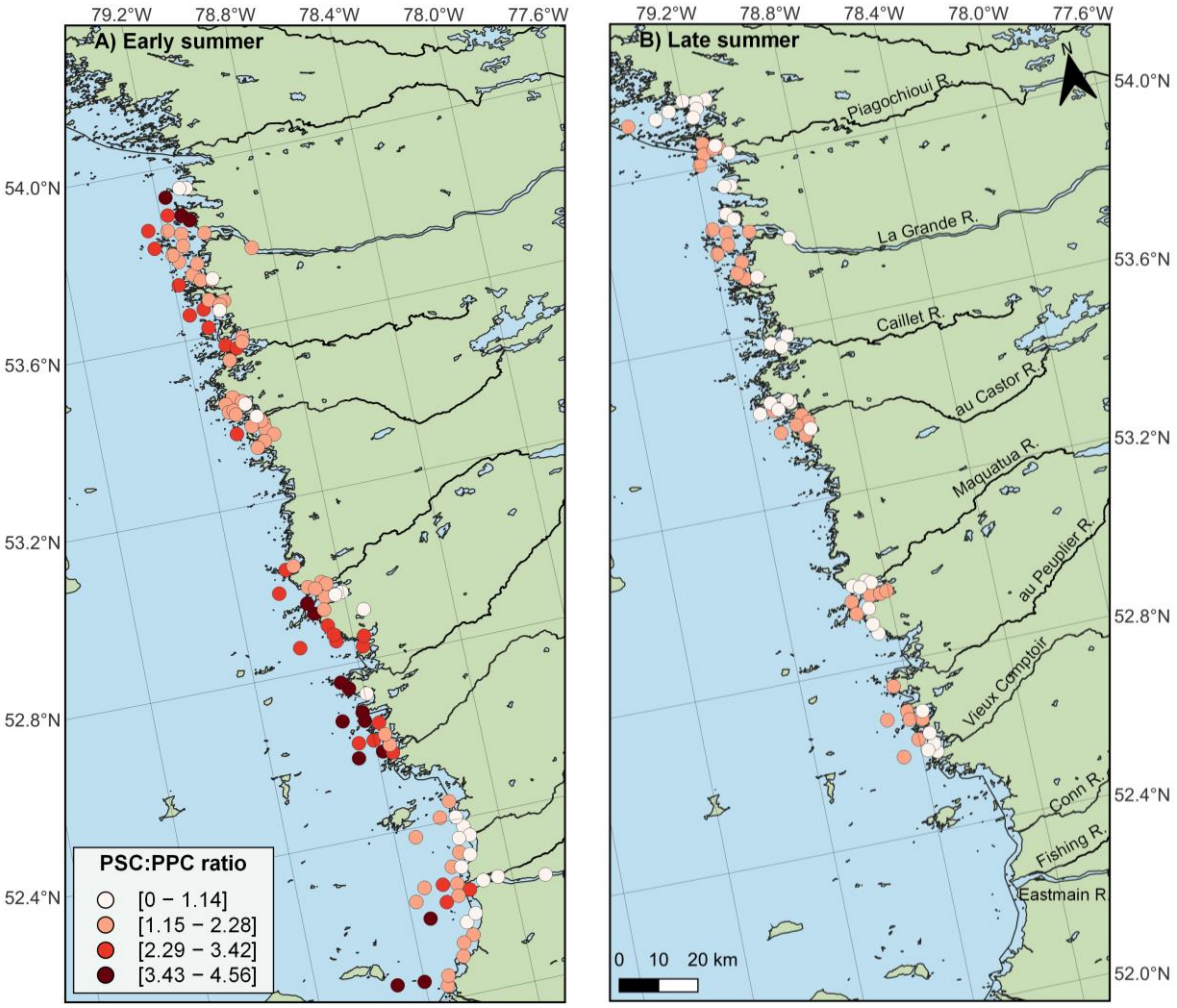

Figure 8. Maps showing the mass ratio of photosynthetic carotenoids to photoprotective carotenoids (PSC:PPC) during **(A)** early and **(B)** late summer.

In contrast to the PSC:TChl *a* ratio which did not change much during both summer periods, the (diadinoxanthin + diatoxanthin):Chl *a* and PPC:TChl *a* ratio were higher during late summer when the water was in general less turbid according to the Secchi depth (Table S1; Figure 9A, B, D). This seasonal difference was also observed in the relationships between (i) PSC:PPC ratio and Secchi depth, (ii) PSC:PPC ratio and water temperature, and (iii) PSC:PPC ratio and relative contribution of prasinophytes to TChl *a*, with slopes always higher in early summer (Figure 9C-E). In contrast to prasinophytes, the slope between the PSC:PPC ratio and relative contribution of diatoms I+II to TChl *a* is positive but do not show a difference over the two summer periods (Figure 9F). These results indicate that phytoplankton communities have relatively more light-harvesting pigments than photoprotective pigments in this low light environment, except in warmer or very turbid water along the James Bay coast where the contribution of prasinophytes to TChl *a* may be large or where the contribution of diatoms I+II is relatively small.

On a local scale, PSC:PPC ratios also varied with distance from the coast, with offshore waters having higher ratios compared to nearshore waters (Figure 8). Taxonomic composition could explain these variations, with a higher abundance of diatoms I+II offshore. As diatoms are larger cells, they will have more pigments per cell, added to the fact that the available light is sufficient for their development. The relation between the PSC:PPC ratio and the abundance of diatoms I+II confirms this explanation. In contrast, nearshore waters are characterized by flagellated cells, such as cryptophytes, dinoflagellates and prasinophytes. The small size of their cells makes them more competitive for light resources, compared to diatoms. Moreover, many genera in the flagellate classes are mixotrophic, as is the case with dinoflagellates *Amphidinium*, *Heterocapsa* and *Gymnodinium/Gyrodinium*, the cryptophytes *Hemiselmis* and *Plagioselmis*, and the prasinophytes *Pyramimonas*, taxa that have been identified by microscopy.

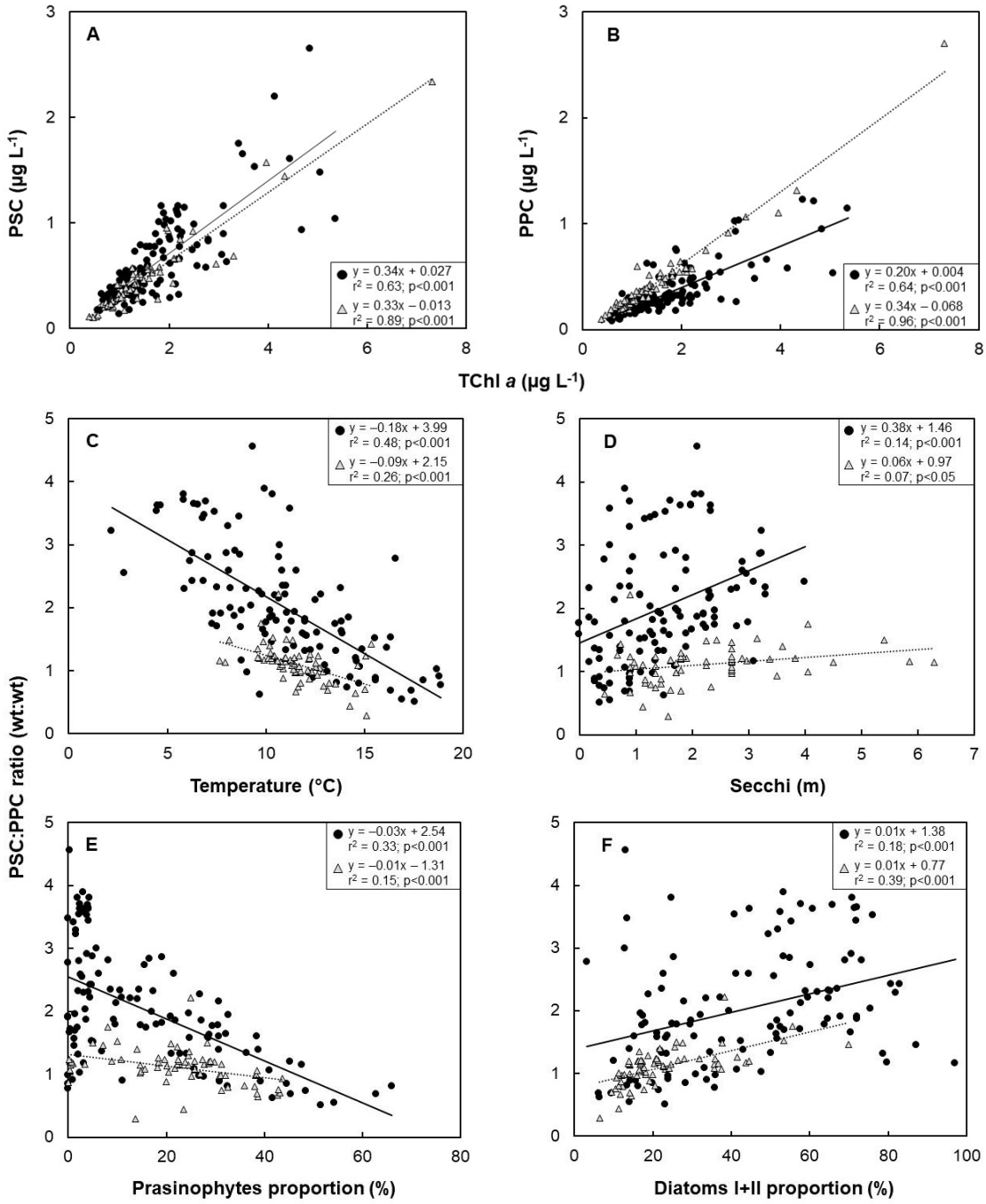

Figure 9. Relationships between **(A)** photosynthetic carotenoid pigment (PSC) concentration and total chlorophyll *a* (TChl *a*) concentration, and **(B)** photoprotective carotenoids (PPC) concentration and TChl *a* concentration. Relationships between PSC:PPC ratio and **(C)** water temperature, **(D)** Secchi depth, **(E)** relative contribution of prasinophytes to TChl *a*, and **(F)** relative contribution of diatoms I+II to TChl *a* during early (circles) and late (triangles) summer. The linear regression line is shown in all panels.

Our results showed that PSC:PPC ratios decreased significantly with increasing temperature ($r^2 = 0.485$; $p < 0.001$ and $r^2 = 0.262$; $p < 0.001$ for early and late summer, respectively) (Figure 9C). This trend was more pronounced in early than late summer. It has also been mentioned in previous studies that some environmental variables, in addition to light, can influence pigment concentrations, such as temperature. For example, Eisner & Cowles (2005), have showed that 36% of the variability in the PSC:PPC ratio could be explained by temperature. They showed that PPC concentrations were higher in waters with higher temperature, since warm waters generally have higher irradiances. However, water temperatures in James Bay are associated with high turbidity rather than high irradiance, which may explain that we do not observe an increase in PPC cell concentrations.

Variations in PSC:PPC ratios may also reflect changes in phytoplankton community structure, since taxa have different carotenoid composition (Eisner & Cowles 2005; Kropuenske et al. 2009; Domingues et al. 2011; Ferreira et al. 2017). Variations have also been noted according to cell size, so that large cells show higher intracellular Chl *a* concentration and PSC:PPC ratio, compared to small cells (Eisner & Cowles 2005). It is known that nanophytoplankton contribute to a large proportion of the biomass where light levels are low (Robinson et al. 2018). This could explain the significant abundance of cryptophytes in the coastal waters of James Bay, which would possess an adaptation to maximize the rate of photosynthesis through changes in pigment composition (Gibb et al. 2001; Robinson et al. 2018). Indeed, small cells such as cryptophytes, chlorophytes or diatoms (< 10 µm) seems to be able to cope with low-light conditions, due to low respiration rates (Hammer et al. 2002). Furthermore, the diatom *Skeletonema* (3 – 16 µm), the second most abundant algal cell > 2 µm, was also present at most stations along the coast during late summer (Table S2). This could be explained by the plasticity of this genus, which enables it to grow in very low-light conditions (Dimier et al. 2007).

1.4 CONCLUSION

The combined use of microscopy, cytometry and pigment signature allowed us to better understand the structure of phytoplankton communities in the coastal waters of James Bay. Results showed that diatoms represented the greatest chlorophyll biomass in early summer, while small flagellated cells were more abundant in late summer, corresponding to the post-bloom period. Results revealed differences at more local scales, between nearshore and offshore waters, which were mainly driven by light availability. Indeed, warm and turbid nearshore waters rich in SPM and CDOM favored the development of pico- and nanoflagellate cells such as cryptophytes, prasinophytes and dinoflagellates. In contrast, offshore waters were dominated by diatoms, where light was less limiting due to lower turbidity. The flow changes had different effects on the La Grande and Eastmain rivers. The partial diversion on the Eastmain River reduced its flow, increasing turbidity due to bank erosion and favoring marine taxa. In contrast, the La Grande River doubled its flow, resulting in low salinity and high nutrient concentrations (NO_3 + NO_2 and $Si(OH)_4$), which favored the development of freshwater taxa in the river plume. PSC:PPC ratios also followed the same trend, increasing with distance from the coast and being higher in the Eastmain River than in the La Grande River. This suggests that light limitation did not maximize PSC concentration, but rather favored the growth of small mixotrophic cells. It may be interesting to estimate the primary productivity of the environment, especially since flagellates of the pico- and nanophytoplankton fraction dominate the turbid waters of James Bay in abundance and sometimes in chlorophyll biomass.

1.5 ACKNOWLEDGEMENTS

This work was funded by the Niskamoon Corporation and by a grant from the Natural Sciences and Engineering Research Council of Canada (NSERG). Partial funding was provided by the Fonds de recherche du Québec – Nature et technologies (FRQNT) through

the Québec-Océan strategic cluster. We thank the Cree local coordinators Ernie Rabbitskin, Geraldine Mark and Ernest Moses, employees of Niskamoon Corporation, and the Cree land users who guided us on the field. We thank Virginie Galindo for coordinating the research project and her contribution to the fieldwork. We are grateful to Sylvie Lessard for phytoplankton identification, Mélanie Simard and Virginie Galindo for HPLC analysis, Claude Belzile for DOM and flow cytometric analyses, and Pascal Guillot for the CTD data processing and quality control. This project is a contribution to the larger Coastal Habitat Comprehensive Research Program aiming to understand changes in the coastal habitats of Eeyou Istchee (James Bay).

CONCLUSION GÉNÉRALE

De nombreuses rivières drainent la région de la baie James, et certaines d'entre elles ont été modifiées par endiguement ou dérivation afin de soutenir le développement de complexes hydroélectriques. Ces infrastructures ont non seulement altéré le débit des rivières, mais également les apports en nutriments et en matière particulaire et dissoute, influençant par conséquent les communautés de phytoplancton dans les eaux côtières avoisinantes. Malgré les changements apportés dans cette région, la baie James demeure encore très peu étudiée, en particulier après la mise en place des complexes hydroélectriques. L'objectif principal de ce projet était donc de caractériser la composition et la variabilité spatiale des communautés phytoplanctoniques le long de la côte est de la baie James au début et à la fin de l'été.

Pour ce faire, l'utilisation combinée de la microscopie optique, de la signature pigmentaire par HPLC et de la cytométrie en flux a permis l'identification et l'estimation de la biomasse chlorophyllienne des principaux groupes algaux : les cryptophytes, les diatomées, les prasinophytes, les dinoflagellés, les cyanobactéries et les chlorophytes. L'identification et le dénombrement cellulaire des taxons par la microscopie a permis la conception de la matrice initiale de CHEMTAX, mais aussi la validation des ratios pigment:Chl *a* calculés par la matrice finale. Grâce aux pigments, la fraction picophytoplanctonique a pu être mise en évidence, suggérant ainsi la présence de petites cellules couramment retrouvées dans les milieux subarctiques, telles que le prasinophyte *Micromonas polaris*, ou encore les cyanobactéries *Synechococcus* et *Cyanobium*. Enfin, la cytométrie en flux a confirmé la très forte abondance des cellules picophytoplanctoniques.

Le début et la fin de l'été se différenciaient par une biomasse plus importante des diatomées tôt en saison, visible en particulier dans la moitié sud de la baie James. La fin de l'été correspondant à la période post-floraison, ce sont donc de petites cellules flagellées qui

se sont mieux développées, telles que les cryptophytes, les prasinophytes et les dinoflagellés. Par ailleurs, nos résultats ont montré des différences dans la composition phytoplanctonique à des échelles plus locales, notamment entre les eaux littorales et du large. C'est la disponibilité de la lumière qui régit principalement la répartition spatiale des groupes. En effet, les eaux turbides riches en matière particulaire en suspension (SPM) et la matière organique dissoute colorée (CDOM) proches de la côte ont été associées à de petites cellules flagellées, favorisées par des températures plus chaudes et de faibles concentrations en nutriments. Inversement, les eaux plus au large étaient dominées par les diatomées, la lumière y étant moins limitante du fait d'une turbidité plus faible. Ces différences ont également été constatées entre les rivières dont le débit a été modifié, en particulier entre La Grande Rivière et la rivière Eastmain. En effet, le détournement partiel de la rivière Eastmain a entraîné une diminution de son débit, conduisant à une augmentation de la salinité de ces eaux, accompagnée par la présence de taxons associés à un environnement marin. En revanche, la Grande Rivière a vu son débit doubler depuis les dernières décennies suite à la dérivation de plusieurs rivières régionales, si bien que les eaux de son panache présentaient une salinité très faible et des concentrations plus élevées en nutriments (en particulier $NO_3 + NO_2$ et $Si(OH)_4$), soutenant le développement des diatomées, en particulier *Urosolenia eriensis* et *Aulacoseira* spp. et d'autres taxons dulcicoles tels que *Scenedesmus bijugus*, *Monoraphidium* spp. et *Pediastrum* spp.

La répartition des principaux groupes algaux face aux variations *in situ* de la lumière suivait également la même tendance que les rapports caroténoïdes photosynthétiques sur caroténoïdes photoprotecteurs (PSC:PPC). En effet, à mesure que la distance à la côte augmentait, ce rapport était également plus élevé, suggérant que les fortes concentrations cellulaires en PSC étaient dues à la plus forte abondance en diatomées. Inversement, les rapports les plus faibles étaient retrouvés dans les eaux plus turbides de la côte, où les petites cellules flagellées étaient les plus abondantes. Ces résultats ont suggéré que la photoacclimatation des cellules ne se faisait pas au niveau des concentrations pigmentaires, mais plutôt au niveau du type nutritionnel employé par les cellules. En effet, une limitation de la lumière, associée à de grande quantité de matière organique, aurait plutôt favorisé la

mixotrophie, comme le montre la présence de dinoflagellés (*Amphidinium*, *Heterocapsa* et *Gymnodinium/Gyrodinium*), de cryptophytes (*Hemiselmis* et *Plagioselmis*) et de prasinophytes (*Pyramimonas*), taxons qui sont reconnus pour employer ce mode de nutrition.

Les résultats obtenus au cours de cette étude ont mis en lumière l'importance de caractériser non seulement les communautés phytoplanctoniques procaryotes et eucaryotes, mais aussi celles des protistes hétérotrophes et mixotrophes vivant dans des eaux côtières subarctiques influencées par des apports de rivières. À notre connaissance, aucune étude récente depuis le développement hydroélectrique n'avait encore été conduite sur les communautés planctoniques unicellulaires de la baie James. Cette étude présente donc des données actualisées de la composition taxonomique du phytoplancton par rapport aux études antérieures qui mettaient l'emphase uniquement sur certains groupes phytoplanctoniques et certaines zones spécifiques de la côte est de la baie James. L'influence des processus physiques et chimique du milieu sur la composition taxonomique a également pu être mise en évidence, contribuant ainsi à pallier les lacunes de nos connaissances sur la dynamique des communautés phytoplanctoniques des eaux côtières. Les résultats obtenus pourront servir de référence à de futures études beaucoup plus approfondies. Cette étude s'inscrit également dans un contexte de perturbations climatiques et anthropiques auxquelles font face les écosystèmes côtiers subarctiques. En effet, étudier simultanément des zones influencées par le développement hydroélectrique (par exemple, La Grande Rivière et la rivière Eastmain) et d'autres non affectées (par exemple, les rivières au Castor et Maquatua) nous a permis d'examiner le fonctionnement de ces environnements en présence et en absence de régulation/diversion des rivières. De plus, considérant la rapidité des changements climatiques auxquels sont soumis ces écosystèmes, il était important d'acquérir ces connaissances pour une meilleure compréhension de la dynamique des communautés phytoplanctoniques qui s'y trouvent, mais aussi pour mieux prévoir leurs réponses face aux futures perturbations environnementales.

Notre étude ayant été réalisée uniquement au début et à la fin de l'été, il est peu probable que nos résultats puissent être extrapolés sur le reste des saisons. En effet, le débit

des rivières et le couvert de la glace de mer sont des variables à considérer, puisqu'elles pourraient influencer la composition taxonomique et la dynamique des communautés phytoplanctoniques. De plus, le débit des rivières régulées et non régulées fluctue au fil des saisons. Les effets des changements climatiques vont s'amplifier au cours des prochaines décennies avec, entre autres, la diminution du couvert de glace et l'intensification des précipitations et de l'érosion. Cela pourrait alors entraîner des conséquences majeures sur la dynamique des communautés phytoplanctoniques et plus largement sur la productivité de ces milieux. Notre étude s'étant essentiellement penchée sur la composition taxonomique du phytoplancton, il pourrait être intéressant d'estimer la productivité primaire du milieu, d'autant plus qu'il n'est pas dominé par les diatomées, groupe phytoplanctonique qui représente généralement la plus grande biomasse pendant les périodes de floraisons. Or, ce sont plutôt des cellules flagellées de la fraction pico- et nanophytoplanctoniques qui dominent en abondance et parfois en biomasse dans les eaux côtières de la baie James. Quantifier la biomasse de chaque groupe avec plus de précision nous permettrait ainsi d'avoir une meilleure vision de la productivité primaire phytoplanctonique dans un milieu caractérisé par des eaux turbides tel que la baie James.

MATÉRIEL SUPPLÉMENTAIRE

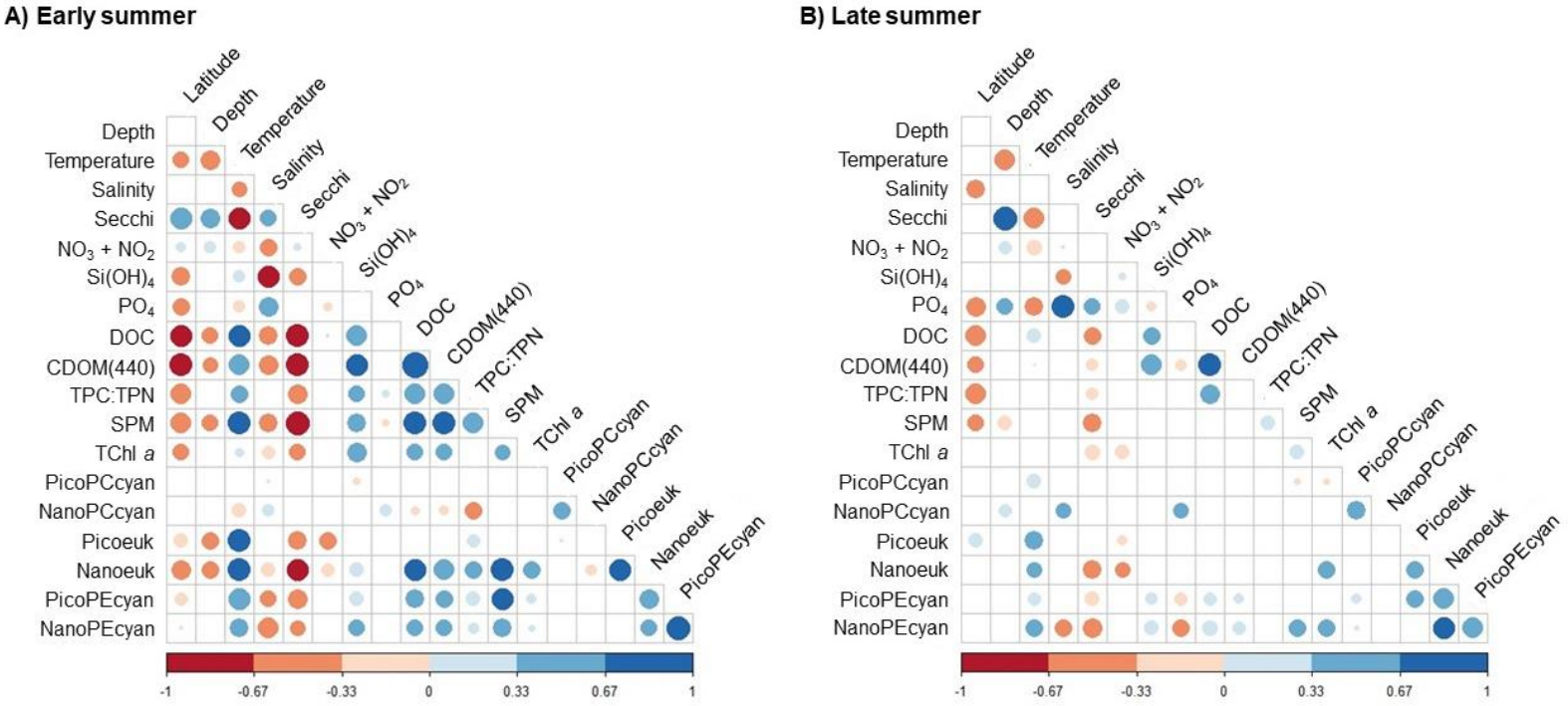

Figure S1. Heat map of the Spearman correlation coefficient between environmental and biological variables. The size of the circle is proportional to the correlation coefficient shown in color.

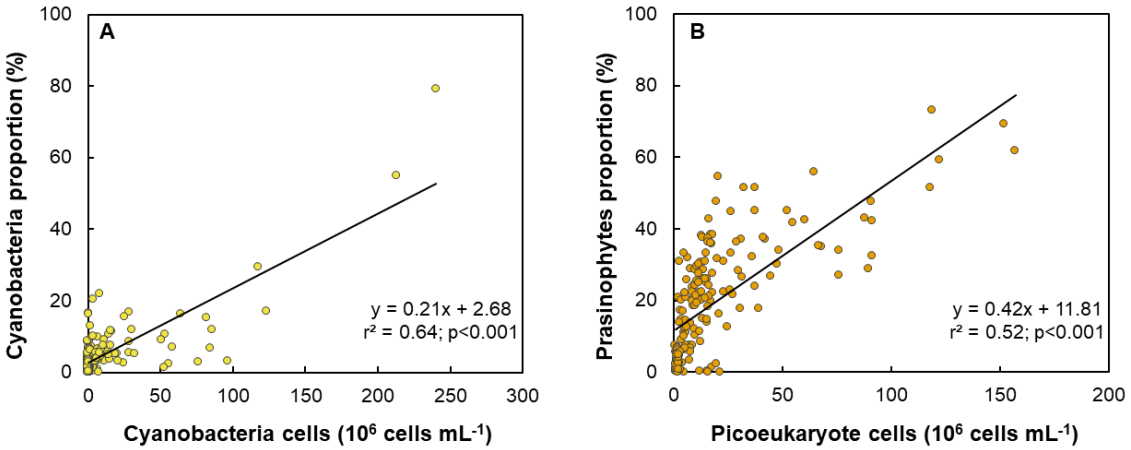

Figure S2. Relationships between **(A)** relative contribution of total cyanobacteria to total chlorophyll *a* concentration and total cyanobacteria cell abundance and **(B)** relative contribution of total prasinophytes (type 2 + type 3) to total chlorophyll *a* concentration and picoeukaryote cell abundance during both sampling periods. Cell abundances were counted by flow cytometry. The linear regression line is shown.

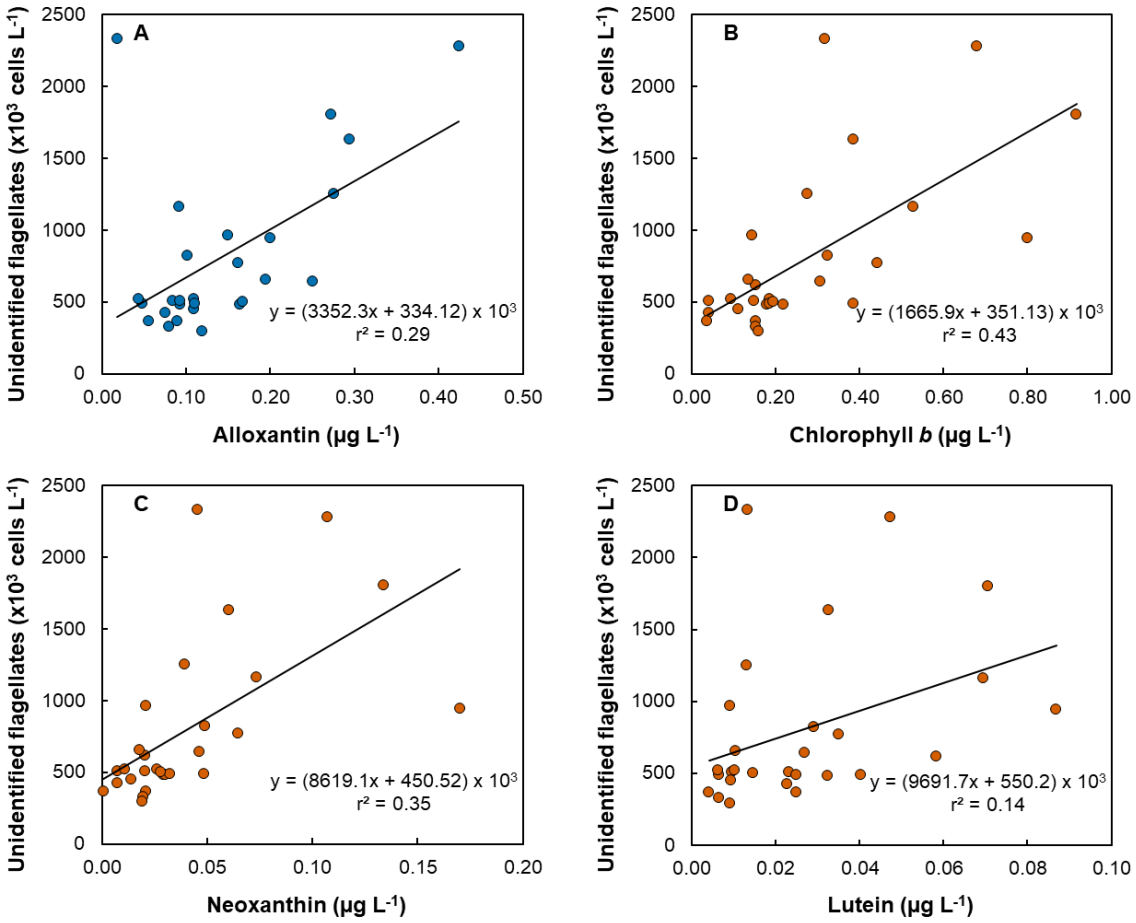

Figure S3. Relationships between unidentified flagellate abundance and **(A)** alloxanthin concentration, **(B)** chlorophyll *b* concentration **(C)** neoxanthin concentration, and **(D)** lutein concentration. Cell abundances were counted by flow cytometry. The linear regression line is shown.

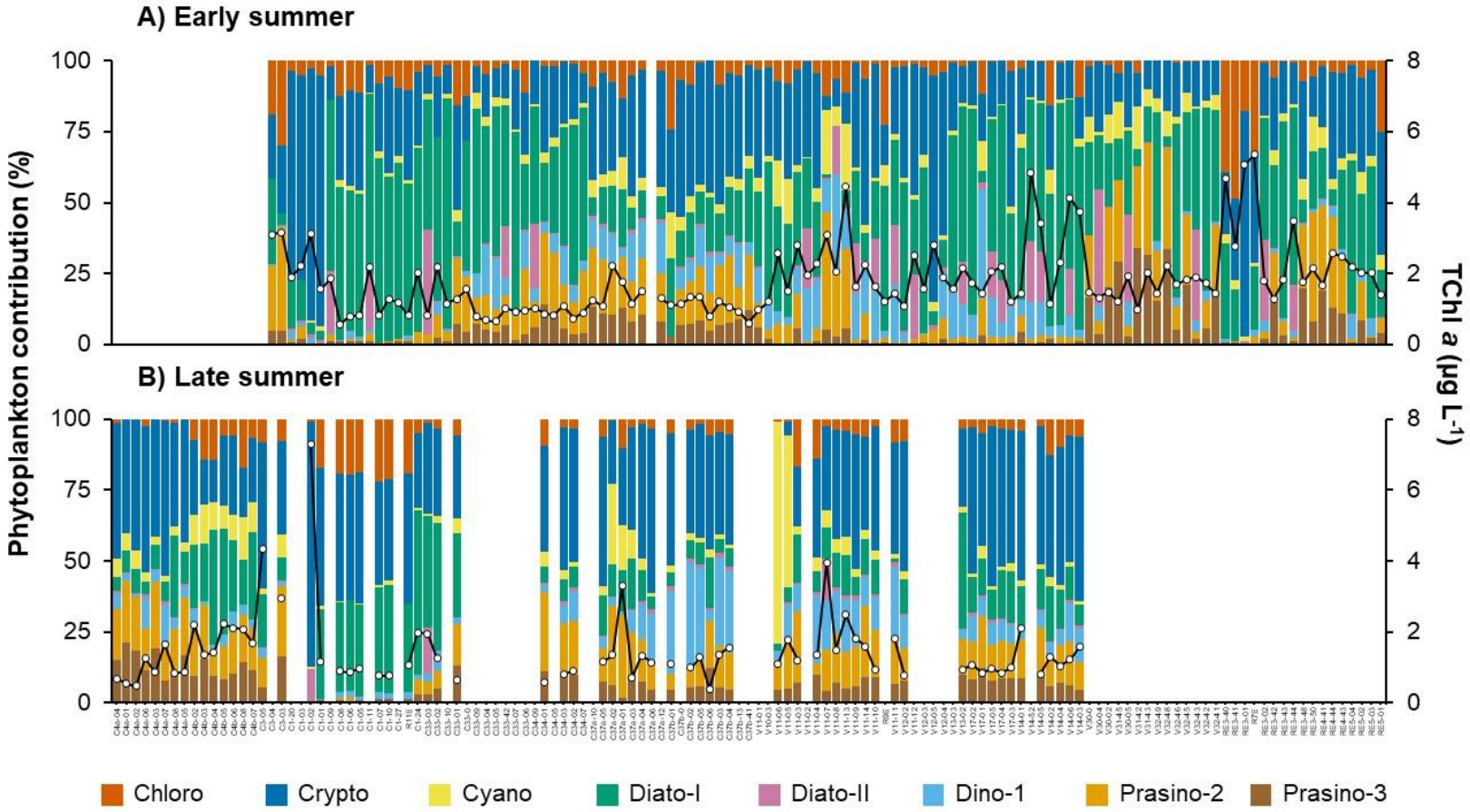

Figure S4. Relative contributions of phytoplanktonic groups to total chlorophyll *a* concentration during **(A)** early and **(B)** late summer. Stations are sorted by latitude (from north on the left to south on the right).

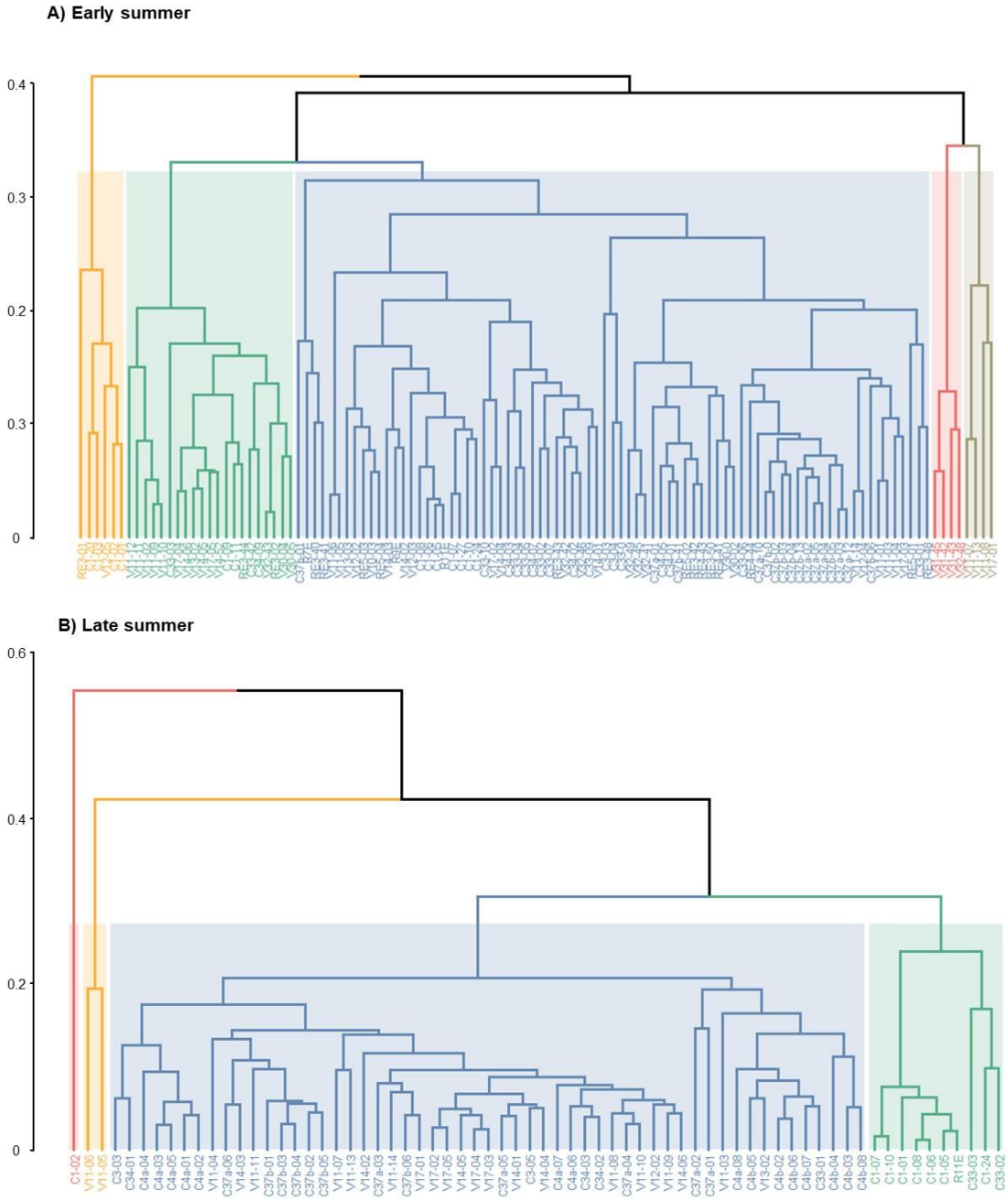

Figure S5. Group-average clustering showing groups of stations with taxonomically similar phytoplankton classes (as determined by CHEMTAX) during **(A)** early (n = 114 stations, similarity level of 70%) and **(B)** late (n = 68 stations, similarity level of 75%) summer.

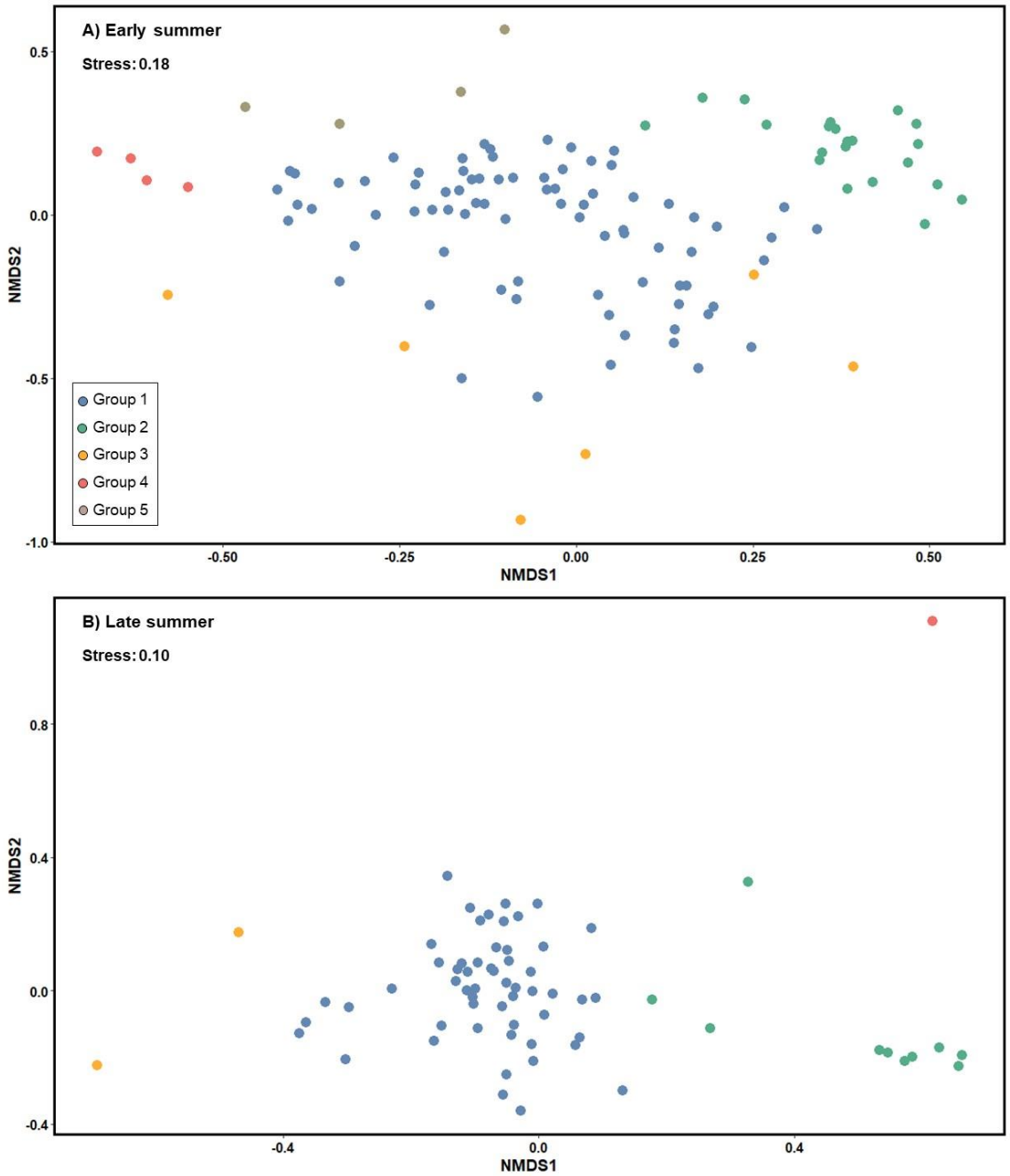

Figure S6. Two-dimensional non-metric multidimensional scaling (NMDS) of stations during **(A)** early (n = 114) and **(B)** late (n = 68) summer. Groups of stations with taxonomically similar phytoplankton classes, as determined with the group-average clustering (see Figure S5), are superimposed on the NMDS.

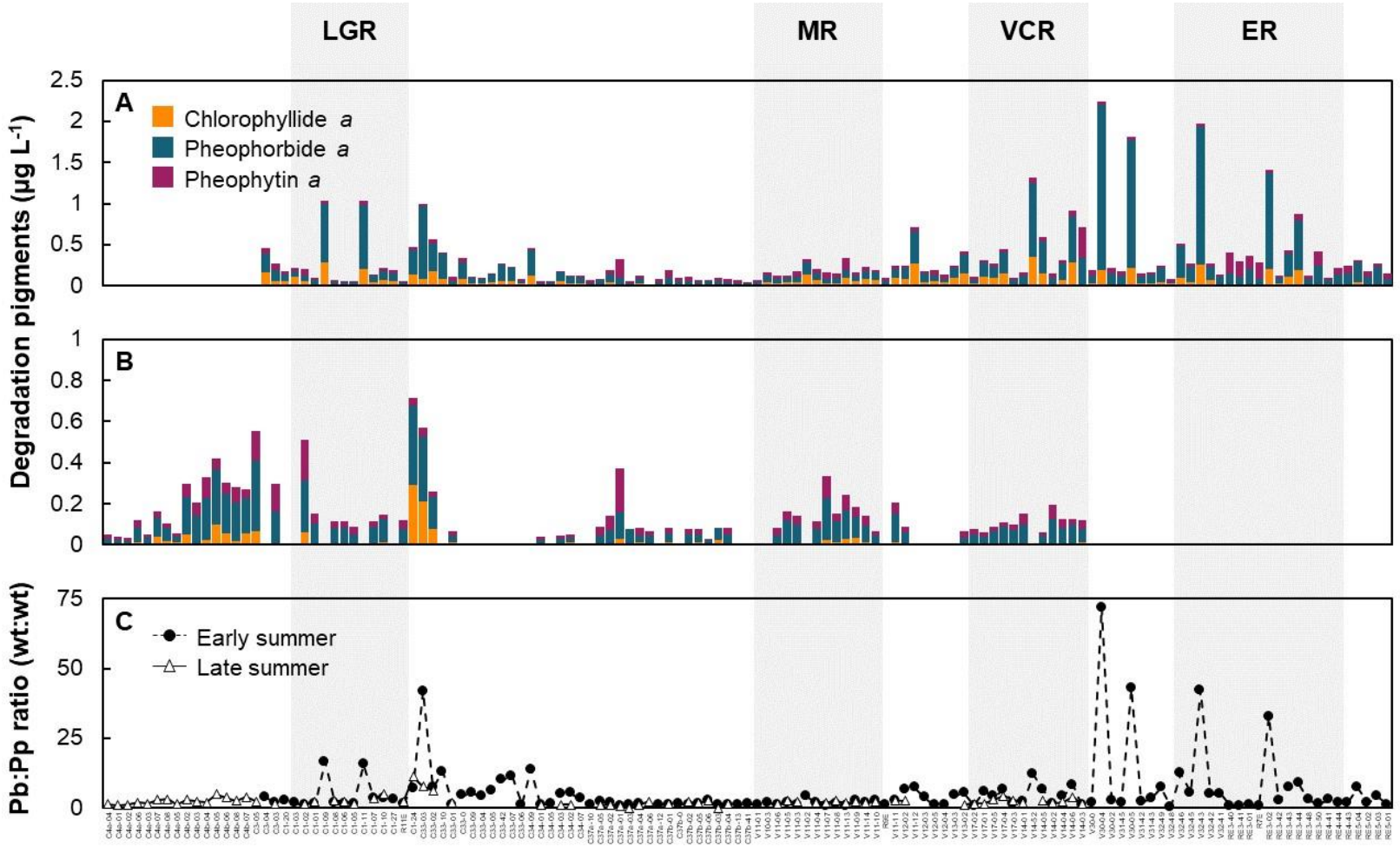

Figure S7. Degradation pigment concentrations during **(A)** early and **(B)** late summer, and **(C)** pheophorbide *a*:pheophytin *a* (Pb:Pp) ratio during early (circles with solid line) and late (triangles with dashed line) summer. Stations are sorted by latitude (from north on the left to south on the right). LGR = La Grande River, MR = Maquatua River, VCR = Vieux Comptoir River, ER = Eastmain River.

Table S1. Relative contribution of accessory pigment to total chlorophyll *a* (%) and photoacclimation index (mean ± SD) during early and late summer.

	Pigments	Early summer	Late summer
Photosynthetic pigments	Chlorophyll *b*	17.44	22.01
	Chlorophyll c_1	0.99	0.31
	Chlorophyll c_2	3.23	2.00
	Chlorophyll c_3	0.25	0.46
	Alloxanthin	11.22	17.02
	Fucoxanthin	27.00	15.49
	MgDVP	1.80	2.09
	Neoxanthin	2.06	3.18
	Peridinin	5.81	7.17
	Prasinoxanthin	4.27	4.25
Photoprotective pigments	β, β-carotene	5.71	6.38
	Antheraxanthin	0.49	0.96
	Diadinoxanthin	10.81	7.22
	Diatoxanthin	0.84	0.63
	Lutein	2.37	2.09
	Violaxanthin	4.26	5.49
	Zeaxanthin	1.45	3.24
Photoacclimation index	Chlide *a*:Chl *a* (wt:wt)	0.037 ± 0.039	0.013 ± 0.027
	PSC:PPC (wt:wt)	2.02 ± 0.93	1.11 ± 0.29
	PPC:PSC (wt:wt)	0.63 ± 0.35	0.99 ± 0.41
	(DD + DT):Chl *a* (wt:wt)	0.10 ± 0.07	0.16 ± 0.05

Table S2. List of planktonic protist and cyanobacteria (> 2 µm) reported from the eastern coast of James Bay during late summer 2018. Minimum (Min), mean and maximum (Max) abundance (cells L^{-1}) for each taxon, and occurrence (O) is shown in percent of the total number of samples collected (n = 28). n.d. = not detected. Note that the limit of detection is 730 cells L^{-1}, however a value of zero was used when calculating the mean abundance.

Taxon	Abundance			O
	Min	Mean	Max	
Diatoms	**34,310**	**333,195**	**1,951,290**	**100**
Centric diatoms	**5,110**	**278,417**	**1,919,900**	**100**
Aulacoseira ambigua (Grunow) Simonsen	n.d.	52	1,460	4
Aulacoseira distans (Ehrenberg) Simonsen	n.d.	600	6,570	14
Aulacoseira islandica (O.Müller) Simonsen	n.d.	104	2,920	4
Aulacoseira italica (Ehrenberg) Simonsen	n.d.	339	6,570	11
Aulacoseira sp. 5	n.d.	1,460	16,790	21
Aulacoseira sp. 6	n.d.	183	5,110	4
Aulacoseira spp.	n.d.	1,095	8,030	32
Chaetoceros contortus F.Schütt	n.d.	78	2,190	4
Chaetoceros fallax Proshkina-Lavrenko	n.d.	26	730	4
Chaetoceros neogracilis VanLandingham	n.d.	26	730	4
Chaetoceros subtilis Cleve	n.d.	78	2,190	4
Chaetoceros wighamii Brightwell	n.d.	365	5,840	11
Chaetoceros spp. (5 – 10 µm) [a]	n.d.	626	3,650	39
Chaetoceros spp. (10 – 20 µm) [a]	n.d.	548	2,190	36
Cyclotella spp. (5 – 10 µm)	n.d.	3,598	35,040	54
Cyclotella spp. (10 – 20 µm)	n.d.	313	2,920	25
Cyclotella spp. (20 – 50 µm)	n.d.	26	730	4
Leptocylindrus minimus Gran [a]	n.d.	3,989	79,570	11
Melosira lineata (Dillwyn) C.Agardh	n.d.	313	5,110	11
Melosira moniliformis C.Agardh	n.d.	130	1,460	11
Melosira nummuloides C.Agardh	n.d.	78	2,190	4
Melosira spp.	n.d.	78	1,460	7

Paralia sulcata (Ehrenberg) Cleve	n.d.	130	3,650	4
Skeletonema cf. *costatum* (Greville) Cleve [a]	n.d.	239,831	1,903,840	96
Sundstroemia pungens (Cleve-Euler) Medlin, Lundholm, Boonprakob & Moestrup	n.d.	26	730	4
Thalassiosira conferta Hasle	n.d.	235	2,920	11
Thalassiosira spp. (5 – 10 µm) [a]	n.d.	104	1,460	7
Thalassiosira spp. (10 – 20 µm) [a]	n.d.	886	8,760	43
Thalassiosira spp. (20 – 50 µm) [a]	n.d.	52	730	7
Urosolenia eriensis (H.L.Smith) Round & R.M.Crawford	n.d.	19,293	192,720	21
Centric diatoms (5 – 10 µm)	n.d.	3,494	40,880	57
Centric diatoms (10 – 20 µm)	n.d.	261	2,920	25
Pennate diatoms	**2,920**	**51,778**	**358,430**	**100**
Achnanthes spp.	n.d.	365	2,920	18
Amphora spp.	n.d.	26	730	4
Asterionella formosa Hassall	n.d.	756	9,490	18
Cocconeis spp.	n.d.	834	3,650	50
Cylindrotheca closterium (Ehrenberg) Reimann & J.C.Lewin	n.d.	6,257	73,730	64
Cylindrotheca gracilis (Brébisson ex Kützing) Grunow	n.d.	104	1,460	7
Cymbella spp.	n.d.	52	730	7
Diatoma cf. *tenuis* C.Agardh	n.d.	26	730	4
Diatoma vulgaris Bory	n.d.	78	1,460	7
Diatoma spp.	n.d.	78	1,460	7
Diploneis spp.	n.d.	26	730	4
Entomoneis paludosa var. ?	n.d.	52	730	14
Fragilaria crotonensis Kitton	n.d.	104	1,460	7
Gomphonema spp.	n.d.	26	730	4
Grammatophora spp.	n.d.	26	730	4
Gyrosigma fasciola (Ehrenberg) J.W.Griffith & Henfrey	n.d.	78	1,460	7
Gyrosigma / *Pleurosigma* spp.	n.d.	156	2,190	14
Hannaea arcus (Ehrenberg) R.M.Patrick	n.d.	26	730	4
Licmophora spp.	n.d.	1,173	18,250	46

Mastogloia spp.	n.d.	104	2,190	7
Navicula directa (W.Smith) Brébisson	n.d.	26	730	4
Navicula transitans var. *derasa* f. *delicatula*	n.d.	313	6,570	14
Navicula spp. (20 – 50 µm)	n.d.	469	3,650	36
Navicula spp. (≥ 50 µm)	n.d.	104	730	14
Nitzschia cf. *laevissima* (Grunow)	n.d.	26	730	4
Nitzschia spp. (20 – 50 µm)	n.d.	183	2,190	18
Nitzschia spp. (50 – 100 µm)	n.d.	26	730	4
Nitzschia spp. (≥ 100 µm)	n.d.	52	730	7
Pinnularia spp.	n.d.	52	730	7
Plagiotropis sp. 1b	n.d.	26	730	4
Rhoicosphenia spp.	n.d.	26	730	4
Stenoneis obtuserostrata (Hustedt) M.Poulin	n.d.	26	730	4
Surirella ovata Kützing	n.d.	26	730	4
Surirella spp. (10 – 20 µm)	n.d.	26	730	4
Tabellaria fenestrata (Lyngbye) Kützing	n.d.	965	9,490	21
Tabellaria flocculosa (Roth) Kützing	n.d.	26	730	4
Fragilariaceae complex [*]	n.d.	6,205	32,120	86
Pennate diatoms (5 – 10 µm)	n.d.	10,950	59,860	96
Pennate diatoms (10 – 20 µm)	n.d.	14,678	108,040	96
Pennate diatoms (20 – 50 µm)	n.d.	5,762	46,720	93
Pennate diatoms (≥ 50 µm)	n.d.	1,408	14,600	57
Dinophyceae	**1,460**	**143,549**	**668,680**	**100**
Naked dinophyceae	**n.d.**	**14,965**	**69,350**	**89**
Amphidinium sphenoides Wulff	n.d.	156	1,460	14
Amphidinium spp. [b]	n.d.	52	730	7
Cochlodinium spp.	n.d.	26	730	4
Gymnodinium cf. *kesslitzii* (J.Schiller) Moestrup	n.d.	10,455	62,780	75
Gymnodinium cf. *parvum* J.Larsen	n.d.	26	730	4
Gyrodinium flagellare J.Schiller	n.d.	26	730	4

Gyrodinium sp. 4	n.d.	26	730	4
Gyrodinium sp. 5	n.d.	78	2,190	4
Gymnodinium/*Gyrodinium* spp. (10 – 20 µm) [a]	n.d.	3,833	10,060	71
Gymnodinium/*Gyrodinium* spp. (20 – 50 µm) [a]	n.d.	156	2,190	14
Lebouridinium glaucum (Lebour) F.Gómez, H.Takayam, D.Moreira & P.López-García	n.d.	26	730	4
Nematopsides vigilans (Marschall) Greuet	n.d.	52	730	7
Torodinium robustum Kofoid & Swezy	n.d.	52	730	7
Thecate dinophyceae	**1,460**	**128,584**	**640,210**	**100**
Apocalathium aciculiferum (Lemmermann) Craveiro, Daugbjerg, Moestrup & Calado	n.d.	26	730	4
Dinophysis acuminata Claparède & Lachmann [a, b]	n.d.	156	1,460	14
Dinophysis spp. [a, b]	n.d.	26	730	4
Heterocapsa rotundata (Lohmann) Gert Hansen	n.d.	124,361	633,640	89
Heterocapsa spp. [b]	n.d.	26	730	4
Parvodinium inconspicuum (Lemmermann) Carty	n.d.	52	730	7
Prorocentrum spp. [a, b]	n.d.	339	4,380	21
Protoperidinium bipes (Paulsen) Balech	n.d.	130	730	18
Protoperidinium brevipes (Paulsen) Balech	n.d.	26	730	4
Scrippsiella spp.	n.d.	26	730	4
Diplopsalis complex [**]	n.d.	52	730	7
Dinophyceae sp. 5	n.d.	548	3,650	21
Dinophyceae sp. 5-1	n.d.	26	730	4
Dinophyceae (10 – 20 µm)	n.d.	1,851	8,030	71
Dinophyceae (20 – 50 µm)	n.d.	886	8,030	32
Dinophyceae cysts (20 – 50 µm)	n.d.	52	730	7
Chlorophyceae	**n.d.**	**19,658**	**83,950**	**75**
Ankistrodesmus arcuatus Korshikov	n.d.	391	2,920	32
Ankistrodesmus fusiformis Corda	n.d.	52	1,460	4
Arthrodesmus spp.	n.d.	26	730	4
cf. *Chlamydomonas* (10 – 20 µm)	n.d.	78	730	11

Chlorella chlorelloides (Naumann) C.Bock, Krienitz & Pröschold	n.d.	209	5,840	4
Coelastrum microporum Nägeli	n.d.	209	5,840	4
Cosmarium spp.	n.d.	52	730	7
Crucigenia spp.	n.d.	156	4,380	4
Dictyosphaerium spp.	n.d.	156	3,650	7
Glochiococcus aciculiferus (Lagerheim) P.C.Silva	n.d.	104	1,460	11
Kirchneriella spp.	n.d.	235	2,920	14
Lemmermannia komarekii (Hindák) C.Bock & Krienitz	n.d.	1,251	20,440	11
Lemmermannia tetrapedia (Kirchner) Lemmermann	n.d.	183	5,110	4
Micractinium belenophorum (Korshikov) T.Proschold, C.Block, W.Luo & L.Kreinitz	n.d.	26	730	4
Monoraphidium contortum (Thuret) Komárková-Legnerová	n.d.	626	3,650	39
Monoraphidium irregulare (G.M.Smith) Komárková-Legnerová	n.d.	339	4,380	18
Monoraphidium spp.	n.d.	3,363	17,520	54
Oocystis borgei J.W.Snow	n.d.	417	5,840	11
Pediastrum spp.	n.d.	886	9,490	18
Quadrigula cf. *pfitzeri* (Schröder) G.M.Smith	n.d.	26	730	4
Scenedesmus bijugus (Turpin) Lagerheim	n.d.	3,389	26,280	21
Scenedesmus spp.	n.d.	600	5,840	18
Spondylosium planum (Wolle) West & G.S.West	n.d.	52	1,460	4
Stauridium privum (Printz) Hegewald	n.d.	1,199	18,980	14
Stauridium tetras (Ehrenberg) E.Hegewald	n.d.	209	2,920	7
Staurodesmus incus (Hassal ex Ralfs) Teiling	n.d.	26	730	4
Staurodesmus spp.	n.d.	26	730	4
Willea irregularis (Wille) Schmidle	n.d.	626	11,680	7
Chlorophyceae (2 – 5 µm, colony)	n.d.	1,564	36,500	11
Chlorophyceae (5 – 10 µm, solitary)	n.d.	339	5,840	14
Chlorophyceae (5 – 10 µm, colony)	n.d.	1,512	17,520	14
Chlorophyceae (5 – 10 µm, filament)	n.d.	130	3,650	4
Chlorophyceae (10 – 20 µm, solitary)	n.d.	52	730	7
Chlorophyceae (10 – 20 µm, colony)	n.d.	626	11,680	14
Chlorophyceae (10 – 20 µm, filament)	n.d.	52	1,460	4

Chlorophyceae (20 – 50 µm, solitary)	n.d.	52	1,460	4
Chlorophyceae (20 – 50 µm, filament)	n.d.	78	2,190	4
Chlorophyceae (≥ 50 µm, solitary)	n.d.	52	730	7
Chlorophyceae (≥ 50 µm, filament)	n.d.	287	8,030	4
Chrysophyceae	**n.d.**	**14,026**	**73,730**	**96**
Chrysolykos angulatus (Willén) Nauwerck	n.d.	26	730	4
Chrysolykos skujae (Nauwerck) Bourrelly	n.d.	704	8,030	14
Chrysolykos spp.	n.d.	52	730	7
Dinobryon bavaricum Imhof	n.d.	2,034	24,090	18
Dinobryon vanhoeffenii H.Bachmann	n.d.	78	2,190	4
Dinobryon borgei Lemmermann	n.d.	652	7,300	14
Dinobryon cf. *divergens* Imhof	n.d.	26	730	4
Dinobryon divergens O.E.Imhof	n.d.	600	16,790	4
Dinobryon faculiferum Willén	n.d.	130	1,460	14
Dinobryon sp. 8	n.d.	156	2,190	11
Dinobryon sp. 9	n.d.	78	1,460	7
Dinobryon spp.	n.d.	886	10,220	11
Kephyrion sp. 1	n.d.	261	3,650	14
Kephyrion sp. 1-1	n.d.	156	1,460	11
Mallomonas spp. [a]	n.d.	78	2,190	4
Chrysophyceae sp. 3	n.d.	469	12,410	7
Chrysophyceae (2 – 5 µm)	n.d.	391	4,380	14
Chrysophyceae (5 – 10 µm)	n.d.	5,658	23,360	86
Chrysophyceae (10 – 20 µm)	n.d.	1,121	5,110	46
Chrysophyceae (stromatocysts)	n.d.	469	6,570	18
Dictyochophyceae	**n.d.**	**28,001**	**175,200**	**93**
Apedinella spinifera (Throndsen) Throndsen	n.d.	11,185	70,810	79
Pseudopedinella pyriformis N.Carter	n.d.	2,946	35,770	54
Pseudopedinella/*Mesopedinella* spp. (2 – 5 µm)	n.d.	4,745	30,660	64

Pseudopedinella/*Mesopedinella* spp. (5 – 10 µm)	n.d.	9,125	45,990	82
Cryptophyceae	**35,040**	**572,607**	**1,929,390**	**100**
Hemiselmis spp.	n.d.	197,882	1,606,000	89
Plagioselmis spp.	n.d.	49,145	154,760	89
Rhodomonas marina (P.A.Dangeard) Lemmermann	n.d.	391	2,920	29
Rhodomonas spp.	n.d.	209	2,190	18
Teleaulax acuta (Butcher) D.R.A.Hill	n.d.	2,659	16,060	43
Teleaulax amphioxeia (W.Conrad) D.R.A.Hill	n.d.	14,157	81,760	82
Teleaulax spp.	n.d.	7,952	49,640	64
Cryptophyceae sp. 5	n.d.	78	1,460	7
Cryptophyceae sp. 11	n.d.	104	2,920	4
Cryptophyceae (2 – 5 µm)	n.d.	78	1,460	7
Cryptophyceae (5 – 10 µm)	8,030	166,675	495,670	100
Cryptophyceae (10 – 20 µm)	24,090	132,704	534,360	100
Cryptophyceae (≥ 20 µm)	n.d.	574	8,760	11
Euglenophyceae	**n.d.**	**4,823**	**41,610**	**50**
Euglena spp. (10 – 20 µm)	n.d.	156	2,920	7
Euglena spp. (20 – 50 µm)	n.d.	652	8,030	14
Eutreptiella braarudii Throndsen	n.d.	26	730	4
Eutreptiella eupharyngea Moestrup & R.E.Norris	n.d.	495	11,680	11
Eutreptiella gymnastica Throndsen	n.d.	626	3,650	36
Eutreptiella spp. (10 – 20 µm)	n.d.	417	4,380	21
Eutreptiella spp. (20 – 50 µm)	n.d.	391	4,380	29
Euglenophyceae (10 – 20 µm)	n.d.	417	3,650	21
Euglenophyceae (20 – 50 µm)	n.d.	1,564	16,060	29
Euglenophyceae (≥ 50 µm)	n.d.	78	2,190	4
Prasinophyceae	**n.d.**	**244,863**	**3,266,750**	**89**
Pseudoscourfieldia marina (J.Throndsen) Manton	n.d.	183	2,190	14

Pyramimonas sp. 1	n.d.	156	4,380	4
Pyramimonas sp. 5	n.d.	104	1,460	7
Pyramimonas sp. 6	n.d.	1,278	6,570	57
Pyramimonas spp. (2 – 5 µm)	n.d.	88,539	519,760	89
Pyramimonas spp. (5 – 10 µm)	n.d.	152,309	2,817,800	89
Pyramimonas spp. (10 – 20 µm)	n.d.	287	4,380	11
Prasinophyceae (5 – 10 µm)	n.d.	2,008	32,120	21
Prymnesiophyceae	**1,460**	**30,165**	**66,430**	**100**
Chrysochromulina spp. (2 – 5 µm) [a, b]	n.d.	9,646	24,820	82
Chrysochromulina spp. (5 – 10 µm) [a, b]	n.d.	9,360	29,200	96
Phaeocystis pouchetii (palmelloid stage) (Hariot) Lagerheim [b]	n.d.	26	730	4
Prymnesiophyceae (2 – 5 µm)	n.d.	5032	14,600	79
Prymnesiophyceae (5 – 10 µm)	n.d.	6,101	12,410	96
Unidentified flagellates	**294,920**	**808,553**	**2,330,890**	**100**
Flagellate sp. 1	n.d.	26	730	4
Flagellate sp. 15	n.d.	626	15,330	11
Flagellates (2 – 5 µm)	201,480	611,427	1,898,000	100
Flagellates (5 – 10 µm)	49,640	183,074	540,200	100
Flagellates (10 – 20 µm)	n.d.	13,270	24,820	96
Flagellates (≥ 20 µm)	n.d.	130	2,190	11
Photosynthetic ciliates	**n.d.**	**16,842**	**420,480**	**64**
Mesodinium rubrum Lohmann [a]	n.d.	16,842	420,480	64
Cyanophyceae	**n.d.**	**51,335**	**675,250**	**61**
Anabaena spp. [a, b]	n.d.	5,996	101,470	14
Chroococcus spp. (2 – 5 µm)	n.d.	365	7,300	7
Cyanodictyon cf. *planctonicum* B.A.Mayer	n.d.	600	16,790	4
Dolichospermum spp. [b]	n.d.	7,769	217,540	4

Lyngbya spp. [a, b]	n.d.	5,996	167,900	4
Merismopedia cf. *tenuissima* Lemmermann	n.d.	626	17,520	4
Merismopedia cf. *tranquilla* (Ehrenberg) Trevisan	n.d.	417	11,680	4
Merismopedia spp.	n.d.	1,695	24,820	14
Oscillatoria spp. [a]	n.d.	521	14,600	4
Cyanophyceae (2 – 5 µm, colony)	n.d.	11,784	155,490	21
Cyanophyceae (2 – 5 µm, filament)	n.d.	11,471	102,930	50
Cyanophyceae (5 – 10 µm, solitary)	n.d.	26	730	4
Cyanophyceae (5 – 10 µm, colony)	n.d.	130	3,650	4
Cyanophyceae (5 – 10 µm, filament)	n.d.	3,468	84,680	7
Cyanophyceae (10 – 20 µm, solitary)	n.d.	78	1,460	7
Cyanophyceae (10 – 20 µm, filament)	n.d.	391	10,950	4
Total number of species		**106**		
Total number of genera		**94**		
Total number of taxonomic entries		**224**		

[*] Complex composed of *Synedra*, *Fragilaria*, *Ulnaria*, *Ctenophora* and *Grammonema*.

[**] Complex composed of *Preperidinium*, *Diplopelta*, *Diplosalopsis*, *Oblea* and *Boreadinium*.

[a] Potentially harmful taxa according to Bates et al. (2020)

[b] Potentially harmful taxa according to Lundholm et al. (2009)

Table S3. Summary of mean values (± standard deviation) for environmental and biological variables measured in the surface waters for five groups of stations with taxonomically similar phytoplankton classes (determined with the group-average clustering) during early summer. The Kruskal-Wallis test (with p-value) and Dunn's post hoc test were performed to seek differences between groups for each variable (letters depict significant differences between groups where a<b<c). n.s.: non significant. PicoPCcyan: pico-phycocyanin-containing cyanobacteria, NanoPCcyan: nano-phycocyanin-containing cyanobacteria, PicoPEcyan: pico-phycoerythrin-containing cyanobacteria, NanoPEcyan: nano-phycoerythrin-containing cyanobacteria, Picoeuk: photosynthetic picoeukaryotes, Nanoeuk: photosynthetic nanoeukaryotes.

Variable	Group 1 (n = 79)		Group 2 (n = 21)		Group 3 (n = 6)		Group 4 (n = 4)		Group 5 (n = 4)		p-value
Temperature (°C)	11.45 ± 3.04	bc	7.03 ± 2.52	a	10.60 ± 3.22	b	16.39 ± 1.22	c	14.72 ± 1.81	c	p < 0.001
Salinity (psu)	12.65 ± 6.96	b	16.70 ± 2.57	c	5.25 ± 3.40	a	13.05 ± 3.18	abc	16.43 ± 0.97	bc	p < 0.01
Secchi depth (m)	1.41 ± 0.91	a	2.05 ± 0.79	b	1.33 ± 0.71	ab	0.68 ± 0.27	a	0.74 ± 0.15	a	p < 0.01
NO_3+NO_2 (µM)	0.32 ± 0.59	a	0.38 ± 0.47	a	0.57 ± 0.54	a	0.11 ± 0.02	a	0.06 ± 0.04	a	n.s.
PO_4 (µM)	0.16 ± 0.08	ab	0.22 ± 0.09	c	0.09 ± 0.07	a	0.15 ± 0.01	abc	0.21 ± 0.05	bc	p < 0.01
$Si(OH)_4$ (µM)	18.08 ± 9.39	a	18.24 ± 4.85	a	24.97 ± 8.38	a	19.34 ± 3.65	a	12.47 ± 2.40	a	n.s.
$a_{CDOM}(440)$ (m^{-1})	3.13 ± 1.96	a	2.31 ± 0.72	a	3.27 ± 2.37	ab	3.90 ± 0.25	b	2.26 ± 0.35	ab	n.s.
SPM (mg L^{-1})	11.00 ± 18.00	b	2.83 ± 1.51	a	9.34 ± 10.34	b	13.02 ± 6.78	b	8.54 ± 0.85	b	p < 0.001
TChl *a* (µg L^{-1})	1.59 ± 0.84	a	2.15 ± 1.03	b	2.94 ± 1.23	b	1.61 ± 0.60	ab	2.76 ± 1.31	b	p < 0.001
Pheo (µg L^{-1})	0.14 ± 0.11	a	0.80 ± 0.61	b	0.14 ± 0.05	a	0.10 ± 0.04	a	0.11 ± 0.06	a	p < 0.01
PicoPCcyan (cells mL^{-1})	6,702 ± 15,027	b	148 ± 237	a	9,725 ± 21,701	b	9,760 ± 10,769	b	4,880 ± 3,233	b	p < 0.001
NanoPCcyan (cells mL^{-1})	315 ± 683	b	17 ± 27	a	472 ± 734	b	184 ± 297	ab	39 ± 17	ab	p < 0.001
PicoPEcyan (cells mL^{-1})	483 ± 1,904	a	11 ± 11	a	19 ± 25	a	0 ± 0	a	36 ± 24	a	n.s.
NanoPEcyan (cells mL^{-1})	17 ± 22	a	21 ± 24	a	15 ± 31	a	2 ± 3	a	22 ± 29	a	n.s.
Picoeuk (cells mL^{-1})	19,144 ± 25,471	b	3,540 ± 4,077	a	8,944 ± 9,136	ab	137,610 ± 1,750	c	26,358 ± 14,316	bc	p < 0.001
Nanoeuk (cells mL^{-1})	6,565 ± 6,085	a	3,671 ± 2,585	a	7,563 ± 7,755	a	15,270 ± 5,499	b	9,835 ± 3,109	a	p < 0.01

Table S4. Summary of mean values (± standard deviation) for environmental and biological variables measured in the surface waters for four groups of stations with taxonomically similar phytoplankton classes (determined with the group-average clustering) during late summer. The Kruskal-Wallis test (with p-value) and Dunn's post hoc test were performed to seek differences between groups for each variable (letters depict significant differences between groups where a<b<c). n.s.: non significant. Abbreviations are defined in Table S3.

Variable	Group 1 (n = 55)		Group 2 (n = 10)		Group 3 (n = 2)		Group 4 (n = 1)		p-value
Temperature (°C)	11.57 ± 1.65	a	10.73 ± 0.64	a	14.68 ± 0.59	b	12.20	ab	p < 0.05
Salinity (psu)	17.86 ± 5.79	b	5.79 ± 8.47	a	9.50 ± 0.57	ab	2.90	ab	p < 0.001
Secchi depth (m)	2.17 ± 1.29	a	2.34 ± 0.93	a	1.35 ± 0.32	a	1.17	a	n.s.
NO_3+NO_2 (µM)	0.21 ± 0.26	a	1.16 ± 0.87	b	0.10 ± 0.03	ab	0.06	ab	p < 0.05
PO_4 (µM)	0.18 ± 0.07	b	0.06 ± 0.07	a	0.03 ± 0.01	a	0.03	ab	p < 0.001
$Si(OH)_4$ (µM)	17.98 ± 6.84	a	26.13 ± 7.41	b	33.39 ± 0.32	b	18.30	ab	p < 0.01
$a_{CDOM}(440)$ (m^{-1})	1.78 ± 0.69	a	1.80 ± 0.24	ab	5.21 ± 0.41	b	1.79	ab	p < 0.05
SPM (mg L^{-1})	4.81 ± 3.39	a	4.76 ± 2.77	a	2.72 ± 0.42	a	3.68	a	n.s.
TChl *a* (µg L^{-1})	1.40 ± 0.80	a	1.17 ± 0.45	a	1.44 ± 0.48	a	7.31	a	n.s.
Pheo (µg L^{-1})	0.10 ± 0.08	a	0.21 ± 0.22	a	0.08 ± 0.05	a	0.31	a	n.s.
PicoPCcyan (cells mL^{-1})	17,066 ± 29,948	a	2,273 ± 290	a	22,515 ± 19,347	b	5,989	ab	p < 0.05
NanoPCcyan (cells mL^{-1})	255 ± 263	a	416 ± 111	b	1,342 ± 67	b	678	ab	p < 0.01
PicoPEcyan (cells mL^{-1})	420 ± 1 264	a	55 ± 36	a	8 ± 4	a	78	a	n.s.
NanoPEcyan (cells mL^{-1})	45 ± 49	a	25 ± 23	a	17 ± 16	a	50	a	n.s.
Picoeuk (cells mL^{-1})	20,998 ± 19,378	b	3,345 ± 3,101	a	25,247 ± 939	b	4,617	ab	p < 0.001
Nanoeuk (cells mL^{-1})	5,645 ± 3,761	b	3,175 ± 1,875	a	9,703 ± 617	b	5,222	ab	p < 0.05

RÉFÉRENCES

Alou-Font, E., C.-J. Mundy, S. Roy, M. Gosselin, and S. Agustí. 2013. Snow cover affects ice algal pigment composition in the coastal Arctic Ocean during spring. Marine Ecology Progress Series. 474: 89–104. doi:10.3354/meps10107

Alou-Font, E., S. Roy, S. Agustí, and M. Gosselin. 2016. Cell viability, pigments and photosynthetic performance of Arctic phytoplankton in contrasting ice-covered and open-water conditions during the spring-summer transition. Marine Ecology Progress Series. 543: 89–106. doi:10.3354/meps11562

Andrews, J., D. Babb, and D. G. Barber. 2018. Climate change and sea ice: shipping in Hudson Bay, Hudson Strait, and Foxe Basin (1980–2016). Elementa: Science of the Anthropocene. 6(19). doi:10.1525/elementa.281

Ansotegui, A., A. Sarobe, J. M. Trigueros, I. Urrutxurtu, and E. Orive. 2003. Size distribution of algal pigments and phytoplankton assemblages in a coastal - estuarine environment: contribution of small eukaryotic algae. Journal of Plankton Research. 25(4): 341–355. doi:10.1093/plankt/25.4.341

Araújo, C. A. S., C. Belzile, J.-É. Tremblay, and S. Bélanger. 2022. Environmental niches and seasonal succession of phytoplankton assemblages in a subarctic coastal bay: Applications to remote sensing estimates. Frontier in Marine Science. 9: 1001098. doi: 10.3389/fmars.2022.1001098

Ardyna, M., C. Mundy, M. M. Mills, L. Oziel, P.-L. Grondin, L. Lacour, G. Verin, G. Van Dijken, J. Ras, E. Alou-Font, M. Babin, M. Gosselin, J.-É. Tremblay, P. Raimbault, P. Assmy, M. Nicolaus, H. Claustre, and K. R. Arrigo. 2020. Environmental drivers of under-ice phytoplankton bloom dynamics in the Arctic Ocean. Elementa: Science of the Anthropocene. 8: 30. doi:10.1525/elementa.430

Armstrong, R. A., C. Lee, J. I. Hedges, S. Honjo, and S. G. Wakeham. 2001. A new, mechanistic model for organic carbon fluxes in the ocean based on the quantitative association of POC with ballast minerals. Deep Sea Research Part II: Topical Studies in Oceanography. 49(1-3): 219–236. doi:10.1016/S0967-0645(01)00101-1

Arrigo, K. R. 2017. Sea ice as a habitat for primary producers. In D. N. Thomas (Ed.), Sea ice. Wiley-Blackwell, Oxford, U. K. (3rd ed., pp. 352–369). https://doi.org/10.1002/9781118778371

Arrigo, K. R., and G. L. van Dijken. 2015. Continued increases in Arctic Ocean primary production. Progress in Oceanography. 136: 60–70. doi:10.1016/j.pocean.2015.05.002

Balzano, S., D. Marie, P. Gourvil, and D. Vaulot. 2012. Composition of the summer photosynthetic pico and nanoplankton communities in the Beaufort Sea assessed by T-RFLP and sequences of the 18S rRNA gene from flow cytometry sorted samples. The ISME Journal. 6(8): 1480–1498. doi:10.1038/ismej.2011.213

Bates, S. S., D. G. Beach, L. A. Comeau, N. Haigh, N. I. Lewis, A. Locke, J. L. Martin, P. McCarron, C. H. McKenzie, C. Michel, C. O. Miles, M. Poulin, Q. Michael, W. A. Rourke, M. G. Scarratt, M. Starr, and T. Wells, 2020. Marine harmful algal blooms and phycotoxins of concern to Canada. Fisheries and Oceans Canada, Gulf Fisheries Centre, Canadian Technical Report of Fisheries and Aquatic Sciences No. 3384, pp. 1–323.

Battin, T. J., L. A. Kaplan, S. Findlay, C. S. Hopkinson, E. Marti, A. I. Packman, J. D. Newbold, and F. Sabater. 2008. Biophysical controls on organic carbon fluxes in fluvial networks. Nature Geoscience. 1(2): 95–100. doi:10.1038/ngeo101

Bazin, P., F. Jouenne, T. Friedl, A.-F. Deton-Cabanillas, B. Le Roy, and B. Véron. 2014. Phytoplankton diversity and community composition along the estuarine gradient of a temperate macrotidal ecosystem: combined morphological and molecular approaches. PloS ONE. 9(4): e94110. doi:10.1371/journal.pone.0094110

Bérard-Therriault, L., M. Poulin, and L. Bossé. 1999. Guide d'identification du phytoplancton marin de l'estuaire et du golfe du Saint-Laurent: incluant également certains protozoaires. Publication spéciale canadienne des sciences halieutiques et aquatiques. 128: 1–387.

Bhiry, N., A. Delwaide, M. Allard, Y. Bégin, L. Filion, M. Lavoie, C. Nozais, S. Payette, R. Pienitz, and É. Saulnier-Talbot. 2011. Environmental change in the Great Whale River region, Hudson Bay: Five decades of multidisciplinary research by Centre d'études nordiques (CEN). Écoscience. 18(3): 182–203. doi:10.2980/18-3-3469

Bidigare, R. R., T. J. Frank, C. Zastrow, and J. M. Brooks. 1986. The distribution of algal chlorophylls and their degradation products in the Southern Ocean. Deep Sea Research Part A. Oceanographic Research Papers. 33(7): 923–937. doi:10.1016/0198-0149(86)90007-5

Blais, M.-A., A. Matveev, C. Lovejoy, and W. F. Vincent. 2022. Size-fractionated microbiome structure in subarctic rivers and a coastal plume across DOC and salinity gradients. Frontiers in Microbiology: 4022. doi:10.3389/fmicb.2021.760282

Blough, N. V., and R. Del Vecchio. 2002. Chromophoric DOM in the coastal environment. In D. A. Hansell, and C. A. Carlson (Eds.), Biogeochemistry of marine dissolved organic matter. Elsevier Science, Amsterdam (pp. 509–546). https://doi.org/10.1016/B978-012323841-2/50012-9

Bock, N. A., S. Charvet, J. Burns, Y. Gyaltshen, A. Rozenberg, S. Duhamel, and E. Kim. 2021. Experimental identification and in silico prediction of bacterivory in green algae. The ISME Journal. 15(7): 1987–2000. doi:10.1038/s41396-021-00899-w

Bourrelly, P. 1970. Les algues d'eau douce. Initiation à la systématique. Tome III: Eugléniens, Peridiniens, Algues rouges et Algues bleues. N. Boubée & Cie, Paris.

Bracher, A., H. A. Bouman, R. J. Brewin, A. Bricaud, V. Brotas, A. M. Ciotti, L. Clementson, E. Devred, A. Di Cicco, and S. Dutkiewicz. 2017. Obtaining phytoplankton diversity from ocean color: a scientific roadmap for future development. Frontiers in Marine Science. 4: 55. doi:10.3389/fmars.2017.00055

Brito, A. C., C. Sá, C. R. Mendes, T. Brand, A. M. Dias, V. Brotas, and K. Davidson. 2015. Structure of late summer phytoplankton community in the Firth of Lorn (Scotland) using microscopy and HPLC-CHEMTAX. Estuarine, Coastal and Shelf Science. 167: 86–101. doi:10.1016/j.ecss.2015.07.006

Brown, R. D. 2010. Analysis of snow cover variability and change in Québec, 1948–2005. Hydrological Processes. 24(14): 1929–1954. doi:10.1002/hyp.7565

Brown, R. D., and R. O. Braaten. 1998. Spatial and temporal variability of Canadian monthly snow depths, 1946–1995. Atmosphere-Ocean. 36(1): 37–54. doi:10.1080/07055900.1998.9649605

Buitenhuis, E. T., W. K. Li, D. Vaulot, M. Lomas, M. Landry, F. Partensky, D. Karl, O. Ulloa, L. Campbell, and S. Jacquet. 2012. Picophytoplankton biomass distribution in the global ocean. Earth System Science Data. 4(1): 37–46. doi:10.5194/essd-4-37-2012

Burchard, H., H. M. Schuttelaars, and D. K. Ralston. 2018. Sediment trapping in estuaries. Annual Review of Marine Science. 10: 371–395. doi:10.1146/annurev-marine-010816-060535

Callieri, C. 2008. Picophytoplankton in freshwater ecosystems: the importance of small-sized phototrophs. Freshwater Reviews. 1(1): 1–28. doi:10.1608/FRJ-1.1.1

Carmack, E. C., M. Yamamoto-Kawai, T. W. Haine, S. Bacon, B. A. Bluhm, C. Lique, H. Melling, I. V. Polyakov, F. Straneo, and M. L. Timmermans. 2016. Freshwater and its role in the Arctic Marine System: Sources, disposition, storage, export, and physical and biogeochemical consequences in the Arctic and global oceans. Journal

of Geophysical Research: Biogeosciences. 121(3): 675–717. doi:10.1002/2015JG003140

Catlett, D., P. G. Matson, C. A. Carlson, E. G. Wilbanks, D. A. Siegel, and M. D. Iglesias-Rodriguez. 2020. Evaluation of accuracy and precision in an amplicon sequencing workflow for marine protist communities. Limnology and Oceanography: Methods. 18(1): 20–40. doi:10.1002/lom3.10343

Chakdar, H., and S. Pabbi. 2016. Cyanobacterial phycobilins: production, purification, and regulation. In P. Shukla (Ed.), Frontier Discoveries and Innovations in Interdisciplinary Microbiology. Springer India, New Delhi (pp. 45–69). https://doi.org/10.1007/978-81-322-2610-9_4

Chapman, W. L., and J. E. Walsh. 1993. Recent variations of sea ice and air temperature in high latitudes. Bulletin of the American Meteorological Society. 74(1): 33–48. doi:10.1175/1520-0477(1993)074<0033:RVOSIA>2.0.CO;2

Chisholm, S. W. 1992. Phytoplankton size. In P. G. Falkowski, A. D. Woodhead, and K. Vivirito (Eds.), Primary productivity and biogeochemical cycles in the sea. Springer New York, NY (pp. 213–237). https://doi.org/10.1007/978-1-4899-0762-2_12

Choi, C. J., M. L. Brosnahan, T. R. Sehein, D. M. Anderson, and D. L. Erdner. 2017. Insights into the loss factors of phytoplankton blooms: The role of cell mortality in the decline of two inshore *Alexandrium* blooms. Limnology and Oceanography. 62(4): 1742–1753. doi:10.1002/lno.10530

Clair, T. A., B. G. Warner, R. Robarts, H. Murkin, J. Lilley, L. Mortsch, and C. Rubec. 1998. Canadian inland wetlands and climate change. In G. Koshida, and W. Avis (Eds.), The Canada country study: climate impacts and adaptation. National sectoral volume. Environment Canada, Ottawa, Ontario, Canada. (pp. 189–218).

Clarke, K., and R. Warwick. 2001. A further biodiversity index applicable to species lists: variation in taxonomic distinctness. Marine Ecology Progress Series. 216: 265–278. doi:10.3354/meps216265

Clarke, K. R. 1993. Non-parametric multivariate analyses of changes in community structure. Australian Journal of Ecology. 18(1): 117–143. doi:10.1111/j.1442-9993.1993.tb00438.x

Cole, J. J., Y. T. Prairie, N. F. Caraco, W. H. McDowell, L. J. Tranvik, R. G. Striegl, C. M. Duarte, P. Kortelainen, J. A. Downing, and J. J. Middelburg. 2007. Plumbing the global carbon cycle: integrating inland waters into the terrestrial carbon budget. Ecosystems. 10: 172–185. doi:10.1007/s10021-006-9013-8

Costanzo, R. 2023. Étude de la variabilité spatio-temporelle des apports d'eau douce dans la baie James. Mémoire de maîtrise. Université du Québec à Rimouski.

Coupel, P., A. Matsuoka, D. Ruiz-Pino, M. Gosselin, D. Marie, J.-É. Tremblay, and M. Babin. 2015a. Pigment signatures of phytoplankton communities in the Beaufort Sea. Biogeosciences. 12(4): 991–1006. doi:10.5194/bg-12-991-2015

Coupel, P., D. Ruiz-Pino, M.-A. Sicre, J. Chen, S. Lee, N. Schiffrine, H. Li, and J.-C. Gascard. 2015b. The impact of freshening on phytoplankton production in the Pacific Arctic Ocean. Progress in Oceanography. 131: 113–125. doi:10.1016/0198-0149(86)90007-5

Curtis, J., G. Wendler, R. Stone, and E. Dutton. 1998. Precipitation decrease in the western Arctic, with special emphasis on Barrow and Barter Island, Alaska. International Journal of Climatology. 18(15): 1687–1707. doi:10.1002/(SICI)1097-0088(199812)18:15<1687::AID-JOC341>3.0.CO;2-2

Dashkova, V., D. Malashenkov, N. Poulton, I. Vorobjev, and N. S. Barteneva. 2017. Imaging flow cytometry for phytoplankton analysis. Methods. 112: 188–200. doi:10.1016/j.ymeth.2016.05.007

de Melo, M. L., M.-L. Gerárdin, C. Fink-Mercier, and P. A. del Giorgio. 2022. Patterns in riverine carbon, nutrient and suspended solids export to the Eastern James Bay: links to climate, hydrology and landscapes. Biogeochemistry. 161: 291–233. doi:10.1007/s10533-022-00983-z

De Sève, M. 1993. Diatom bloom in the tidal freshwater zone of a turbid and shallow estuary, Rupert Bay (James Bay, Canada). Hydrobiologia. 269(1): 225–233. doi:10.1007/BF00028021

Del Bel Belluz, J., M. A. Peña, J. M. Jackson, and N. Nemcek. 2021. Phytoplankton composition and environmental drivers in the northern Strait of Georgia (Salish Sea), British Columbia, Canada. Estuaries and Coasts. 44: 1419-1439. doi:10.1007/s12237-020-00858-2

Déry, S. J., T. J. Mlynowski, M. A. Hernández-Henríquez, and F. Straneo. 2011. Interannual variability and interdecadal trends in Hudson Bay streamflow. Journal of Marine Systems. 88(3): 341–351. doi:10.1016/j.jmarsys.2010.12.002

Déry, S. J., T. A. Stadnyk, M. K. MacDonald, and B. Gauli-Sharma. 2016. Recent trends and variability in river discharge across northern Canada. Hydrology and Earth System Sciences. 20(12): 4801–4818. doi:10.5194/hess-20-4801-2016

Dimier, C., F. Corato, F. Tramontano, and C. Brunet. 2007. Photoprotection and xanthophyll-cycle activity in three marine diatoms. Journal of Phycology. 43(5): 937–947. doi:10.1111/j.1529-8817.2007.00381.x

Domingues, R. B., T. P. Anselmo, A. B. Barbosa, U. Sommer, and H. M. Galvão. 2011. Light as a driver of phytoplankton growth and production in the freshwater tidal zone of a turbid estuary. Estuarine, Coastal and Shelf Science. 91(4): 526–535. doi:10.1016/j.ecss.2010.12.008

Domingues, R. B., A. B. Barbosa, U. Sommer, and H. M. Galvão. 2012. Phytoplankton composition, growth and production in the Guadiana estuary (SW Iberia): Unraveling changes induced after dam construction. Science of the Total Environment. 416: 300–313. doi:10.1016/j.scitotenv.2011.11.043

DuRand, M. D., R. E. Green, H. M. Sosik, and R. J. Olson. 2002. Diel variations in optical properties of *Micromonas pusilla* (Prasinophyceae). Journal of Phycology. 38(6): 1132–1142. doi:10.1046/j.1529-8817.2002.02008.x

Duthie, H. C. 1979. Limnology of subarctic Canadian lakes and some effects of impoundment. Arctic and Alpine Research. 11(2): 145–158. doi:10.1080/00040851.1979.12004127

Eisner, L. B., and T. J. Cowles. 2005. Spatial variations in phytoplankton pigment ratios, optical properties, and environmental gradients in Oregon coast surface waters. Journal of Geophysical Research: Oceans. 110(C10): 1–17. doi:10.1029/2004JC002614

El-Sabh, M. I., and V. G. Koutitonsky. 1977. An oceanographic study of James Bay before the completion of the La Grande hydroelectric complex. Arctic. 30(3): 169–186.

Estrada, R., M. Harvey, M. Gosselin, M. Starr, P. S. Galbraith, and F. Straneo. 2012. Late-summer zooplankton community structure, abundance, and distribution in the Hudson Bay system (Canada) and their relationships with environmental conditions, 2003–2006. Progress in Oceanography. 101(1): 121–145. doi:10.1016/j.pocean.2012.02.003

Évrard, A., C. Fink-Mercier, V. Galindo, U. Neumeier, M. Gosselin, and H. Xie. 2023. Regulated *vs.* unregulated rivers: Impacts on CDOM dynamics in the eastern James Bay. Marine Chemistry. 256: 104309. doi:10.1016/j.marchem.2023.104309

Falkowski, P. G., and T. G. Owens. 1980. Light—shade adaptation: two strategies in marine phytoplankton. Plant Physiology. 66(4): 592–595. doi:10.1104/pp.66.4.592

Falkowski, P. G., and J. A. Raven. 2007. Aquatic photosynthesis (2nd ed.). Princeton University Press, Princeton.

Ferland, J., M. Gosselin, and M. Starr. 2011. Environmental control of summer primary production in the Hudson Bay system: The role of stratification. Journal of Marine Systems. 88(3): 385–400. doi:10.1016/j.jmarsys.2011.03.015

Ferreira, A., Á. M. Ciotti, C. R. B. Mendes, J. Uitz, and A. Bricaud. 2017. Phytoplankton light absorption and the package effect in relation to photosynthetic and photoprotective pigments in the northern tip of Antarctic Peninsula. Journal of Geophysical Research: Oceans. 122(9): 7344–7363. doi:10.1002/2017JC012964

Findlay, S. E. 2005. Increased carbon transport in the Hudson River: unexpected consequence of nitrogen deposition? Frontiers in Ecology and the Environment. 3(3): 133–137. doi:10.1890/1540-9295(2005)003[0133:ICTITH]2.0.CO;2

Finkel, Z. V. 2001. Light absorption and size scaling of light-limited metabolism in marine diatoms. Limnology and Oceanography. 46(1): 86–94. doi:10.4319/lo.2001.46.1.0086

Foy, M. G., and S. I. C. Hsiao, 1976. Phytoplankton data from James Bay, 1974. Fisheries and Marine Service, Research and Development, Technical Report 631: 1–73.

Freeman, C., C. Evans, D. Monteith, B. Reynolds, and N. Fenner. 2001. Export of organic carbon from peat soils. Nature. 412(6849): 785–785. doi:10.1038/35090628

Gagnon, A. S., and W. A. Gough. 2005. Climate change scenarios for the Hudson Bay region: an intermodel comparison. Climatic Change. 69(2-3): 269–297. doi:10.1007/s10584-005-1815-8

Galbraith, P. S., and P. Larouche. 2011. Sea-surface temperature in Hudson Bay and Hudson Strait in relation to air temperature and ice cover breakup, 1985–2009. Journal of Marine Systems. 88(3): 463–475. doi:10.1016/j.jmarsys.2011.06.006

Gallegos, C. L., D. L. Correll, and J. W. Pierce. 1990. Modeling spectral diffuse attenuation, absorption, and scattering coefficients in a turbid estuary. Limnology and Oceanography. 35(7): 1486–1502. doi:10.4319/lo.1990.35.7.1486

Gameiro, C., J. Zwolinski, and V. Brotas. 2011. Light control on phytoplankton production in a shallow and turbid estuarine system. Hydrobiologia. 669: 249–263. doi:10.1007/s10750-011-0695-3

Gattuso, J.-P., B. Gentili, C. M. Duarte, J. Kleypas, J. J. Middelburg, and D. Antoine. 2006. Light availability in the coastal ocean: impact on the distribution of benthic photosynthetic organisms and their contribution to primary production. Biogeosciences. 3(4): 489–513. doi:10.5194/bg-3-489-2006

Geider, R. J., H. L. MacIntyre, and T. M. Kana. 1996. A dynamic model of photoadaptation in phytoplankton. Limnology and Oceanography. 41(1): 1–15. doi:10.4319/lo.1996.41.1.0001

Gibb, S. W., D. G. Cummings, X. Irigoien, R. G. Barlow, R. Fauzi, and C. Mantoura. 2001. Phytoplankton pigment chemotaxonomy of the northeastern Atlantic. Deep Sea Research Part II: Topical Studies in Oceanography. 48(4-5): 795–823. doi:10.1016/S0967-0645(00)00098-9

Goericke, R., and J. P. Montoya. 1998. Estimating the contribution of microalgal taxa to chlorophyll *a* in the field-variations of pigment ratios under nutrient- and light-limited growth. Marine Ecology Progress Series. 169: 97–112. doi:10.3354/meps169097

Goldman, J. C., and M. R. Dennett. 1985. Susceptibility of some marine phytoplankton species to cell breakage during filtration and post-filtration rinsing. Journal of experimental marine biology and ecology. 86(1): 47–58. doi:10.1016/0022-0981(85)90041-3

Goodenough, U., R. Roth, T. Kariyawasam, A. He, and J.-H. Lee. 2018. Epiplasts: membrane skeletons and epiplastin proteins in euglenids, glaucophytes, cryptophytes, ciliates, dinoflagellates, and apicomplexans. MBio. 9(5): 10–1128. doi:10.1128/mbio.02020-18

Gough, W. A., and E. Wolfe. 2001. Climate change scenarios for Hudson Bay, Canada, from general circulation models. Arctic. 5(2): 142–148.

Graff, J. R., T. K. Westberry, A. J. Milligan, M. B. Brown, G. D. Olmo, K. M. Reifel, and M. J. Behrenfeld. 2016. Photoacclimation of natural phytoplankton communities. Marine Ecology Progress Series. 542: 51–62. doi:10.3354/meps11539

Granskog, M. A., Z. Z. A. Kuzyk, K. Azetsu-Scott, and R. W. Macdonald. 2011. Distributions of runoff, sea-ice melt and brine using $\delta^{18}O$ and salinity data—A new view on freshwater cycling in Hudson Bay. Journal of Marine Systems. 88(3): 362–374. doi:10.1016/j.jmarsys.2011.03.011

Grasshoff, K., K. Kremling, and M. Ehrhardt. 1999. Methods of seawater analysis. Wiley-VCH, New-York. (3rd ed)

Grobbelaar, J. U. 1990. Modelling phytoplankton productivity in turbid waters with small euphotic to mixing depth ratios. Journal of Plankton Research. 12(5): 923–931. doi:10.1093/plankt/12.5.923

Gustafson Jr, D. E., D. K. Stoecker, M. D. Johnson, W. F. Van Heukelem, and K. Sneider. 2000. Cryptophyte algae are robbed of their organelles by the marine ciliate *Mesodinium rubrum*. Nature. 405(6790): 1049–1052. doi:10.1038/35016570

Hackett, J. D., L. Maranda, H. S. Yoon, and D. Bhattacharya. 2003. Phylogenetic evidence for the cryptophyte origin of the plastid of *Dinophysis* (dinophysiales, dinophyceae). Journal of Phycology. 39(2): 440–448. doi:10.1046/j.1529-8817.2003.02100.x

Hallegraeff, G., and S. Jeffrey. 1984. Tropical phytoplankton species and pigments of continental shelf waters of north and north-west Australia. Marine Ecology Progress Series. 20(1): 59–74.

Hallegraeff, G. M. 2010. Ocean climate change, phytoplankton community responses, and harmful algal blooms: a formidable predictive challenge. Journal of Phycology. 46(2): 220–235. doi:10.1111/j.1529-8817.2010.00815.x

Hammer, A., R. Schumann, and H. Schubert. 2002. Light and temperature acclimation of *Rhodomonas salina* (Cryptophyceae): photosynthetic performance. Aquatic Microbial Ecology. 29(3): 287–296. doi:10.3354/ame029287

Hein, M., M. F. Pedersen, and K. Sand-Jensen. 1995. Size-dependent nitrogen uptake in micro- and macroalgae. Marine Ecology Progress Series. 118(1): 247–253. doi:10.3354/meps157097

Hendry, G. 1993. Plant pigments. In P. Lea, and R. C. Leegood (Eds.), Plant biochemistry and molecular biology. Wiley, Chichester, England (2nd ed., pp. 181–196).

Henriksen, P., B. Riemann, H. Kaas, H. M. Sørensen, and H. L. Sørensen. 2002. Effects of nutrient-limitation and irradiance on marine phytoplankton pigments. Journal of Plankton Research. 24(9): 835–858. doi:10.1093/plankt/24.9.835

Hernández-Henríquez, M. A., T. J. Mlynowski, and S. J. Déry. 2010. Reconstructing the natural streamflow of a regulated river: A case study of La Grande Rivière, Québec, Canada. Canadian Water Resources Journal. 35(3): 301–316. doi:10.4296/cwrj3503301

Hernando, M., I. R. Schloss, G. Malanga, G. O. Almandoz, G. A. Ferreyra, M. B. Aguiar, and S. Puntarulo. 2015. Effects of salinity changes on coastal Antarctic phytoplankton physiology and assemblage composition. Journal of Experimental Marine Biology and Ecology. 466: 110–119. doi:10.1016/j.jembe.2015.02.012

Higgins, H. W., S. W. Wright, and L. Schluter. 2011. Quantitative interpretation of chemotaxonomic pigment data. In S. Roy, C. A. Llewellyn, E. S. Egeland, andG. Johnsen (Eds.), Phytoplankton pigments: characterization, chemotaxonomy and applications in Oceanography. Cambridge University Press, United Kingdom (pp. 257–313).

Hillebrand, H., C. D. Dürselen, D. Kirschtel, U. Pollingher, and T. Zohary. 1999. Biovolume calculation for pelagic and benthic microalgae. Journal of Phycology. 35(2): 403–424. doi:10.1046/j.1529-8817.1999.3520403.x

Hochheim, K., and D. Barber. 2010. Atmospheric forcing of sea ice in Hudson Bay during the fall period, 1980–2005. Journal of Geophysical Research: Oceans. 115(C05009). doi:10.1029/2009JC005334

Holmes, R. M., J. W. McClelland, B. J. Peterson, S. E. Tank, E. Bulygina, T. I. Eglinton, V. V. Gordeev, T. Y. Gurtovaya, P. A. Raymond, and D. J. Repeta. 2012. Seasonal and annual fluxes of nutrients and organic matter from large rivers to the Arctic Ocean and surrounding seas. Estuaries and Coasts. 35: 369–382. doi:10.1007/s12237-011-9386-6

Hop, H., M. Vihtakari, B. A. Bluhm, P. Assmy, M. Poulin, R. Gradinger, I. Peeken, C. von Quillfeldt, L. M. Olsen, and L. Zhitina. 2020. Changes in sea-ice protist diversity with declining sea ice in the Arctic Ocean from the 1980s to 2010s. Frontiers in Marine Science. 7: 243. doi:10.3389/fmars.2020.00243

Hopwood, M. J., D. Carroll, T. Dunse, A. Hodson, J. M. Holding, J. L. Iriarte, S. Ribeiro, E. P. Achterberg, C. Cantoni, and D. F. Carlson. 2020. How does glacier discharge affect marine biogeochemistry and primary production in the Arctic? The Cryosphere. 14(4): 1347–1383. doi:10.5194/tc-14-1347-2020

Horvat, C., D. R. Jones, S. Iams, D. Schroeder, D. Flocco, and D. Feltham. 2017. The frequency and extent of sub-ice phytoplankton blooms in the Arctic Ocean. Science Advances. 3(3): e1601191. doi:10.1126/sciadv.1601191

Ibarbalz, F. M., N. Henry, M. C. Brandão, S. Martini, G. Busseni, H. Byrne, L. P. Coelho, H. Endo, J. M. Gasol, and A. C. Gregory. 2019. Global trends in marine plankton diversity across kingdoms of life. Cell. 179(5): 1084–1097. doi:10.1016/j.cell.2019.10.008

Ingram, R. G., L. Legendre, Y. Simard, and S. Lepage. 1985. Phytoplankton response to freshwater runoff: The diversion of the Eastmain River, James Bay. Canadian Journal of Fisheries and Aquatic Sciences. 42(6): 1216–1221. doi:10.1139/f85-149

Irigoien, X., B. Meyer, R. Harris, and D. Harbour. 2004. Using HPLC pigment analysis to investigate phytoplankton taxonomy: the importance of knowing your species. Helgoland Marine Research. 58(2): 77–82. doi:10.1007/s10152-004-0171-9

Irwin, A. J., and Z. V. Finkel. 2018. Phytoplankton functional types: a trait perspective. In J. M. Gasol, and D. L. Kirchman (Eds.), Microbial ecology of the oceans. John Wiley & Sons, Hoboken, NJ (pp. 435–465). https://doi.org/10.1101/148312

Jacquemot, L., D. Kalenitchenko, L. C. Matthes, A. Vigneron, C. J. Mundy, J.-É. Tremblay, and C. Lovejoy. 2021. Protist communities along freshwater–marine transition zones in Hudson Bay (Canada). Elementa: Science of the Anthropocene. 9(1): 00111. doi:10.1525/elementa.2021.00111

Jeffrey, S. 1961. Chromatographic separation of chlorophylls and carotenoids from marine algae. Biochemical Journal. 80(2): 336–342. doi:10.1042/bj0800336

Jeffrey, S. 1968. Quantitative thin-layer chromatography of chlorophylls and carotenoids from marine algae. Biochimica et Biophysica Acta (BBA)-Bioenergetics. 162(2): 271–285. doi:10.1016/0005-2728(68)90109-6

Jeffrey, S., and G. Hallegraeff. 1987. Chlorophyllase distribution in ten classes of phytoplankton: a problem for chlorophyll analysis. Marine Ecology Progress Series. 35(3): 293–304.

Jeffrey, S., S. W. Wright, and M. Zapata. 2011. Microalgal classes and their signature pigments. In S. Roy, C. A. Llewellyn, E. S. Egeland, and G. Johnsen (Eds.), Phytoplankton pigments: characterization, chemotaxonomy and applications in Oceanography. Cambridge University Press, United Kingdom (pp. 3–77).

Jimenez, V., J. A. Burns, F. Le Gall, F. Not, and D. Vaulot. 2021. No evidence of phago-mixotrophy in *Micromonas polaris* (Mamiellophyceae), the dominant picophytoplankton species in the Arctic. Journal of Phycology. 57(2): 435–446. doi:10.1111/jpy.13125

John, D. M., B. A. Whitton, and A. J. Brook. 2011. The Freshwater Algal Flora of the British Isles: An Identification Guide to Freshwater and Terrestrial Algae. (2nd ed.). Natural History Museum and British Phycological Society.

Joosten, A. M. T. 2006. Flora of blue-green algae of Netherlands I. The non-filamentous species of inland waters. KNNV Publishing.

Kauko, H. M., A. K. Pavlov, G. Johnsen, M. A. Granskog, I. Peeken, and P. Assmy. 2019. Photoacclimation state of an Arctic underice phytoplankton bloom. Journal of Geophysical Research: Oceans. 124(3): 1750–1762. doi:10.1029/2018JC014777

Keller, W., A. M. Paterson, K. M. Rühland, and J. M. Blais. 2014. Introduction—environmental change in the Hudson and James Bay Region. Arctic, Antarctic, and Alpine Research. 46(1): 2–5. doi:10.1657/1938-4246-46.1.2

Kirk, J. T. O. 2011. Light and photosynthesis in aquatic ecosystems (3rd ed.). Cambridge University Press, Cambridge, UK.

Klauschies, T., B. Bauer, N. Aberle-Malzahn, U. Sommer, and U. Gaedke. 2012. Climate change effects on phytoplankton depend on cell size and food web structure. Marine Biology. 159: 2455–2478. doi:10.1007/s00227-012-1904-y

Klein, K. P., H. Lantuit, B. Heim, D. Doxaran, B. Juhls, I. Nitze, D. Walch, A. Poste, and J. E. Søreide. 2021. The Arctic Nearshore Turbidity Algorithm (ANTA)-A multi sensor turbidity algorithm for Arctic nearshore environments. Science of Remote Sensing. 4: 100036. doi:10.1016/j.srs.2021.100036

Komárek, J. 2013. Cyanoprokaryota. 3. Teil / Part 3: Heterocytous Genera. Süßwasserflora von Mitteleuropa Freshwater Flora of Central Europe. Springer Spektrum Akademischer Verlag Heidelberg.

Komárek, J., and K. Anagnostidis. 2008. Cyanoprokaryota. 1. Teil / Part 1: Chroococcales. Süßwasserflora von Mitteleuropa Freshwater Flora of Central Europe. Springer Spektrum Akademischer Verlag Heidelberg.

Kramer, S. J., L. M. Bolaños, D. Catlett, A. P. Chase, M. J. Behrenfeld, E. S. Boss, E. T. Crockford, S. J. Giovannoni, J. R. Graff, and N. Haëntjens. 2024. Toward a synthesis of phytoplankton communities composition methods for global-scale application. Limnology and Oceanography: Methods. doi:10.1002/lom3.10602

Krause-Jensen, D., P. Archambault, J. Assis, I. Bartsch, K. Bischof, K. Filbee-Dexter, K. H. Dunton, O. Maximova, S. B. Ragnarsdóttir, and M. K. Sejr. 2020. Imprint of climate change on pan-Arctic marine vegetation. Frontiers in Marine Science. 7: 617324. doi:10.3389/fmars.2020.617324

Kropuenske, L. R., M. M. Mills, G. L. van Dijken, S. Bailey, D. H. Robinson, N. A. Welschmeyer, and K. R. Arrigo. 2009. Photophysiology in two major Southern Ocean phytoplankton taxa: photoprotection in *Phaeocystis antarctica* and *Fragilariopsis cylindrus*. Limnology and Oceanography. 54(4): 1176–1196. doi:10.4319/lo.2009.54.4.1176

Kuczynska, P., M. Jemiola-Rzeminska, and K. Strzalka. 2015. Photosynthetic pigments in diatoms. Marine Drugs. 13(9): 5847–5881. doi:10.3390/md13095847

Kuzyk, Z. Z. A., R. W. Macdonald, J.-É. Tremblay, and G. A. Stern. 2010. Elemental and stable isotopic constraints on river influence and patterns of nitrogen cycling and biological productivity in Hudson Bay. Continental Shelf Research. 30(2): 163–176. doi:10.1016/j.csr.2009.10.014

Lannuzel, D., L. Tedesco, M. Van Leeuwe, K. Campbell, H. Flores, B. Delille, L. Miller, J. Stefels, P. Assmy, and J. Bowman. 2020. The future of Arctic sea-ice biogeochemistry and ice-associated ecosystems. Nature Climate Change. 10(11): 983–992. doi:10.1038/s41558-020-00940-4

Latasa, M. 2007. Improving estimations of phytoplankton class abundances using CHEMTAX. Marine Ecology Progress Series. 329: 13–21. doi:10.3354/meps329013

Latasa, M., R. Scharek, F. L. Gall, and L. Guillou. 2004. Pigment suites and taxonomic groups in Prasinophyceae. Journal of Phycology. 40(6): 1149–1155. doi:10.1111/j.1529-8817.2004.03136.x

Lawrenz, E., J. L. Pinckney, M. L. Ranhofer, H. L. MacIntyre, and T. L. Richardson. 2010. Spectral irradiance and phytoplankton community composition in a blackwater-dominated estuary, Winyah Bay, South Carolina, USA. Estuaries and Coasts. 33: 1186–1201. doi:10.1007/s12237-010-9310-5

Leblanc, M. L., M. I. O'Connor, Z. Z. A. Kuzyk, F. Noisette, K. E. Davis, E. Rabbitskin, L. L. Sam, U. Neumeier, R. Costanzo, and J. K. Ehn. 2022. Limited recovery following a massive seagrass decline in subarctic eastern Canada. Global Change Biology. 29(2): 432–450. doi:10.1111/gcb.16499

Lebrun, A., S. Comeau, F. Gazeau, and J.-P. Gattuso. 2022. Impact of climate change on Arctic macroalgal communities. Global and Planetary Change. 219: 103980. doi:10.1016/j.gloplacha.2022.103980

Lee, J., A. Tefs, V. Galindo, T. A. Stadnyk, M. Gosselin, and J.-É. Tremblay. 2023. Nutrient inputs from subarctic rivers into Hudson Bay. Elementa: Science of the Anthropocene. 11: 00085. doi:10.1525/elementa.2021.00085

Legendre, L., B. Robineau, M. Gosselin, C. Michel, R. Ingram, L. Fortier, J. Therriault, S. Demers, and D. Monti. 1996. Impact of freshwater on a subarctic coastal ecosystem under seasonal sea ice (southeastern Hudson Bay, Canada) II. Production and export of microalgae. Journal of Marine Systems. 7(2-4): 233–250. doi:10.1016/0924-7963(95)00007-0

Legendre, L., and Y. Simard. 1978. Dynamique estivale du phytoplancton dans l'estuaire de la baie de Rupert (baie de James). Naturaliste canadien. 105: 243–258.

Legendre, P., and L. Legendre. 2012. Numerical ecology. Elsevier.

Li, W. K., F. A. McLaughlin, C. Lovejoy, and E. C. Carmack. 2009. Smallest algae thrive as the Arctic Ocean freshens. Science. 326(5952): 539–539. doi:10.1126/science.1179798

Liu, K. K., L. Atkinson, C. Chen, S. Gao, J. Hall, R. Macdonald, L. T. McManus, and R. Quinones. 2000. Exploring continental margin carbon fluxes on a global scale. Eos, Transactions American Geophysical Union. 81(52): 641–644. doi:10.1029/EO081i052p00641-01

Llewellyn, C. A., J. R. Fishwick, and J. C. Blackford. 2005. Phytoplankton community assemblage in the English Channel: a comparison using chlorophyll *a* derived from HPLC-CHEMTAX and carbon derived from microscopy cell counts. Journal of Plankton Research. 27(1): 103–119. doi:10.1093/plankt/fbh158

Lohr, M. 2011. Carotenoid metabolism in phytoplankton. In S. Roy, C. A. Llewellyn, E. S. Egeland, and G. Johnsen (Eds.), Phytoplankton pigments: characterization, chemotaxonomy and applications in Oceanography. Cambridge University Press, New-York (pp. 113–161).

Lovejoy, C., W. F. Vincent, S. Bonilla, S. Roy, M. J. Martineau, R. Terrado, M. Potvin, R. Massana, and C. Pedrós-Alió. 2007. Distribution, phylogeny, and growth of cold-adapted picoprasinophytes in Arctic seas. Journal of Phycology. 43(1): 78–89. doi:10.1111/j.1529-8817.2006.00310.x

Lund, J., C. Kipling, and E. Le Cren. 1958. The inverted microscope method of estimating algal numbers and the statistical basis of estimations by counting. Hydrobiologia. 11(2): 143–170. doi:10.1007/BF00007865

Lundholm, N., C. Churro, S. Fraga, M. Hoppenrath, M. Iwataki, J. Larsen, K. Mertens, Ø. Moestrup, and A. Zingone. 2009. IOC-UNESCO taxonomic reference list of harmful micro algae. Accessed at https://www.marinespecies.org/hab on 2023-07-15. doi:10.14284/362

Mabit, R., C. A. Araújo, R. K. Singh, and S. Bélanger. 2022. Empirical remote sensing algorithms to retrieve SPM and CDOM in Québec coastal waters. Frontiers in Remote Sensing. 3: 15. doi:10.3389/frsen.2022.834908

Mackey, D., H. Higgins, M. Mackey, and D. Holdsworth. 1998. Algal class abundances in the western equatorial Pacific: estimation from HPLC measurements of chloroplast pigments using CHEMTAX. Deep Sea Research Part I: Oceanographic Research Papers. 45(9): 1441–1468. doi:10.1016/S0967-0637(98)00025-9

Mackey, M., D. Mackey, H. Higgins, and S. Wright. 1996. CHEMTAX-a program for estimating class abundances from chemical markers: application to HPLC measurements of phytoplankton. Marine Ecology Progress Series. 144: 265–283. doi:10.3354/meps144265

Marañón, E., P. Cermeno, M. Latasa, and R. D. Tadonléké. 2012. Temperature, resources, and phytoplankton size structure in the ocean. Limnology and Oceanography. 57(5): 1266–1278. doi:10.4319/lo.2012.57.5.1266

Matthes, L., J. Ehn, L. Dalman, D. Babb, I. Peeken, M. Harasyn, S. Kirillov, J. Lee, S. Bélanger, and J.-É. Tremblay. 2021. Environmental drivers of spring primary

production in Hudson Bay. Elementa: Science of the Anthropocene. 9: 00160. doi:10.1525/elementa.2020.00160

McCabe, G. J., M. P. Clark, and M. C. Serreze. 2001. Trends in Northern Hemisphere surface cyclone frequency and intensity. Journal of Climate. 14(12): 2763–2768. doi:10.1175/1520-0442(2001)014<2763:TINHSC>2.0.CO;2

McClelland, J., A. Townsend-Small, R. Holmes, F. Pan, M. Stieglitz, M. Khosh, and B. Peterson. 2014. River export of nutrients and organic matter from the North Slope of Alaska to the Beaufort Sea. Water Resources Research. 50(2): 1823–1839. doi:10.1002/2013WR014722

McClelland, J. W., R. Holmes, K. Dunton, and R. Macdonald. 2012. The Arctic Ocean Estuary. Estuaries and Coasts. 35(2): 353–368. doi:10.1007/s12237-010-9357-3

McCrystall, M. R., J. Stroeve, M. Serreze, B. C. Forbes, and J. A. Screen. 2021. New climate models reveal faster and larger increases in Arctic precipitation than previously projected. Nature Communications. 12: 6765. doi:10.1038/s41467-021-27031-y

McKie-Krisberg, Z. M., R. W. Sanders, and R. J. Gast. 2018. Evaluation of mixotrophy-associated gene expression in two species of polar marine algae. Frontiers in Marine Science. 5: 273. doi:10.3389/fmars.2018.00273

Meilleur, C., M. Kamula, Z. Kuzyk, and C. Guéguen. 2023. Insights into surface circulation and mixing in James Bay and Hudson Bay from dissolved organic matter optical properties. Journal of Marine Systems. 238: 103841. doi:10.1016/j.jmarsys.2022.103841

Messier, D., R. Ingram, and D. Roy. 1986. Physical and biological modifications in response to La Grande hydroelectric complex. In I. P. Martini (Ed.), Canadian inland seas. Elsevier Oceanography series (Vol. 44, pp. 403–424). https://doi.org/10.1016/S0422-9894(08)70913-9

Millette, N., J. Pierson, A. Aceves, and D. Stoecker. 2017. Mixotrophy in *Heterocapsa rotundata*: a mechanism for dominating the winter phytoplankton. Limnology and Oceanography. 62(2): 836–845. doi:10.1002/lno.10470

Millette, N. C., R. J. Gast, J. Y. Luo, H. V. Moeller, K. Stamieszkin, K. H. Andersen, E. F. Brownlee, N. R. Cohen, S. Duhamel, and S. Dutkiewicz. 2023. Mixoplankton and mixotrophy: future research priorities. Journal of Plankton Research. 45(4): 576–596. doi:10.1093/plankt/fbad020

Morel, A., Y.-H. Ahn, F. Partensky, D. Vaulot, and H. Claustre. 1993. *Prochlorococcus* and *Synechococcus*: A comparative study of their optical properties in relation to their size and pigmentation. Journal of Marine Research. 51(3): 617–649.

Mundy, C., M. Gosselin, M. Starr, and C. Michel. 2010. Riverine export and the effects of circulation on dissolved organic carbon in the Hudson Bay system, Canada. Limnology and Oceanography. 55(1): 315–323.

Muylaert, K., K. Sabbe, and W. Vyverman. 2009. Changes in phytoplankton diversity and community composition along the salinity gradient of the Schelde estuary (Belgium/The Netherlands). Estuarine, Coastal and Shelf Science. 82(2): 335–340. doi:10.1016/j.ecss.2009.01.024

Naeem, S., M. Solan, R. Aspden, and D. Paterson. 2012. Ecological consequences of declining biodiversity: a biodiversity-ecosystem function (BEF) framework for marine systems. In M. Solan, R. J. Aspden, and D. M. Paterson (Eds.), Marine Biodiversity and Ecosystem Functioning. Oxford University Press, Oxford, UK. (pp. 34–51).

Nair, A., S. Sathyendranath, T. Platt, J. Morales, V. Stuart, M.-H. Forget, E. Devred, and H. Bouman. 2008. Remote sensing of phytoplankton functional types. Remote Sensing of Environment. 112(8): 3366–3375. doi:10.1016/j.rse.2008.01.021

Needham, D. M., and J. A. Fuhrman. 2016. Pronounced daily succession of phytoplankton, archaea and bacteria following a spring bloom. Nature Microbiology. 1(4): 1–7. doi:10.1038/nmicrobiol.2016.5

Nemcek, N., M. Hennekes, A. Sastri, and R. I. Perry. 2023. Seasonal and spatial dynamics of the phytoplankton community in the Salish Sea, 2015-2019. Progress in Oceanography. 217: 103108. doi:10.1016/j.pocean.2023.103108

Neukermans, G., K. Ruddick, H. Loisel, and P. Roose. 2012. Optimization and quality control of suspended particulate matter concentration measurement using turbidity measurements. Limnology and Oceanography: Methods. 10(12): 1011–1023. doi:10.4319/lom.2012.10.1011

Nielsen, D. M., P. Pieper, A. Barkhordarian, P. Overduin, T. Ilyina, V. Brovkin, J. Baehr, and M. Dobrynin. 2022. Increase in Arctic coastal erosion and its sensitivity to warming in the twenty-first century. Nature Climate Change. 12(3): 263–270. doi:10.1038/s41558-022-01281-0

Not, F., R. Massana, M. Latasa, D. Marie, C. Colson, W. Eikrem, C. Pedrós-Alió, D. Vaulot, and N. Simon. 2005. Late summer community composition and abundance of photosynthetic picoeukaryotes in Norwegian and Barents Seas. Limnology and Oceanography. 50(5): 1677–1686. doi:10.4319/lo.2005.50.5.1677

Nozais, C., W. F. Vincent, C. Belzile, M. Gosselin, M.-A. Blais, J. Canário, and P. Archambault. 2021. The Great Whale River ecosystem: ecology of a subarctic river

and its receiving waters in coastal Hudson Bay, Canada. Écoscience. 28(3-4): 327–346. doi:10.1080/11956860.2021.1926137

Osterkamp, T., and V. Romanovsky. 1996. Characteristics of changing permafrost temperatures in the Alaskan Arctic, USA. Arctic and Alpine Research. 28(3): 267–273.

Otero, J., X. A. Álvarez-Salgado, and A. Bode. 2020. Phytoplankton diversity effect on ecosystem functioning in a coastal upwelling system. Frontiers in Marine Science. 7: 592255. doi:10.3389/fmars.2020.592255

Paerl, H. W., and D. Justic. 2011. Primary producers: phytoplankton ecology and trophic dynamics in coastal waters. In E. Wolanski, and D. S. McLusky (Eds.), Treatise on Estuarine and Coastal Science. Academic Press, Waltham (Vol. 6, pp. 23–42).

Pang, M., K. Liu, and H. Liu. 2022. Evidence for mixotrophy in pico-chlorophytes from a new *Picochlorum* (Trebouxiophyceae) strain. Journal of Phycology. 58(1): 80–91. doi:10.1111/jpy.13218

Parsons, T., Y. Maita, and C. Lalli. 1984. A manual of biological and chemical methods for seawater analysis. Pergamon Press, Oxford.

Pennock, J. R. 1985. Chlorophyll distributions in the Delaware estuary: regulation by light-limitation. Estuarine, Coastal and Shelf Science. 21(5): 711–725. doi:10.1016/0272-7714(85)90068-X

Pennock, J. R., and J. H. Sharp. 1986. Phytoplankton production in the Delaware Estuary: temporal and spatial variability. Marine Ecology Progress Series. 34(1-2): 143–155.

Peterson, B. J., R. M. Holmes, J. W. McClelland, C. J. Vorosmarty, R. B. Lammers, A. I. Shiklomanov, I. A. Shiklomanov, and S. Rahmstorf. 2002. Increasing river discharge to the Arctic Ocean. Science. 298(5601): 2171–2173. doi:10.1126/science.1077445

Pfander, H. 1992. Carotenoids: an overview. Methods in Enzymology. 213: 3–13. doi:10.1016/0076-6879(92)13105-7

Poulin, M., N. Daugbjerg, R. Gradinger, L. Ilyash, T. Ratkova, and C. von Quillfeldt. 2011. The pan-Arctic biodiversity of marine pelagic and sea-ice unicellular eukaryotes: a first-attempt assessment. Marine Biodiversity. 41: 13–28. doi:10.1007/s12526-010-0058-8

Prinsenberg, S. 1984. Freshwater contents and heat budgets of James Bay and Hudson Bay. Continental Shelf Research. 3(2): 191–200. doi:10.1016/0278-4343(84)90007-4

Rae, R., and W. F. Vincent. 1998. Phytoplankton production in subarctic lake and river ecosystems: development of a photosynthesis-temperature-irradiance model. Journal of Plankton Research. 20(7): 1293–1312. doi:10.1093/plankt/20.7.1293

Raimbault, P. 1988. Size fraction of phytoplankton in the Ligurian Sea and the Algeria Basin (Mediterranean Sea): size distribution versus total concentration. Marine Microbial Food Webs. 3: 1–7.

Raymond, P. A., J. Hartmann, R. Lauerwald, S. Sobek, C. McDonald, M. Hoover, D. Butman, R. Striegl, E. Mayorga, and C. Humborg. 2013. Global carbon dioxide emissions from inland waters. Nature. 503(7476): 355–359. doi:10.1038/nature12760

Richardson, T. L. 2022. The colorful world of cryptophyte phycobiliproteins. Journal of Plankton Research. 44(6): 806–818. doi:10.1093/plankt/fbac048

Robinson, A., H. A. Bouman, G. H. Tilstone, and S. Sathyendranath. 2018. Size class dependent relationships between temperature and phytoplankton photosynthesis-irradiance parameters in the Atlantic Ocean. Frontiers in Marine Science. 4: 435. doi:10.3389/fmars.2017.00435

Rodriguez, F., M. Varela, and M. Zapata. 2002. Phytoplankton assemblages in the Gerlache and Bransfield Straits (Antarctic Peninsula) determined by light microscopy and CHEMTAX analysis of HPLC pigment data. Deep Sea Research Part II: Topical Studies in Oceanography. 49(4-5): 723–747. doi:10.1016/S0967-0645(01)00121-7

Roy, D., and D. Messier. 1989. A review of the effects of water transfers in the La Grande hydroelectric complex (Quebec, Canada). Regulated Rivers: Research & Management. 4(3): 299–316. doi:10.1002/rrr.3450040308

Roy, S., F. Blouin, A. Jacques, and J.-C. Therriault. 2008. Absorption properties of phytoplankton in the Lower Estuary and Gulf of St. Lawrence (Canada). Canadian Journal of Fisheries and Aquatic Sciences. 65(8): 1721–1737. doi:10.1139/F08-089

Roy, S., J.-P. Chanut, M. Gosselin, and T. Sime-Ngando. 1996. Characterization of phytoplankton communities in the lower St. Lawrence Estuary using HPLC-detected pigments and cell microscopy. Marine Ecology Progress Series. 142: 55–73. doi:10.3354/meps142055

Roy, S., C. A. Llewellyn, E. S. Egeland, and G. Johnsen. 2011. Phytoplankton pigments: characterization, chemotaxonomy and applications in Oceanography. Cambridge University Press, United Kingdom.

RStudioTeam, 2021. R: Integrated Development Environment for R. In RStudio, PBC, Boston, MA. https://www.rstudio.com/

Sarker, S., P. Lemke, and K. H. Wiltshire. 2018. Does ecosystem variability explain phytoplankton diversity? Solving an ecological puzzle with long-term data sets. Journal of Sea Research. 135: 11–17. doi:10.1016/j.seares.2018.02.002

Sathish, K., J. Patil, and A. Anil. 2020. Phytoplankton chlorophyll-breakdown pathway: Implication in ecosystem assessment. Journal of Environmental Management. 258: 109989. doi:10.1016/j.jenvman.2019.109989

Schagerl, M., and K. Donabaum. 2003. Patterns of major photosynthetic pigments in freshwater algae. Cyanoprokaryota, Rhodophyta and Cryptophyta. International Journal of Limnology. 39(1): 35–47. doi:10.1051/limn/2003003

Schloss, I. R., G. A. Ferreyra, M. E. Ferrario, G. O. Almandoz, R. Codina, A. A. Bianchi, C. F. Balestrini, H. A. Ochoa, D. R. Pino, and A. Poisson. 2007. Role of plankton communities in sea–air variations in pCO_2 in the SW Atlantic Ocean. Marine Ecology Progress Series. 332: 93–106. doi:10.3354/meps332093

Schlüter, L., T. L. Lauridsen, G. Krogh, and T. Jørgensen. 2006. Identification and quantification of phytoplankton groups in lakes using new pigment ratios–a comparison between pigment analysis by HPLC and microscopy. Freshwater Biology. 51(8): 1474–1485. doi:10.1111/j.1365-2427.2006.01582.x

Schlüter, L., F. Møhlenberg, H. Havskum, and S. Larsen. 2000. The use of phytoplankton pigments for identifying and quantifying phytoplankton groups in coastal areas: testing the influence of light and nutrients on pigment/chlorophyll *a* ratios. Marine Ecology Progress Series. 192: 49–63. doi:10.3354/meps192049

Simo-Matchim, A.-G., M. Gosselin, M. Poulin, M. Ardyna, and S. Lessard. 2017. Summer and fall distribution of phytoplankton in relation to environmental variables in Labrador fjords, with special emphasis on *Phaeocystis pouchetii*. Marine Ecology Progress Series. 572: 19–42. doi:10.3354/meps12125

Simon, N., E. Foulon, D. Grulois, C. Six, Y. Desdevises, M. Latimier, F. Le Gall, M. Tragin, A. Houdan, and E. Derelle. 2017. Revision of the genus *Micromonas* Manton et Parke (Chlorophyta, Mamiellophyceae), of the type species *M. pusilla* (Butcher) Manton & Parke and of the species *M. commoda* van Baren, Bachy and Worden and description of two new species based on the genetic and phenotypic characterization of cultured isolates. Protist. 168(5): 612–635. doi:10.1016/j.protis.2017.09.002

Smith, S., and J. Hollibaugh. 1993. Coastal metabolism and the oceanic organic carbon balance. Reviews of Geophysics. 31(1): 75–89. doi:10.1029/92RG02584

Sosik, H. M., R. J. Olson, and E. V. Armbrust. 2010. Flow cytometry in phytoplankton research. In D. Suggett, O. Prášil, and M. A. Borowitzka (Eds.), Chlorophyll *a*

fluorescence in aquatic sciences: methods and applications. Springer, Dordrecht (Vol. 4, pp. 171–185). https://doi.org/10.1007/978-90-481-9268-7_8

Stieglitz, M., S. Déry, V. Romanovsky, and T. Osterkamp. 2003. The role of snow cover in the warming of arctic permafrost. Geophysical Research Letters. 30(13). doi:10.1029/2003GL017337

Stockner, J. G. 1988. Phototrophic picoplankton: an overview from marine and freshwater ecosystems. Limnology and Oceanography. 33: 765–775. doi:10.4319/lo.1988.33.4part2.0765

Stoecker, D. K., and P. J. Lavrentyev. 2018. Mixotrophic plankton in the polar seas: A pan-arctic review. Frontiers in Marine Science. 5: 292. doi:10.3389/fmars.2018.00292

Stroeve, J., and D. Notz. 2018. Changing state of Arctic sea ice across all seasons. Environmental Research Letters. 13(10): 103001. doi:10.1088/1748-9326/aade56

Suzuki, R., and Y. Fujita. 1986. Chlorophyll decomposition in *Skeletonema costatum*: a problem in chlorophyll determination of water samples. Marine Ecology Progress Series. 28: 81–85.

Szymczak-Żyla, M., G. Kowalewska, and J. W. Louda. 2008. The influence of microorganisms on chlorophyll *a* degradation in the marine environment. Limnology and Oceanography. 53(2): 851–862. doi:10.4319/lo.2008.53.2.0851

Takano, Y., G. Hansen, D. Fujita, and T. Horiguchi. 2008. Serial replacement of diatom endosymbionts in two freshwater dinoflagellates, *Peridiniopsis* spp. (Peridiniales, Dinophyceae). Phycologia. 47(1): 41–53. doi:10.2216/07-36.1

Thinh, L.-V. 1983. Effect of irradiance on the physiology and ultrastructure of the marine cryptomonad, *Cryptomonas* strain Lis (Cryptophyceae). Phycologia. 22(1): 7–11. doi:10.2216/i0031-8884-22-1-7.1

Throndsen, J., G. R. Hasle, and K. Tangen. 2007. Phytoplankton of Norwegian coastal waters. Almater, Oslo.

Tomas, C. R. 1997. Identifying marine phytoplankton. Academic Press, Elsevier, Amsterdam.

Tremblay, G., C. Belzile, M. Gosselin, M. Poulin, S. Roy, and J.-É. Tremblay. 2009. Late summer phytoplankton distribution along a 3500 km transect in Canadian Arctic waters: strong numerical dominance by picoeukaryotes. Aquatic Microbial Ecology. 54: 55–70. doi:10.3354/ame01257

Tremblay, J.-É., D. Robert, D. E. Varela, C. Lovejoy, G. Darnis, R. J. Nelson, and A. R. Sastri. 2012. Current state and trends in Canadian Arctic marine ecosystems: I. Primary production. Climatic Change. 115: 161–178. doi:10.1007/s10584-012-0496-3

Tremblay, J., J. Lee, M. Gosselin, S. Bélanger, S. Kuzyk, and L. Candlish. 2019. Nutrient dynamic and marine biological productivity in the greater Hudson Bay marine region. In Z. Z. Kuzyk, and L. Candlish (Eds.), In the Greater Hudson Bay marine region - An integrated regional impact study (IRIS) of climate change and modernization. Québec, Canada: ArcticNet (pp. 225–244).

Uncles, R., J. Stephens, and R. Smith. 2002. The dependence of estuarine turbidity on tidal intrusion length, tidal range and residence time. Continental Shelf Research. 22(11-13): 1835–1856. doi:10.1016/S0278-4343(02)00041-9

Unrein, F., R. Massana, L. Alonso-Sáez, and J. Gasol. 2007. Significant year-round effect of small mixotrophic flagellates on bacterioplankton in an oligotrophic coastal system. Limnology and Oceanography. 52(1): 456–469. doi:10.4319/lo.2007.52.1.0456

Utermöhl, H. 1958. Zur vervollkommnung der quantitativen phytoplankton-methodik. Internationale Vereinigung für theoretische und angewandte Limnologie: Mitteilungen. 9(1): 1–38. doi:10.1080/05384680.1958.11904091

Van De Poll, W. H., M. A. Van Leeuwe, J. Roggeveld, and A. G. Buma. 2005. Nutrient limitation and high irradiance acclimation reduce PAR and UV-induced viability loss in the Antarctic diatom *Chaetoceros brevis* (Bacillariophyceae). Journal of Phycology. 41(4): 840-850. doi:10.1111/j.1529-8817.2005.00105.x

Van Oostende, N., S. Fawcett, D. Marconi, J. Lueders-Dumont, A. Sabadel, E. Woodward, B. Jönsson, D. M. Sigman, and B. Ward. 2017. Variation of summer phytoplankton community composition and its relationship to nitrate and regenerated nitrogen assimilation across the North Atlantic Ocean. Deep Sea Research Part I: Oceanographic Research Papers. 121: 79–94. doi:10.1016/j.dsr.2016.12.012

Vancoppenolle, M., K. M. Meiners, C. Michel, L. Bopp, F. Brabant, G. Carnat, B. Delille, D. Lannuzel, G. Madec, and S. Moreau. 2013. Role of sea ice in global biogeochemical cycles: emerging views and challenges. Quaternary Science Reviews. 79: 207–230. doi:10.1016/j.quascirev.2013.04.011

Vigil, P., P. D. Countway, J. Rose, D. J. Lonsdale, C. J. Gobler, and D. A. Caron. 2009. Rapid shifts in dominant taxa among microbial eukaryotes in estuarine ecosystems. Aquatic Microbial Ecology. 54(1): 83–100. doi:10.3354/ame01252

Vincent, W. F. 2000. Cyanobacterial dominance in the polar regions. In B. A. Whitton, and M. Potts (Eds.), The ecology of cyanobacteria: Their diversity in time and space. Springer, Dordrecht (pp. 321–340). https://doi.org/10.1007/0-306-46855-7_12

Vincent, W. F., and A. Quesada. 2012. Cyanobacteria in high latitude lakes, rivers and seas. In B. Whitton (Ed.), Ecology of cyanobacteria II: their diversity in space and time. Springer, Dordrecht (pp. 371–385). https://doi.org/10.1007/978-94-007-3855-3_13

Waite, A., A. Fisher, P. A. Thompson, and P. J. Harrison. 1997. Sinking rate *versus* cell volume relationships illuminate sinking rate control mechanisms in marine diatoms. Marine Ecology Progress Series. 157: 97–108. doi:10.3354/meps157097

Waleron, M., K. Waleron, W. F. Vincent, and A. Wilmotte. 2007. Allochthonous inputs of riverine picocyanobacteria to coastal waters in the Arctic Ocean. FEMS Microbiology Ecology. 59(2): 356–365. doi:10.1111/j.1574-6941.2006.00236.x

Walsh, J. 2000. Global atmospheric circulation patterns and relationships to Arctic freshwater fluxes. In E. L. Lewis, E. P. Jones, P. Lemke, T. D. Prowse, and P. Wadhams (Eds.), The Freshwater Budget of the Arctic Ocean. NATO Science Series. Springer, Dordrecht (Vol. 70, pp. 21-43). https://doi.org/10.1007/978-94-011-4132-1_2

Wang, H., J. Liu, M. Klaar, A. Chen, L. Gudmundsson, and J. Holden. 2024. Anthropogenic climate change has influenced global river flow seasonality. Science. 383(6686): 1009–1014. doi:10.1126/science.adi9501

Wang, J.-X., F.-Z. Kong, H.-X. Geng, Q.-C. Zhang, Y.-Q. Yuan, and R.-C. Yu. 2021. CHEMTAX analysis of phytoplankton assemblages revealed potential indicators for blooms of haptophyte *Phaeocystis globosa*. Ecological Indicators. 131: 108177. doi:10.1016/j.ecolind.2021.108177

Warner, S. 1999. The Cree people of James Bay: assessing the social impacts hydroelectric dams and reservoirs. In J. F. Horning (Ed.), Social and Environmental Impacts of the James Bay Hydroelectric Project. McGill-Queen's, Montréal, Ithaca (pp. 93–120). https://doi.org/10.1515/9780773567733-008

Westmacott, J. R., and D. H. Burn. 1997. Climate change effects on the hydrologic regime within the Churchill-Nelson River Basin. Journal of Hydrology. 202(1-4): 263–279. doi:10.1016/S0022-1694(97)00073-5

Wiltshire, K. H., M. Boersma, K. Carstens, A. C. Kraberg, S. Peters, and M. Scharfe. 2015. Control of phytoplankton in a shelf sea: determination of the main drivers based on the Helgoland Roads Time Series. Journal of Sea Research. 105: 42–52. doi:10.1016/j.seares.2015.06.022

Woelfel, J., R. Schumann, F. Peine, A. Flohr, A. Kruss, J. Tegowski, P. Blondel, C. Wiencke, and U. Karsten. 2010. Microphytobenthos of Arctic Kongsfjorden (Svalbard, Norway): biomass and potential primary production along the shore line. Polar Biology. 33: 1239–1253. doi:10.1007/s00300-010-0813-0

Wofsy, S. 1983. A simple model to predict extinction coefficients and phytoplankton biomass in eutrophic waters. Limnology and Oceanography. 28(6): 1144–1155. doi:10.4319/lo.1983.28.6.1144

Wright, S. 2017. Chemtax version 1.95 for calculating the taxonomic composition of phytoplankton populations, Ver. 3. Australian Antarctic Data Centre. https://doi.org/10.4225/15/59fff1c5ea8fc

Wright, S., S. Jeffrey, R. Mantoura, C. Llewellyn, T. Bjørnland, D. Repeta, and N. Welschmeyer. 1991. Improved HPLC method for the analysis of chlorophylls and carotenoids from marine phytoplankton. Marine Ecology Progress Series. 77: 183–196.

Wright, S., D. Thomas, H. Marchant, H. Higgins, M. Mackey, and D. Mackey. 1996. Analysis of phytoplankton of the Australian sector of the Southern Ocean: comparisons of microscopy and size frequency data with interpretations of pigment HPLC data using the 'CHEMTAX' matrix factorisation program. Marine Ecology Progress Series. 144: 285–298. doi:10.3354/meps144285

Wright, S. W., A. Ishikawa, H. J. Marchant, A. T. Davidson, R. L. van den Enden, and G. V. Nash. 2009. Composition and significance of picophytoplankton in Antarctic waters. Polar Biology. 32(5): 797–808. doi:10.1007/s00300-009-0582-9

Wright, S. W., and S. Jeffrey. 2006. Pigment markers for phytoplankton production. In J. K. Volkman (Ed.), Marine organic matter: biomarkers, isotopes and DNA. Springer-Verlag, Berlin, Heidelberd (pp. 71–104). https://doi.org/10.1007/698_2_003

Zapata, M., S. Jeffrey, S. W. Wright, F. Rodríguez, J. L. Garrido, and L. Clementson. 2004. Photosynthetic pigments in 37 species (65 strains) of Haptophyta: implications for Oceanography and chemotaxonomy. Marine Ecology Progress Series. 270: 83–102. doi:10.3354/meps270083

Zapata, M., F. Rodríguez, and J. L. Garrido. 2000. Separation of chlorophylls and carotenoids from marine phytoplankton: a new HPLC method using a reversed phase C8 column and pyridine-containing mobile phases. Marine Ecology Progress Series. 195: 29–45. doi:10.3354/meps195029

Ziegler, A. D., J. Sheffield, E. P. Maurer, B. Nijssen, E. F. Wood, and D. P. Lettenmaier. 2003. Detection of intensification in global- and continental-scale hydrological

cycles: Temporal scale of evaluation. Journal of Climate. 16(3): 535–547. doi:10.1175/1520-0442(2003)016<0535:DOIIGA>2.0.CO;2